



Role of the transcription factor NFATc1
during the early stages of thymocyte development

Die Bedeutung des Transkriptionsfaktors NFATc1
für frühe Differenzierungsprozesse der
Thymozytenreifung

Doctoral Thesis for a Doctoral Degree at the
Graduate School of Life Sciences,
Julius-Maximilians-Universität Würzburg
Section Infection and Immunity

submitted by

Sabrina Giampaolo

from Atessa (CH), Italy

Würzburg 2021

Submitted on:

Office stamp

Members of the Thesis Committee

Chairperson: Prof. Dr. med. Georg Gasteiger

Primary Supervisor: Prof. Dr. Edgar Serfling

Supervisor (Second): PD Dr. Friederike Berberich-Siebelt

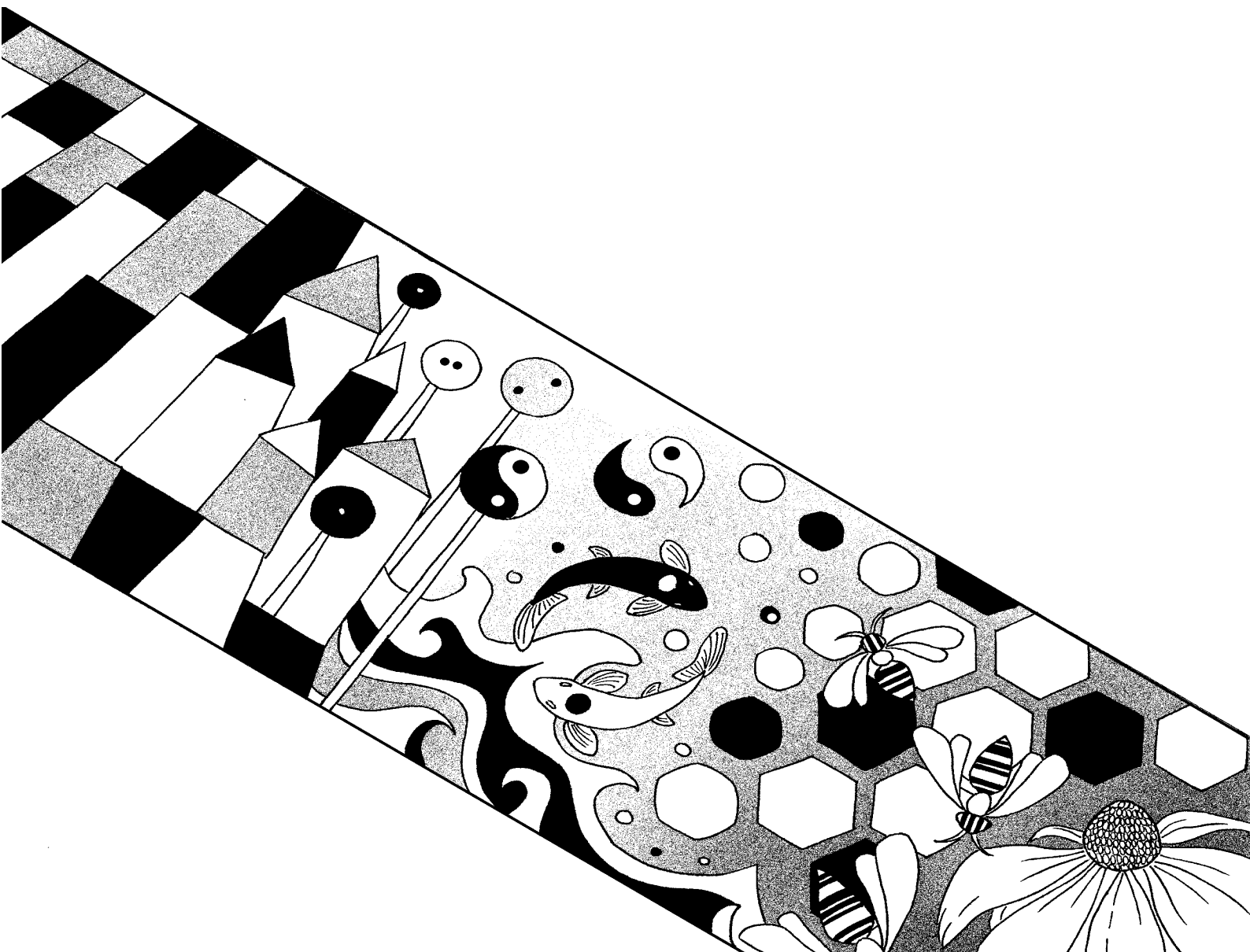
Supervisor (Third): PD Dr. med. Niklas Beyersdorf

Supervisor (Fourth): Prof. Dr. Amiya Patra

Date of Public Defence:

Date of Receipt of Certificates:

To my grandmother Savina,
from who I have inherited my strenght



1	Affidavit/Declaration	1
2	Abstract/Summary	2
3	Zusammenfassung.....	3
4	Introduction	4
4.1	The thymus and T cell development	4
4.2	Regulation of T cell development	6
4.3	<i>Tcrb</i> locus rearrangement, β -Selection, and pre-TCR formation	12
4.3.1	The pre-TCR signaling	14
4.4	Role of chemokines in T cell development	15
4.5	$\gamma\delta$ T cell development	17
4.5.1	$\gamma\delta$ T cells as effector cells	20
4.6	Nuclear Factor of Activated T Cells (NFAT)	21
4.6.1	The transcription factor NFATc1	24
4.6.1.1	NFATc1 in T cell development	26
4.7	Aim of the study and outcome	27
5	Materials and Methods.....	28
5.1	Materials	28
5.2	Chemicals and reagents	28
5.2.1	Consumables	29
5.2.2	Instruments	30
5.2.3	Buffers	31
5.2.4	Kits	33
5.2.5	Oligonucleotides	33
5.2.5.1	Genotyping	34
5.2.5.2	ChIP	34
5.2.5.3	Real-time PCR	34

5.2.6	Cells	35
5.2.6.1	Media and cell culture supplements	36
5.2.6.2	Ligands and chemicals for cell stimulation	36
5.2.7	Antibodies and conjugates	36
5.2.7.1	ChIP	36
5.2.7.2	Antibody-conjugates for flow cytometry	36
5.2.7.3	Primary and secondary antibodies for Western Blots	37
5.2.8	Data analysis software and online tools	37
5.2.9	Mice	38
5.3	Methods	39
5.3.1	Generation of transgenic mice lines	39
5.3.1.1	Genotyping and Polymerase Chain Reaction (PCR)	39
5.3.1.2	Gel electrophoresis of DNA	41
5.3.2	Cell culture	41
5.3.2.1	Cell counting	41
5.3.2.2	Cell culture media	41
5.3.2.3	Preparation of single-cell suspension of murine thymocytes	41
5.3.2.4	Isolation of DN, DP thymocytes, and $\gamma\delta$ T Cells	42
5.3.2.5	Cultivation and stimulation of thymocytes	42
5.3.3	Molecular methods	43
5.3.3.1	Purification by affinity-based chromatin immunoprecipitation and sequencing (ChIP-seq)	43
5.3.3.1.1	ChIP-seq analysis	45
5.3.3.2	RNA isolation from thymocytes and cDNA synthesis	45
5.3.3.3	Real-time PCR (qRT-PCR)	46
5.3.3.4	Preparation of cDNA libraries and NGS-RNA-sequencing	47
5.3.3.5	Protein extraction and quantification	48
5.3.3.6	Western Blot	48
5.3.4	Flow cytometry (FACS)	49
5.3.5	Statistical analysis	50
6	Results	51
6.1	The <i>Nfatc1/A-Bio.BirA</i> mouse model, an excellent tool for more specific ChIP-seq assays	51
6.2	Identification of NFATc1/A binding sites	53

6.3	Identification of NFATc1/A binding sites in thymocytes <i>in vivo</i>	56
6.4	NFATc1/A binding sites and gene expression in thymocytes	58
6.5	NFATc1/A binding at the <i>Tcrb</i> and <i>Tcra</i> loci	60
6.6	Lack of NFATc1 expression in DN thymocytes leads to a moderate decrease in thymic cellularity	62
6.7	Lack of expression of the NFATc1/ α inducible isoforms during DN stages leads to a moderate reduction in thymic cellularity	64
6.8	Lack of NFATc1 activity leads to an increase of $\gamma\delta$ thymocytes in the thymus	67
6.9	The deficiency of the NFATc1/ α isoforms leads to an increase of $\gamma\delta$ T cells in the thymus	71
6.10	NFATc1 deficiency increases the level of CD4 ⁺ $\gamma\delta$ T cells	73
6.11	CD24 ^{low/-} $\gamma\delta$ T cells increase upon loss of NFATc1	75
6.12	NFATc1 regulates important genes for $\gamma\delta$ T cells development	78
6.13	Differential expression of the Bcl2 family members in NFATc1-deficient $\gamma\delta$ T cells	81
7	Discussion	84
7.1	Identification of NFATc1/A target genes that control thymocyte development	84
7.2	$\gamma\delta$ T cells increase in the absence of NFATc1	87
7.3	NFATc1 controls the thymocyte lineage fate of $\alpha\beta$ and $\gamma\delta$ T cells	91
8	Annex	94
8.1	Supplementary information	94
8.2	List of abbreviations	96
9	Bibliography	100
10	Acknowledgments	112

1 Affidavit/Declaration

I hereby confirm that my thesis entitled "Role of the transcription factor NFATc1 during the early stages of thymocyte development" is the result of my own work. I did not receive any help or support from commercial consultants.

All sources and/or materials applied are listed and specified in the thesis.

Furthermore, I confirm that this thesis has not yet been submitted as part of another examination process neither in identical nor in similar form.

Place, Date

Signature

Eidesstattliche Erklärung

Hiermit erkläre ich an Eides statt, die Dissertation „Die Bedeutung des Transkriptionsfaktors NFATc1 für frühe Differenzierungsprozesse der Thymozytenreifung“ eigenständig, d.h. insbesondere selbständig und ohne Hilfe eines kommerziellen Promotionsberaters, angefertigt und keine anderen als die von mir angegebenen Quellen und Hilfsmittel verwendet zu haben.

Ich erkläre außerdem, dass die Dissertation weder in gleicher noch in ähnlicher Form bereits in einem anderen Prüfungsverfahren vorgelegen hat.

Ort, Datum

Unterschrift

2 Abstract/Summary

T lymphocytes (T cells) represent one of the major cell populations of the immune system. Named by the place of their development, the thymus, several types can be distinguished as the $\alpha\beta$ T cells, the $\gamma\delta$ T cells, the mucosa-associated invariant T cells (MAIT), and the natural killer T (NKT) cells. The $\alpha\beta$ lineages of CD4⁺ T_{Helper} and the CD8⁺ T_{Cytotoxic} cells with the T cell receptor (TCR) composed of α - and β -chain are major players of the adaptive immune system. In the thymus, CD4⁺ and CD8⁺ single positive (SP) $\alpha\beta$ cells represent the ultimate result of positive and negative selection of CD4⁺CD8⁺ double positive (DP) thymocytes. The DP population derives from the double negative (DN) thymocytes that develop from bone marrow-derived progenitors through different stages (DN1-DN4) that are characterized by CD25 and CD44 surface expression^{1, 2, 3}.

NFATc1, a member of the Nuclear Factor of Activated T cells (NFAT) transcription factors family, is critically involved in the differentiation and function of T cells. During thymocyte development, the nuclear expression of NFATc1 reaches the highest level at the DN3 (CD44⁻CD25⁺) stage. The hematopoietic cell-specific ablation of NFATc1 activity results in an arrest of thymocyte differentiation at the DN1 (CD44⁺CD25⁻) stage⁴. On the other hand, overexpression of a constitutively active version of NFATc1 results in an impaired transition of DN3 cells to the DN4 (CD44⁻CD25⁻) stage, suggesting that a certain threshold level of NFATc1 activity is critical at this point⁵.

ChIP-seq and RNA-seq analysis allowed us the identification of NFATc1/A target genes involved in lineage development as the *Tcra* and *Tcrb* gene loci. Furthermore, we identified multiple NFATc1-regulated genes that are involved in $\gamma\delta$ T cell development. In the mouse models, *Rag1Cre-Nfatc1^{fl/fl}* and *Rag1Cre-E2^{fl/fl}*, in which the activity of NFATc1 or inducible NFATc1 in the latter is impaired during the early stages of thymocyte development, we observed increased numbers of $\gamma\delta$ T cells. These $\gamma\delta$ T cells showed an unusual overexpression of CD4, a lack of CD24 expression, and overexpression of the anti-apoptotic gene *Bcl2a1a*.

We hypothesize that during the DN stages NFATc1 plays an important role in regulating crucial steps of $\alpha\beta$ thymocyte development and when NFATc1 activity is missing this may disturb $\alpha\beta$ development resulting in alternative cell fates like $\gamma\delta$ T cells.

3 Zusammenfassung

T-Lymphozyten (T-Zellen) sind eine wichtige Säule des Immunsystems. Benannt nach dem Ort ihrer Entstehung, dem Thymus, werden sie verschiedenen Linien zugeordnet, den $\alpha\beta$ -T-Zellen, den $\gamma\delta$ -T-Zellen, den Mukosa assoziierten invarianten T-Zellen (MAIT) und den natürlichen Killer T-Zellen (NKT). Bei den $\alpha\beta$ -T-Zellen mit einem T-Zell-Rezeptor (TZR) aus α - und β -Kette unterscheidet man die $CD4^+$ Helfer T. von den $CD8^+$ zytotoxischen T-Zellen. Beide sind zentrale Bestandteile des adaptiven Immunsystems. Einfach positive (SP) $CD4^+$ und $CD8^+$ $\alpha\beta$ -T-Zellen gehen aus der positiven und negativen Selektion doppelt-positiver (DP) $CD4^+CD8^+$ Zellen hervor. Zuvor durchlaufen sie als doppelt-negative (DN) Thymozyten, die von Vorläufern aus dem Knochenmark abstammen, verschiedene Stadien (DN1-DN4), die durch unterschiedliche Expression der Adhäsionsmoleküle CD25 und CD44 gekennzeichnet sind^{1,2,3}.

Der Transkriptionsfaktor NFATc1, ein Mitglied der Familie Nukleärer Faktoren Aktivierter T-Zellen (NFAT), ist maßgeblich an der Differenzierung und der Funktion von T-Zellen beteiligt. Während der Thymozytenreifeung kann eine zunehmende nukleäre Expression von NFATc1 beobachtet werden, die im DN3-Stadium ($CD44^+CD25^+$) den höchsten Wert erreicht. Eine Deletion der NFATc1-Aktivität in frühen Vorläuferzellen führte zu einem Arrest der Thymozytendifferenzierung im DN1-Stadium ($CD44^+CD25^-$)⁵. Andererseits hemmte die Überexpression einer konstitutiv aktiven Form von NFATc1 den Übergang von DN3-Zellen in das DN4-Stadium ($CD44^+CD25^-$), was vermuten lässt, dass ein bestimmter Schwellenwert der NFATc1-Aktivität zu diesem Zeitpunkt von entscheidender Bedeutung ist⁶

Mittels ChIP- und RNA-Sequenzierung gelang es, NFATc1-Zielgene im Thymus zu identifizieren. Hierzu zählten unter anderen die *Tcra* und *Tcrb* Gene. Transkriptionsanalysen an isolierten DN-Thymozyten offenbarten daneben mehrere NFATc1-regulierte Gene, die an der Entwicklung von $\gamma\delta$ -T-Zellen beteiligt sind. In den Mausmodellen, *Rag1Cre-Nfatc1^{fl/fl}* und *Rag1Cre-E2^{fl/fl}*, bei denen die Aktivität von NFATc1 bzw. der induzierbaren NFATc1-Aktivität zu frühen Stadien der Thymozytenentwicklung beeinträchtigt ist, stieg die Zahl von $\gamma\delta$ -T-Zellen an. Diese $\gamma\delta$ -T-Zellen zeigen eine unübliche Überexpression des CD4 Markers, eine fehlende Expression des Oberflächenmarkers CD24 und eine Überexpression des antiapoptotischen Gens *Bcl2a1a*. Wir vermuten daher, dass NFATc1 an der erfolgreichen Reifeung von $\alpha\beta$ -T-Zellen direkt beteiligt ist und fehlende NFATc1-Aktivität die Entwicklung alternativer Linien wie von $\gamma\delta$ -T-Zellen befördert.

4 Introduction

4.1 The thymus and T cell development

The thymus is one of the primary lymphoid organs and is the site where lymphoid progenitors, coming from fetal liver or bone marrow, develop to give rise to mature naïve T cells. In human and mouse, the thymus is located in the anterior superior mediastinum, in front of the heart, and behind the sternum. During the mouse embryogenesis, the thymus primordium appears at the ventral aspect of the third pharyngeal pouch at E10.5 and E11.5 and continues to develop for 3-4 weeks after birth (E, Embryonic day).

The thymus is composed of two identical lobes surrounded by a capsule of connective tissue that injects extensions (septa) into the organ, dividing lobes into lobules. Each lobule again consists of two zones: an outer cortex and an inner medulla. The junction between the two is designed as a cortico-medullary junction (CMJ) and the most outer region of the cortex is known as the subcapsular zone (SCZ) (Figure 4.1). The thymus is highly vascularized with thymic arteries and veins connected with more central blood vessels of the body. Blood vessels that support the thymus are organized along the septa and enrich the cortico-medullary zone. Histologically, the cellular structure of the thymus is spatially well organized to release all necessary signals to the developing thymocytes^{6,7}.

The thymus is primarily composed of the hematopoietic progenitors of T cells that undergo steps of differentiation and selection, thymic stroma, a highly organized three-dimensional network of cortical and medullary thymic epithelial cells (cTECs and mTECs), dendritic cells (DCs), macrophages, and other non-hematopoietic stromal elements as fibroblast and endothelial cells². All immune cells arise from hematopoietic stem cells (HSCs), which show long-term self-renewal (potential to continuously re-generating) and stemness capacities (can develop in either lymphoid or myeloid lineages). As in all mammals, during mouse development, the first site of hematopoiesis is the yolk sac. Hematopoiesis is observed already at this site at E7. In the yolk sac, the very first multipotent hematopoietic progenitors with lymphohematopoietic potential are generated around day E9.5. These embryonic stem cells (ES) that express c-kit (Tyrosine kinase receptor or receptor for stem cell factor or CD117), AA4.1 (CD93), and CD45 (lymphocyte common antigen)⁸, can differentiate either in erythro-myeloid (monocytes and granulocytes) or lymphoid lineages to generate T, B, and NK cells when cultured *in vitro* on stromal cells^{9,10}. At E10-11, HSCs from the yolk sac start to colonize the mouse fetal liver moving along the vitelline vein. By day E12, the fetal liver becomes the main source of hematopoiesis. The fetal liver contains multipotential progenitor cells with lymphoid-myeloid age characteristics and expresses CD45⁺c-Kit⁺Flt3⁺Il7R α ⁺ surface markers. At this stage, some lymphoid progenitors start to move to the thymus^{7,11}. The first waves of

thymus-seeding precursors are a mix of T-lymphoid, B-lymphoid, and myeloid progenitor cells¹². During fetal life, T cell commitment occurs before reaching thymus primordium¹³. The first progenitor population colonizes the thymus primordium at E11 of mouse development. Soon, they start to proliferate intensively and establish the earliest population of Double Negative thymocytes (DN)^{14, 15, 16}.

During adult life, the thymus does not contain hematopoietic self-renewal cells, but it is continuously seeded by the bone marrow (BM). Common Lymphoid Progenitors (CLPs) from the BM enter the thymus from the blood at the cortico-medullary junction, migrate toward the cortex, subcapsular zone, and back to medulla as they differentiate to become T cells. This migration through the organ is mediated by crosstalk of various chemokines and cytokines (Figure 4.1)^{17, 18, 19}

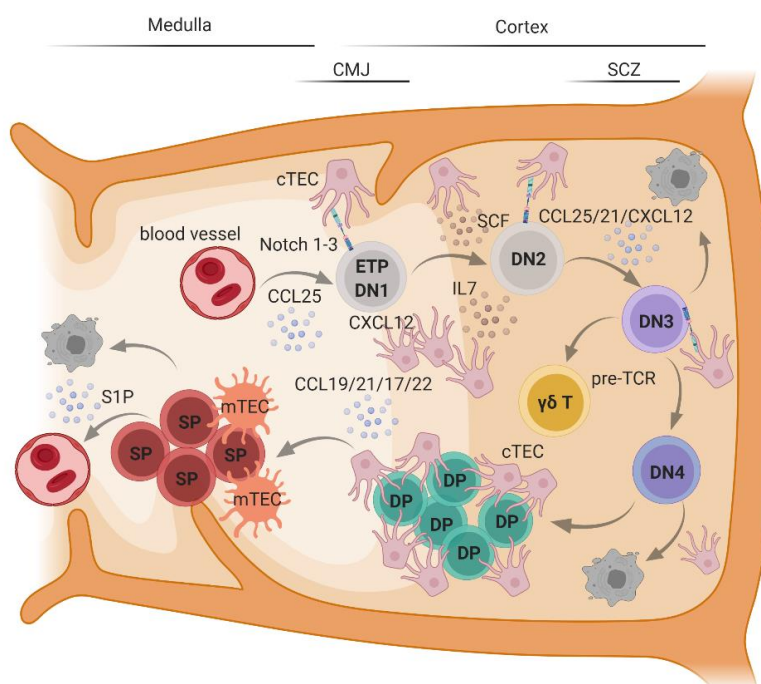


Figure 4.1 The thymus at different stages of thymocyte development.

The thymocytes differentiate in the thymus passing through the four Double Negative (ETP/DN1, DN2, DN3, and DN4), Double Positive (DP), and Single Positive (SP) stages. Notch, IL7, and SCF (c-kit ligand) signaling are known to be important for the early stages of development until stage DN3. The chemokines CCL25, CCL21, CXCL12, CCL19, CCL22, and SP1 are expressed by the thymic stroma and bind to their respective chemokine receptors on thymocytes.

cTECs and mTECs release all the microenvironmental cues necessary for thymocyte development.

The picture was generated with Biorender.com and adapted from Takahama Y., *Nat Rev Immunol.*, 2006.

4.2 Regulation of T cell development

The thymocyte development is a precisely coordinated process that is orchestrated by environmental cues, transcription factors (TFs), and chromatin re-modeling complexes¹⁷. All these elements need to act spatially and temporally to establish the T cell lineage identity, proliferation, TCR rearrangement and expression, and the positive and negative selection processes^{11, 20, 21}. Among the TFs that regulate T cell development, cell-type-specific “master regulators” have not been identified. Instead, numerous TFs coordinately regulate each other’s transcription and specific events during thymocyte development. Moreover, these TFs induce multiple chromatin modifications, such as DNA methylations, and make distinct regions of the chromatin accessible for gene expression necessary for T cell differentiation.

Thymocyte development consists of different stages characterized by the expression of surface markers, including co-receptors and the respective T cell receptors (TCR).

The earliest stage is indicated as DN thymocytes that lack both the co-receptors CD4 and CD8. They represent ~5% of the population of thymocytes in the thymus. DN thymocytes consist of four distinct populations according to the surface expression of CD44 and CD25 molecules: ETP-DN1 (CD44⁺ CD25⁻); DN2 (CD44⁺ CD25⁺); DN3 (CD44⁻ CD25⁺); DN4 (CD44⁻ CD25⁻) cells, which are at various stages of differentiation, including also CD24 (heat-stable antigen, HSA), CD45 (Ly-5), CD90 (Thy-1), CD117 (c-kit), and CD127 (IL7R α) expression. Subsequently, the thymocytes express the TCR and the co-receptors CD4 and CD8, and, therefore, they are defined as Double Positive (DP) cells. DP thymocytes undergo the process of negative and positive selection to give rise to the single positive (SP) cells, where the thymocytes express either CD4 or CD8 co-receptors (Figure 4.2 A). The first population of cells detected in the post-natal thymus is the early T lymphocyte progenitors (ETPs) or DN1 cells. ETPs/DN1 cells (CD3⁻ CD4⁻ CD8⁻ CD117⁺ CD44⁺ CD25⁻) retain the capacity to generate DCs, NK cells, macrophages, mast cells, granulocytes, and B and T cells, but have lost the potential for erythroid and megakaryocytes. Based on CD24 and CD117 markers, the DN1 cells can further be divided into five heterogeneous populations. They differentiate for the expression of genes like CD3 ϵ and *Rag1*, *Tcrb* locus rearrangement status, proliferation rate, and their potential to generate T or non-T lineage cells¹⁸. The subsequent developmental stage, DN2 (CD44⁺, CD25⁺, CD117⁺) cells, show a highly proliferative rate and the retention of some characteristics of stemness. This stage can be further subdivided into two subpopulations depending on the expression of Lck and c-kit: DN2a (Lck⁻, c-kit^{hi}, CD25⁺) cells can give rise to NK, DCs, and myeloid cells. DN2b cells (Lck⁺, c-kit^{int}, CD25⁺) lost the capacity to give rise to all other lineages. Instead, they are more committed to the T cell lineage.

A

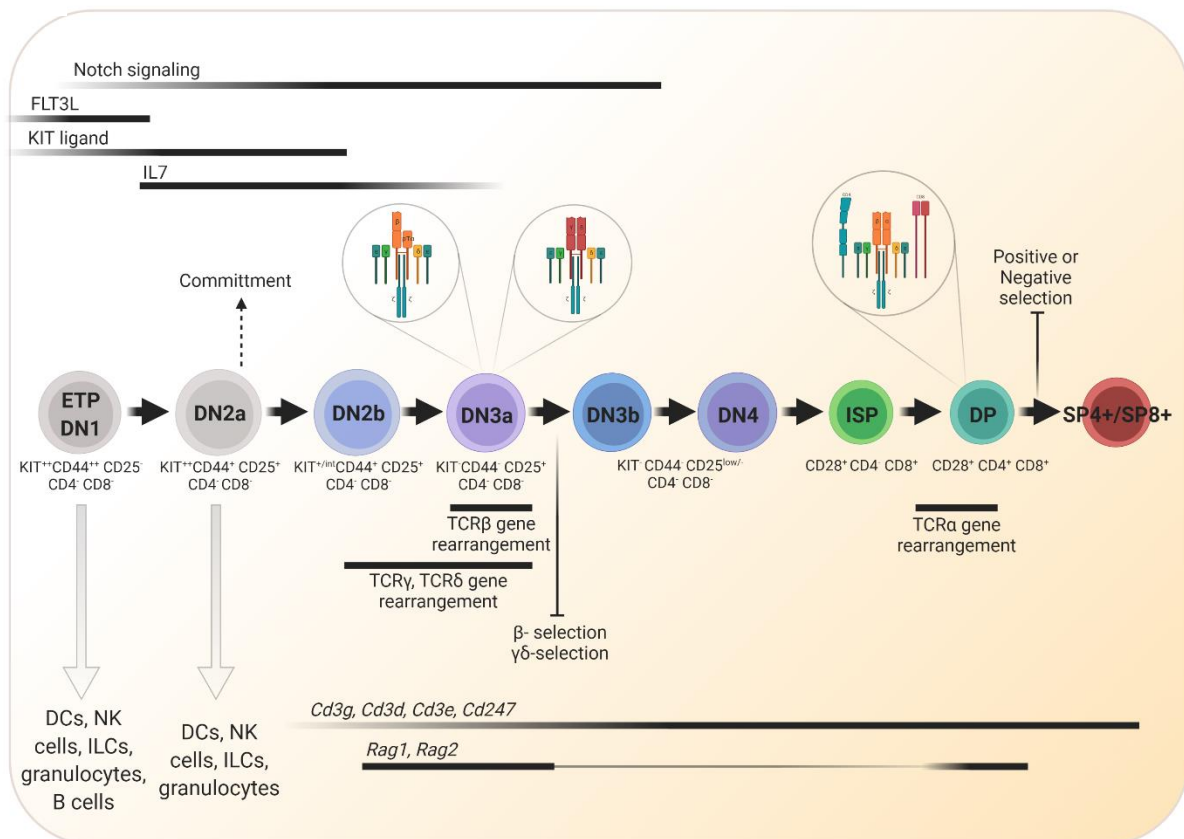


Figure 4.2 A Stages of thymocyte development in the thymus.

The thymocyte developmental stages are indicated, starting from early T cell progenitor (ETP) cells, passing through the different DN steps (DN1-DN4), to reach the DP and SP T cell stages. The thymic environmental cues are necessary for thymocyte survival and commitment, as Notch, IL7, KIT ligand, and FLT3L signals (on the top, indicated by black lines). At precise phases, genes essential for thymocyte development are expressed (below, indicated by black lines).

During the earliest developmental steps, when Notch signaling is missing (indicated by gray arrows) cells retain the potential to become DCs, NK cells, ILCs, granulocytes, and B cells.

At the DN3a step, the cells get selected upon the expression of the pre-TCR or the $\gamma\delta$ -TCR (indicated in the callouts). At the DP stage, thymocytes will be positively or negatively selected (indicated in the callouts). The picture was created with Biorender.com and adapted from Hosokawa, H. & Rothenberg E.V., *Nat.Rev. Immunol.*, 2020.

Upon expression of the two *Rag1* and *Rag2* genes (recombinase activating gene 1 and 2), thymocytes start to rearrange their *Tcry*, *Tcrδ* and *Tcrb* loci and express TCR $\gamma\delta$ or the β -chain of the T cell receptor. TCR β associates with a surrogate of the α chain (pre-T α) giving rise to the pre-T cell receptor (pre-TCR). The DN2b stage corresponds to the commitment of the progenitors to the T cell lineage. Therefore, at this stage, the bifurcation of $\alpha\beta$ or $\gamma\delta$ T cell lineages occurs. It is still controversial which signals induce the common DN progenitor to follow one or the other lineage. Some lines of evidence suggest the existence of a pre-

committed lineage fate reinforced by TCR $\alpha\beta$ or $\gamma\delta$ expression, or a role for TCR to induce lineage decision. Concerning this last hypothesis, some studies suggest an association between TCR signaling strength and lineage outcome: weak signals coming from the pre-TCR induce the $\alpha\beta$ lineage, whereas stronger signal supports the generation of $\gamma\delta$ lineage⁷.

Irreversible T cell commitment is achieved at the DN3 stage (CD3⁻ CD4⁻ CD8⁻ CD117⁻CD44⁻ CD25⁺) at which thymocytes are selected through an antigen-independent mechanism called β -selection. It ensures that only thymocytes expressing a functional TCR β chain proceed in development (See below " β -selection and pre-TCR signaling"). The DN3 stage can be further divided into DN3a and DN3b thymocyte populations. DN3a cells are characterized by a more resting population, with a gene expression program associated with the recombination of *Tcr* loci (mediated by *Rag1* and *Rag2*, *pT α*). DN3b cells are characterized by intense proliferation, a sign of post-selected thymocytes²². Selected thymocytes start to proliferate extensively reaching the DN4 stage (CD44⁻ CD25⁻ CD117⁻). At this stage, thymocytes start to recombine the *Tcra* locus and express mature $\alpha\beta$ TCR complexes on their surface.

Expression of both co-receptors CD4 and CD8 on the surface marks the entry of thymocytes into the DP stage. DP immature thymocytes represent ~80% of the thymocytes population. At this stage, thymocytes get "instructed" by the cTECs and mTECs to recognize non-self-antigens and not respond to self-antigens.

This "training" is designated as positive and negative selection: interactions between MHC/self-antigen complexes, expressed by cTEC, mTEC, and DCs, and newly formed T cell receptors induce in DP thymocytes signals of different strengths and, therefore, with different outcomes. This phenomenon is indicated as affinity hypothesis: low avidity interaction elicits survival signals (positive selection), whereas high avidity signals induce cell death by apoptosis or clonal deletion (negative selection). Positive selection is mediated by cTECs in the cortex. TCRs of non-selected DP thymocytes bind MHC class I and II/self-peptide complexes exposed on cTECs cell surface. Low strength signaling through the TCRs rescues thymocytes from apoptosis via induction of *Bcl2*, while non-recognition of TCRs leads to "death by neglect". Only 3-5 % of DP cells survive this checkpoint step and move to the SP stage²³. At this point, T cells express CD4⁺ or CD8⁺ co-receptors on their surface.

Negative selection of SP CD4⁺ or CD8⁺ T cells, where strong signals coming from TCR and MHC I and II/self-peptide complexes induce cell death by apoptosis, is orchestrated by mTECs. Expression of self-peptides derived from tissue-restricted-antigens (TRA) in mTECs is coordinated by the *Aire* (autoimmune regulator) gene and supported by the mechanism of autophagy^{24, 25}. mTECs establish the "central tolerance" by positive and negative selection processes and the generation of CD4⁺ FoxP3⁺ CD25⁺ regulatory T cells (Treg) in the thymus. Treg precursors recognize MHC II/self-antigen complexes with high affinity but the response is a positive selection and the generation of cells with self-tolerance. This mechanism is

termed agonist selection²⁶. CD4⁺ comprise approximately ~10%, and CD8⁺ cells ~5% of total thymocytes. In mouse, SP cells are retained in the thymus medulla for 12 days and go through a process of further maturation and selection, aimed to delete self-reactive thymocytes escaped from negative selection²⁷.

This process is characterized by the expression of CD62 ligand (CD62L is also known as Lymphocytes-(L)-selectin) and CD69. These first semi-mature naïve T cells are CD62L^{low}CD69^{hi}. Finally, they proceed to fully matured thymocytes expressing CD62L^{hi}CD69^{low} that are ready to be exported to the periphery as mature naïve T cells¹⁷.

Unconventional T cells such as $\gamma\delta$ T cells, $\gamma\delta$ NKT cells or invariant NKT cells (iNKT), and CD8 $\alpha\alpha^+$ TCR $\alpha\beta$ intraepithelial lymphocytes (IELPs) are also generated in the thymus²⁸.

The early T cell development path can be divided into three phases depending on their commitment status and Notch-dependence: phase 1 ETPs-DN2a, phase 2 DN2b-DN3a, and phase 3 DN3b-DP²⁹. Each phase is characterized by the activation or repression of specific TFs (Figure 4.2 B).

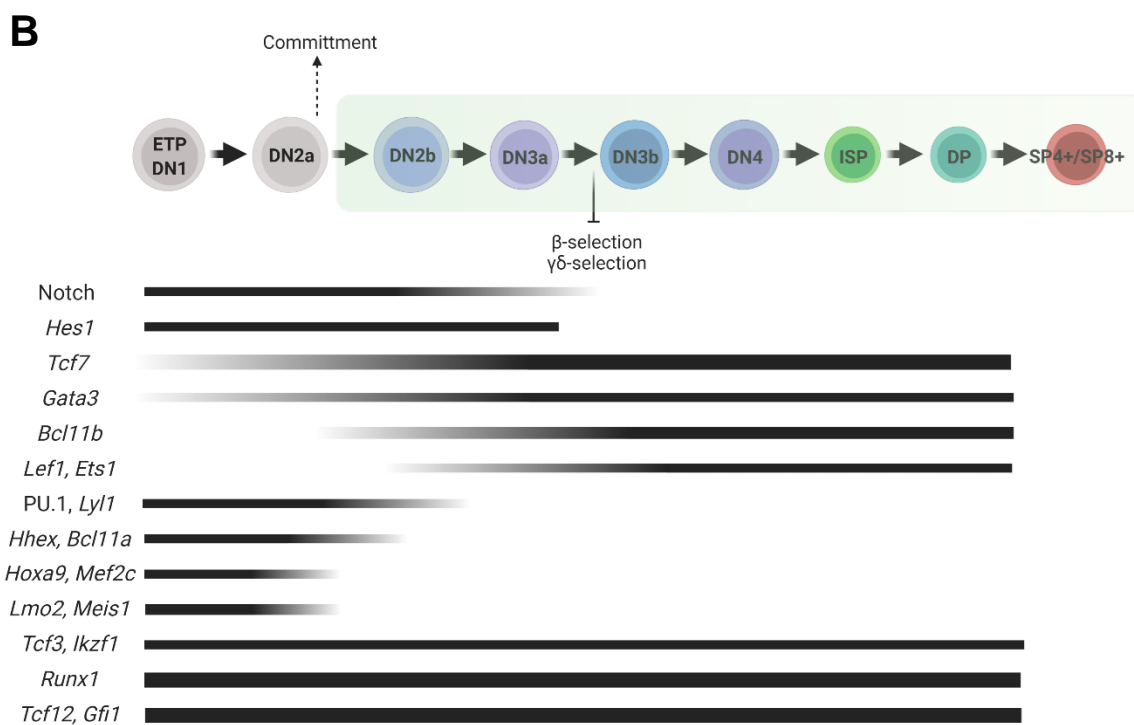


Figure 4.2 B Important TFs that control thymocyte development.

Important TFs involved in thymocyte development are listed on the left. Black bars indicate the expression level and the timing of expression during the developmental stages.

The picture was created with Biorender.com and adapted from Hosokawa, H & Rothenberg E.V., *Nat.Rev. Immunol.*, 2020.

One of the most essential and important pathways during the first two phases of development is Notch signaling^{30, 31, 32}. Deletion of *Notch1* in hematopoietic stem progenitor cells, or of any components of the pathway, led to a complete block in T cell development and the appearance of B cells in the thymus^{33, 34}.

Three members of the **Notch** family, Notch1, Notch2, and Notch3, are expressed in the thymus. They are transmembrane cell-surface receptors and their ligands, Jagged-1 (*Jag1*), Jagged-2 (*Jag2*), Jagged-3 (*Jag3*), Delta-like 1 (*Dll1*), and Delta-like 4 (*Dll4*), are expressed by cTECs³⁵. The engagement of Notch with their ligands induces the proteolytic release of Notch intracellular domain (NICD)³⁶. The NICD translocates into the nucleus and becomes a co-activator for the DNA-binding protein RBPJ.

Notch signaling triggers the expression of genes associated with T cell lineage specification, such as *Tcf7* (encoding TCF-1) and *Gata3*, which promote T cell development, survival, and proliferation of thymocytes until the β -selection step^{37, 38}.

During the ETP stage, a group of TFs associated with hematopoietic stem/ progenitor cell characteristics is still expressed and needed to be turned off at the T cell commitment step. These factors are PU.1, LMO2, MEF2C, BCL-11A, HHEX, LYL1, GFI1B, ERG, MYCN, and HOXA9^{39, 40, 41}.

PU.1 (*Spi1*), a member of the ETS family member of TFs supports the proliferation of thymocyte progenitors and inhibits further T cell differentiation^{42, 43, 44}. It activates *Bcl11a*, *Lmo2*, and *Mef2c* expression that controls the progenitor phenotype⁴⁵. PU.1 activity is induced by Notch signaling^{46, 47} and turned off by GATA3, RUNX1, and TCF1⁴⁸. PU.1 expression is associated with the differentiation of DCs, myeloid cells, and B cells. The Notch pathway triggers also the expression of the transcriptional repressor HES1 (*Hes1*). It is activated at the ETP stage until the DN3 stage, and it plays a role in T cell commitment by excluding the myeloid lineage development, and the survival of DN3 cells once they pass through the β -selection checkpoint^{49, 50, 51}.

The survival and the high proliferative rate of the first phase of pre-committed cells are supported by thymic microenvironmental cues, such as the KIT ligand (SCF, stem cell factor) and interleukin-7 (IL-7), that bind to the c-kit and the IL7R, respectively, on thymocytes. During the early stages of development, IL-7 signals control the expression and the balance of the pro-apoptotic and anti-apoptotic Bcl-2 family members⁵². The great proliferation rate is also supported by the expression of the TFs Lyl1 and Hhex^{53, 54}.

Loss of function of TCF-1 has been associated with a defect in survival and differentiation of early stages of development^{55, 56}. TCF-1 can activate genes specific for the T cell lineage, such as the *Gata3*, *Bcl11b*, *Lck*, *Cd3g*, and *Rag2* genes⁵⁶. TCF1 can also act as a pioneer-like factor inducing the opening of chromatin regions of the transcriptional T cell landscape⁵⁷.

The expression of GATA3 increases at the DN2a stage. GATA3 collaborates with NOTCH to exclude B cell development during the early stages of development and regulates T cell commitment and β -selection in a controlled limited-expression manner^{58, 59, 60}. TCF-1 and GATA3 also interact with MYB, RUNX1, CBFb, IKAROS, GFI1, and E2A required for T cell development.

RUNX1 is the most prominent RUNX member in DN thymocytes and acts in a switch-like mode, activating and repressing genes between the developmental stages⁶¹.

The activities of Notch, TCF-1, GATA3, and RUNX1 collaborate in the transcriptional activation of the *Bcl11b* gene at the late DN2a stage of T cell commitment⁶².

BCL-11B is important for the passage of DN2a cells to the DN2b commitment phase, for the passage through the β -selection, and for many further aspects of $\alpha\beta$ T cell development^{63, 64}. Its expression endures until mature DP stages and is sustained also in all effector cells of $\alpha\beta$ T cell lineages, as in NKT cells, regulatory T cells (Treg), cytotoxic T cells, and T helper cells⁶⁵. Inactivation of *Bcl11b* in hematopoietic cell progenitors causes a developmental block of thymocytes at the DN2-DN3 stage^{66, 67}. Depending on the presence of Notch signaling, these abnormal cells assume a phenotype typical for NK, dendritic, or myeloid cells⁶⁸. Therefore, BCL-11B is important for excluding developing T cells from different cell fates.

During the DN3a stage, Notch signaling controls the expression of the *CD25 (Il2ra)*, *Notch3*, *Ptcra*, *Rag1*, *Rag2*, and *Cd3e* genes⁶⁹. At this stage, Notch signaling promotes the activation and collaborates with so-called E box proteins. E box proteins associate as homodimers or heterodimers with other basic helix-loop-helix (bHLH) factors and bind at an E-box (Enhancer-box; CANNTG) consensus motif to the DNA. This family of bHLH factors is already expressed in lymphoid precursors before the cell enters the thymus^{70, 71, 72}. The E protein family is composed of the E2A (*Tcf3*), HEB (*Tcf12*), and E2-2 (*Tcf4*) members. E proteins play an important role in the generation of hematopoietic stem cells, lymphoid-primed multipotent progenitors, B, and T cells, and later during the commitment phase, as they activate the definitive T cell program^{73, 74}. The E protein E2A, in collaboration with Notch signaling, promotes the T cell commitment⁷⁵. In addition, E2A defines the fate choice between T cell and innate lymphoid cells (ILC) in the thymus. At the DN2b-DN3a stage, the homodimer formation between E2A and HEB is essential for *Tcr γ* , *Tcr δ* , and *Tcrb* rearrangement⁷⁶. In the fetal thymus, they assemble at genomic regions of genes specific for the T cell program, such as at the *Notch1*, *Rag1*, *Rag2*, *Ptcra*, *Cd3g*, *Cd3d*, *Cd3e*, and *Tcrb* genes⁷⁷.

Another important function of the E2A-HEB heterodimers is the control of proliferation arrest of cells until a proper pre-TCR or TCR is expressed on the surface, and proper signaling is generated^{78, 79}. pre-TCR signaling induces the expression of the class IV HLH family inhibitors of DNA binding (ID) factor, the ID1 (*Id1*), ID2 (*Id2*), and ID3 (*Id3*) proteins. ID factors lack the basic -DNA-binding domain⁸⁰. Therefore, associating with E proteins, they impede the binding

of the complex on the DNA. ID factors attenuate the E proteins activity and Notch signaling. During the third developmental phase, the thymocytes that receive a proper pre-TCR or TCR signaling, pass through the β -selection, during which Notch is still required, and this is a high proliferative step when cells can dispense from Notch signaling and move toward the DN4 step.

The DP step is characterized by the expression of further TFs, such as IKZF3 (*Aiolos*) and ROR γ (*Rorc*). To sustain the survival of DP thymocytes in the process of *Tcra* rearrangement and TCR α expression, MYB, together with TCF1, high HEB/E2A, and ROR γ t helps to induce BCL-XL (*Bcl2l1*) expression in the future DP cells^{81, 82, 83}.

4.3 *Tcrb* locus rearrangement, β -Selection, and pre-TCR formation

During the early DN3 stage, thymocytes start to rearrange their *Tcrb* locus and express functional TCR β chains. TCR β chain expression is coordinated with the expression of invariant pre-T α chain that, together with CD3 γ , δ , ϵ , and ζ chains, generate the pre-TCR complex. The pre-TCR signaling leads the thymocytes to cross the first important checkpoint: the β -selection. This process ensures that only thymocytes expressing a proper TCR β chain can proceed for further differentiation. Cells that receive the proper pre-TCR signaling become Notch- and IL7-independent for their survival and proliferation⁸⁴.

Genomic recombination of the *Tcrb* locus is an irreversible process that modifies the original locus configuration, or germinal configuration. Each cell contains two allelic copies of the *Tcrb* locus, one on each homologous chromosome.

In the mouse genome, the *Tcrb* locus is located on chromosome 6 and spans approximately 670 kb DNA (Figure 4.3).

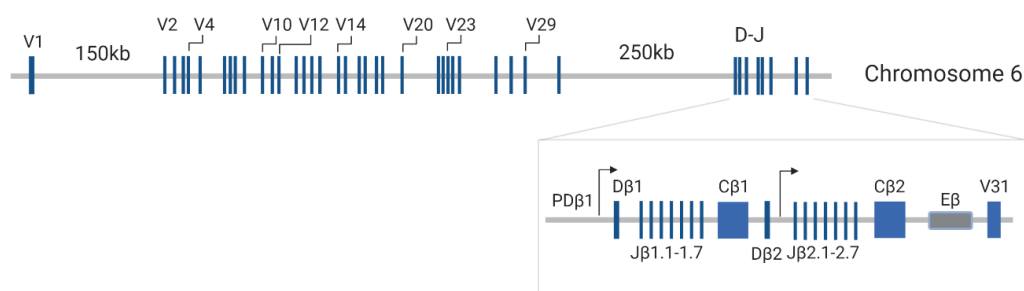


Figure 4.3 Schematic diagram of the mouse *Tcrb* locus.

The *Tcrb* locus lies on mouse chromosome 6. It is composed of 31 variable (V) segments and two clusters of Diversity (D) and Joining (J) segments. At the 3' end of the locus, the promoter of D-J clusters, the two constant regions (C β), and the Enhancer (E β) are located.

The picture is created with Biorender.com and it is adapted from Majumder K. *et al*, *JEM*, 2015.

It consists of four regions containing gene segments for Variable (V), including a ~390-kb 5' domain containing 21 Vb gene segments, Joining (J), Diversity (D), and Constant (C). In addition, a 26-kb 3' domain comprises a duplicated cluster of Db-Jb-Cb gene segments, followed by a single Vb gene segment, Vb31 (Figure 4.3)⁸⁵. The 560-bp *Tcrb* gene enhancer (E β) lies at the center of the ~10-kb Cb2-Vb31 intervening region^{86, 87}. Knockout mouse models have revealed a critical function of E β displaying impaired TCR β chain production and $\alpha\beta$ T cell development^{88, 89}. The activity of the E β enhancer is required to initiate V(D)J recombination at the *Tcrb* locus.

During the DN2 stage, RAG1 and RAG2 are expressed and recognize specific genomic sequences, the recombination signal sequences (RSS) that flank gene segments. RSSs are cleaved by recombinases, generating double-strand breaks that will be recognized and repaired by non-homologous end-joining DNA break systems.

When the *Tcrb* locus is properly recombined, transcription starts from a leader sequence of the V gene segment and proceeds until the constant gene segment.

If an error occurs during the recombination process, other rearrangements are attended until there are no more available exons. After the splicing process that removes intronic sequences, a mature *Tcrb* mRNA transcript is generated and TCR β protein chains are expressed. Pre-T α pairs spontaneously with the TCR β chain in forming a patch distribution in the cell membrane. The colocalization occurs into glycolipids rafts on the cell membrane through which signaling events are initiated⁹⁰.

The pre-T α chain is expressed from the *Ptcra* gene on mouse chromosome 17. *Ptcra* depletion leads to a block of thymocytes development at the DN3 stage⁹¹. The interactions with the downstream signaling components are mediated by its characteristic long cytoplasmic tail. *Ptcra* is expressed gradually along the DN stages until the late DN4 when the *Tcra* locus starts to recombine and TCR α chains are expressed and displaces pre-T α chain for the heterodimerization with the TCR β chain⁹². Pre-TCR initiates signaling in the cell in an autonomous manner, MHC-antigen-independent way. The autonomous pre-TCR signaling is mediated by the spontaneous aggregation of adjacent pre-T α chains through lateral interaction, induced by charged residues in their extracellular domain. Lipid rafts are membrane microdomains enriched with signaling molecules. The association of pre-TCR with lipid rafts and the low threshold of DN activation can mediate signaling cascades.

During β -selection, the coupling of the pre-T α to a mature TCR β induces inhibitory feedback signaling. This induces the cessation of *Tcrb* locus rearrangement (allelic exclusion), the rearrangement of *Tcra* locus, the induction of CD4 and CD8 expression, down-regulation of CD25, the escape from apoptosis, and the proliferation of selected thymocytes. The allelic exclusion is the process through which recombination stops at one of the two alleles. Allelic

exclusion ensures that each T cell expresses only one copy of a recombined *Tcrb* locus increasing the antigen recognition specificity and protecting against autoimmunity.

4.3.1 The pre-TCR signaling

The downstream components that mediate pre-TCR signals are similar to those that transmit signals for T cell activation, i.e. phosphorylation and activation of the Src-family kinase Lck associated with Immunoreceptor Tyrosine-Based Activation Motifs (ITAMs) of the cytoplasmic domain of CD3 molecules, phosphorylation and activation of the tyrosine kinase ZAP-70, phosphorylation of adaptor protein linker for activated T cells (LAT), SH-domain-containing Leukocyte-specific Phosphoprotein of 76 kDa (SLP-76) and Vav, a guanine-nucleotide exchange factor (GEF) for Rho-family GTPases. Following ZAP-70 activation, the enzyme Phosphatidylinositol kinase 3 (PI 3-kinase) is recruited to the cell surface and becomes activated. PI 3-kinase generates Phosphatidylinositol (3,4,5)-trisphosphate (PIP₃) on the membrane surface. PIP₃ binds the protein complex formed by LAT/Gads/SLP-76 inducing activation of the phosphatase C-γ (PLC-γ). PLC-γ needs also phosphorylation by Itk (Interleukin-2-inducible T-cell kinase), a member of the Tec family of cytoplasmic tyrosine kinases.

Activation of PLC-γ leads to the breakdown of the membrane lipid phosphatidylinositol (4,5)-diphosphate (PIP₂) generating Diacylglycerol (DAG) and diffusible second messenger inositol 1,4,5-trisphosphate (IP₃). The activation of PLC-γ induces three different downstream effects: Ca²⁺ influx and an increase of Ca²⁺ concentration in the cell, activation of Ras-MAPK-MEK1-Erk pathway, and activation of protein kinase C-θ (PKC-θ). Diffusible IP₃ binds at Ca²⁺ channel-IP₃ receptors of the endoplasmic reticulum (ER), inducing the release of calcium in the cytosol. Decreased calcium in ER leads to the clustering of the transmembrane protein STIM1 on the ER membrane and its association with the calcium release-activated calcium channel (CRAC channel) and its components Orai1 and Orai2. On the other hand, DAG induces activation of Protein Kinase θ, PKCα and PKCβ. These kinases phosphorylate and promote the CBM complex consisting of CARMA1, BCL10, and MALT1.

Two transcription factor pathways are then activated: the NF-κB (Nuclear Factor κB), and NFAT (Nuclear Factor of Activated T Cell) factors. Both are localized in the cytosol in an inactive form. In lymphocytes, the most activated NF-κB member is a heterodimer composed of p50 and p65 (RelA) proteins. In the cytosol, the dimer is held in an inactive state bound to the inhibitor κB (IκB). The CBM complex induces the activation of serine kinase IκB complex that is comprised of IKKα, IKKβ, and NEMO (IKKγ), the phosphorylation of the inhibitor, and its ubiquitination and degradation via the proteasome. NF-κB promotes the differentiation,

cellular expansion, and survival of thymocytes that transit from the β -selection checkpoint to DP cells.

Increased Ca^{2+} in cytosol binds the calcium-binding protein calmodulin that in turn activates the protein phosphatase calcineurin (CN). CN activation leads to the dephosphorylation of NFAT factors and their translocation from the cytosol to the nucleus where they bind to the promoters of genes involved in T cell proliferation during β -selection. It has been shown that the block of NFAT activity in pre-TCR- selected DN thymocytes, treated in vitro with cyclosporin A, induces a defect in CD25 downregulation that is associated with a block of development at the DN stage⁹³.

A downstream component of the Ras pathway is extracellular signal-related kinase (ERK) whose activation induces the activation of ETS-1 and the early growth response gene (EGR) transcription factors. EGR1, EGR2, and EGR3 regulate in cooperation with ROR γ T the proliferation of thymocytes along with the selection steps in the thymus.

PI3-kinase activation and PIP₃ generation also recruit at the cell surface the serine/threonine kinase Akt (protein kinase B) that binds through its pleckstrin homology (PH) domain to PIP₃. PDK-1 (Phosphoinositide-Dependent Kinase-1) also is recruited to the cell membrane via PH domain binding. PDK-1 is close to Akt and mediates its phosphorylation and activation. This pathway is essential for promoting cell survival and inhibiting cell death via multiple mechanisms.

Although compared to TCR signals, similar transcription factors are activated by pre-TCR signals, the transcriptomes induced by pre-TCR and TCR signals differ substantially. Thus, the *Rag1* and *Rag2* genes are down-regulated due to the upregulation of *Id3*, and this induces a block of further *Tcrb* locus recombination⁹⁴. The upregulation of cyclin D3 is important for supporting the burst of proliferation that accompany the thymocytes to move further into the DN4 stage. To support the survival of selected DN thymocytes, the *Bcl2a1* gene encoding the anti-apoptotic protein Bcl2-A1 (a member of the Bcl-2 family) is induced by pre-TCR signalling⁹⁵.

4.4 Role of chemokines in T cell development

Chemokines are secreted cytokines that bind their specific chemokine receptors on the cell membrane. They are involved in the directional migration of cells along a concentration gradient, a process called chemotaxis. Under homeostatic conditions, chemotaxis induces homing of leukocytes to respective organs and during inflammation leads to recruitment of cells to the site of the damage.

In the thymus, chemokines are expressed and released by the TECs while thymocytes express the corresponding chemokine receptors. Multiple chemokines can bind single

receptors and single chemokines can bind multiple receptors. Specific chemokine receptor binding induces biased signaling into the cell⁹⁶.

There are four classes of chemokines characterized by the C-X-C, C-C, C-X-3C, and X-C structures according to the interaction of the first cysteine at the N- and the last one at the C-terminus of proteins. Chemokine receptors belong to the class A rhodopsin-like family of G protein-coupled receptors that associate with G α i heterotrimeric G proteins⁹⁶.

The binding of chemokines to their receptors induces the motility of thymocytes, their interaction with stromal cells, differentiation, proliferation, and egression from the thymus⁹⁷. Expression of specific chemokines by endothelial cells and TECs is important for the proper localization of developing thymocytes in thymic microenvironments (niches). These niches provide all cues for thymocyte proliferation and differentiation. The DN subpopulations, DP, and SP populations are distributed in specific zones of thymus parenchyma, and chemokines mediate their movement within the organ. Progenitors enter at the CMJ. DN thymocytes migrate along the outward cortex to the SCZ to become DP, and selected thymocytes move back to the medulla as SP cells and egress from the thymus⁹⁸.

At E11, CLPs start to colonize the fetal thymus primordium, and this mechanism is thought to be mediated by a vasculature independent pathway⁹⁹.

Lymphoid progenitors are chemo-attracted to the thymus primordium through the CC-chemokine ligand 21 (CCL21) and CCL25 recognition of their respective receptors, CCR7 and CCR9, expressed on thymocytes. Deficiency of CCR7 and CCR9 shows a decrease in thymic cellularity at E14.5 and E17.5^{100, 101}.

At the latest stage of embryogenesis and in the adult mouse, thymocyte progenitors, moving from the BM, enter the thymus through the vasculature-dependent pathway, at the CMJ, which is abundantly vascularized. Entry is regulated by CCR9, CCR7, and by interactions of Platelet (P)-Selectin Glycoprotein Ligand 1 (PSGL1), expressed by progenitors, with its ligand P-selectin, expressed by thymic endothelium, and also with Vascular Cell Adhesion Molecule-1 (VCAM-1) and Intercellular Adhesion Molecule-1 (ICAM-1). CCR9 and CCR7 are involved in the accumulation and proliferation of DN1 thymocytes at CMJ for ten days before migrating to the cortex region. In the cortex, DN2 thymocytes start to rearrange the *Tcrb* locus and reach the subcapsular zone at the DN3 stage where they pass the β -selection process and proliferate. Thymocyte movement along the cortex to the subcapsular zone is mediated by CCR7, CCR9, and CXCR4^{102, 103, 104}. In the cortex, newly generated DP thymocytes undergo positive and negative selection scanning MHC-peptide complexes displayed by cTECs and DCs. CCR7 and CCR4 receptors are important at this stage for the interactions between thymocytes and thymic antigen-presenting cells (APCs), mTECs, and DCs.

Positively selected DP cells increase their expression of CCR7 and CCR4 while mTECs and DCs express CCL19, CCL21, CCL17, and CCL22 inducing thymocytes to move to the medulla.

Egression of mature SP cells is, at last, mediated by Sphingosine-1-Phosphate Receptor 1 (S1P1) and S1P present in high concentration in plasma^{17, 104, 105, 106}

4.5 $\gamma\delta$ T cell development

$\gamma\delta$ T cells are a unique and well-conserved group of lymphoid cells. Together with $\alpha\beta$ T cells and B cells, they rearrange their antigen receptor loci to generate a TCR that recognizes different epitopes on antigens. Differently from $\alpha\beta$ T and B cells, $\gamma\delta$ T cells show both characteristics of cells of innate and adaptive immune systems. In mice, they represent 4% of all circulating T cells in the thymus and secondary lymphoid organs. $\gamma\delta$ T cells are the first population seeding the fetal thymus¹⁰⁷. The earliest progenitor population is indicated with CD25⁺, CD27⁺, and CD24⁺ cells. $\alpha\beta$ and $\gamma\delta$ T cells share a common progenitor along the DN stages of thymocyte development. At the DN2-DN3 stage, as previously mentioned, the rearrangement of *Tcr β* , *Tcr γ* , and *Tcr δ* loci occur. DN2-DN3 transition represents the time point of $\alpha\beta$ and $\gamma\delta$ bifurcation. Before this stage, thymocyte progenitors retain the potential of giving rise to both lineages. Current studies favor the TCR-dependent two-steps strength-model¹⁰⁸: the strength of the TCR signaling defines the choice between $\alpha\beta$ and $\gamma\delta$ T cells in thymocytes progenitors, irrespectively of the TCR complex on the cell surface^{109, 110, 111, 112} and the acquisition of a functional phenotype, T $\gamma\delta$ 17 or T $\gamma\delta$ 1 effector phenotypes^{113, 114, 115, 110, 116}. The strong TCR signaling is likely to be achieved by the enhanced or prolonged activation of the ERK pathway and its downstream EGR and ID3 targets that are important mediators for strong signals that promote $\gamma\delta$ commitment¹¹⁰.

As previously described, at the DN3 stage, thymocytes undergo the first process of selection mediated by TCR signaling: the β -selection or the $\gamma\delta$ -selection, carried out by a β -chain that associates with the invariant preT α chain or by TCR $\gamma\delta$, respectively. Like pre-TCR complexes, $\gamma\delta$ TCR complexes dimerize autonomously, in a ligand-independent way, and the signaling has the same amplitude as that of the pre-TCR¹¹⁷.

$\gamma\delta$ T cells, unlike $\alpha\beta$ T cells, cross only one step of selection and do not progress through the DP stage, but retain their DN status. Therefore, they don't undergo the positive and negative selection processes, as $\alpha\beta$ T cells. For this reason, a specific ligand recognition is not required for $\gamma\delta$ repertoire shaping, development, or exit from the thymus. The encounter with the antigen in the thymus only defines the effector phenotype of the cells¹¹⁷. It has been shown that only the DETC (Dendritic Epidermal T Cell) population requires a SKINT-1 ligand-dependent selection for developing and homing to epidermis^{118, 119}.

$\gamma\delta$ T cells develop in the thymus and egress the organ to colonize peripheral tissues in a series of “waves”^{120, 121}. The different usage of specific variable γ segments (V γ) during the TCR γ chain rearrangement enables the generation of different waves of $\gamma\delta$ T cells at a discrete-time point during development, from fetal to adult life. They emerge from the thymus both as naïve and effector cells and colonize different tissues. In Table 4.1 the different waves, the time of development, and the tissue residency of $\gamma\delta$ T cells are indicated¹²².

Table 4.1 The different “waves” of $\gamma\delta$ T cell development during embryonic and adult life¹⁴³.

Subset	Timing of development	Tissue residence	Cytokines produced
Vγ1	Perinatal and adult	Liver, lymphoid tissue	IFN γ and IL4
Vγ4	E18 to adult	Dermis, lungs, liver, lymphoid tissue	IL17A or IFN γ
Vγ5 (DETC)	E13-E16	Epidermis	IFN γ
Vγ6	E16-birth	Uterus, lungs, tongue, liver, placenta, kidneys	IL17A
Vγ7	neonatal	Epithelial layers of the small intestine	IFN γ

$\gamma\delta$ T cells can be distinguished into “Innate-like”, “natural” and “pre-programmed” or “inducible” T cells. Innate-like $\gamma\delta$ T cells achieve their characteristic of effector cells already during development in the thymus, and they develop mostly during embryonic life from fetal liver progenitors^{121, 122, 123, 124}. These innate-like $\gamma\delta$ T cells assume differential effector phenotypes, depending on the amount of TCR signals they receive in the thymus (the strength-based differentiation model)^{117, 125}. IFN γ -producing T $\gamma\delta$ 1 cells arise upon strong signaling or ligand engagement in the thymus. Instead, weaker or no TCR engagement signals lead to IL17-producing T $\gamma\delta$ 17 cells. They produce a massive amount of IL17A once they are activated¹¹⁷. These conclusions are also supported by single-cell RNA-sequencing analysis (scRNAseq)¹²⁶. The IL17-producing $\gamma\delta$ T cells seem to be a “default” phenotype¹²⁷. These innate IL17-producing $\gamma\delta$ T cells, comprising the three embryonic waves of V γ 4⁺, V γ 6⁺, and V γ 1⁺ cells, can only develop in a developmental time window during embryonic life (between E15.5 and E18.5). In this time frame, they acquire the capacity to produce IL17, achieved in a TCR-independent manner¹²¹. Innate-IL17 producing $\gamma\delta$ T cells can not develop in adult thymus. The T $\gamma\delta$ 17 cells found in adult mice are long-lived and self-renewing cells generated during fetal

life¹²¹. The innate IFN γ -producing population is instead represented by NK1.1⁺ V γ 1⁺ thymocytes²⁸.

In adult mice, BM progenitors give rise to $\gamma\delta$ T cells that leave the thymus as naïve T cells (CD122^{lo}CD62L⁺ CD44^{lo}) and acquire effector characteristics in the periphery after antigen encounter and activation through TCR signaling.

Table 4.2 lists the lineage determining transcription factors (LDTFs) essential for the commitment, and specification of $\gamma\delta$ T cells^{122, 128, 129, 130, 131, 132, 133}.

These factors are part of a complex network that provides a dual action of the lineage choice in thymocyte progenitors ($\alpha\beta$ or $\gamma\delta$) and effector fate.

Table 4.2 List of genes encoding important LDTFs (line-defining transcription factors) for the commitment, and specification of $\gamma\delta$ T cells¹⁴³.

T$\gamma\delta$1	T$\gamma\delta$17
<i>Tbx21</i>	<i>Rorc</i>
<i>Tcf7</i>	<i>Maf</i>
<i>Lef1</i>	<i>Sox13</i>
<i>Eomes</i>	<i>Sox4</i>
<i>Notch1</i>	<i>Blk</i>
<i>Egr1-Egr3</i>	<i>Tcf3-Tcf12</i>
<i>Id3</i>	<i>Hes1</i>
	<i>IL7-IL7r</i> (high levels)
	<i>Tgfb1</i>

As reported before, strong TCR signals mediate the expression of EGR2 and EGR3 TFs. ID3, controlled by EGR2 and EGR3, in turn, inhibits E47, a key factor of *Rorc* expression¹³⁴. TCR signaling also downregulates *Sox13* expression and, therefore, inhibits the development of T $\gamma\delta$ 17 cells.

ROR γ t induction via a TCR-independent mechanism may depend on the expression of the two high-mobility group box TFs SOX4, and SOX13 that have been shown to induce *Rorc* expression¹³³.

The IL7/IL7R pathway is essential for thymocyte development in general, but $\gamma\delta$ T cells seem to be more dependent on IL-7 for their development. IL7R-deficient mice completely lack $\gamma\delta$ T

cells, as they have a block in V-J recombination. It has been shown that IL7 signals control the accessibility of TCR γ locus¹³².

Notch signaling is essential for $\alpha\beta$ T cells during cell commitment, survival, proliferation, and differentiation until the β -selection step (DN3). DN1 and DN2 populations still maintain the potential to give rise to $\alpha\beta$ and $\gamma\delta$ T cells. During the DN3 step, cells are fully committed and they do not retain the bi-potential characteristic. Committed $\gamma\delta$ cells don't require anymore Notch signaling, in contrast to $\alpha\beta$ cells that need these signals for β -selection and further proliferation and differentiation after this stage¹³⁵. More specifically, Notch signals target TCF-1 that promotes the expression of *Lef1*. Both factors control T $\gamma\delta$ 1 cell differentiation. On the other hand, it has been demonstrated that *Hes-1*, another Notch signaling target gene, is specifically expressed in T $\gamma\delta$ 17 cells¹³⁶.

4.5.1 $\gamma\delta$ T cells as effector cells

$\gamma\delta$ effector T cells can be defined by the expression of distinct surface markers and specific TFs: IFN γ producing cells are CD44⁺, CD45RB⁺, CD27⁺, CD122⁺, NK1.1⁺, and the key TF is T-bet, while IL17A producing cells are CD44^{hi}, CD45RB^{lo}, CD27⁻, CD122⁻, NK1.1⁻, express CCR6, and ROR γ t is their main TF. Mice deficient in these key TFs lack the respective cytokine-producing $\gamma\delta$ T cell population.

Most innate-like $\gamma\delta$ T cells are tissue-resident lymphocytes with a limited TCR repertoire. During an immune response, they get activated in a TCR-independent manner, such as through the NKG2D receptor that recognizes cellular stress signals, pathogen pattern recognition receptors (PRRs), and/or by inflammatory cytokine receptors. They respond rapidly to several types of antigens, including self-proteins (products of cell dysregulation), non-self peptide antigens, non-peptide antigens¹³⁷, insulin peptide B:9-23¹³⁸, glycoproteins, phycoerythrin, and also lipid antigens such as cardiolipin¹³⁹. The antigen recognition strategy is still not clear, but some $\gamma\delta$ T cell subsets can recognize MHC class II molecules, and others recognize β_2 M-associated MHC class 1b T10 and T22 molecules^{140, 141, 142}. They home to and are enriched in barrier tissues such as the epidermis, dermis, small intestine, lung, and uterus. They also display tissue sensing capacities^{122, 123, 57}. As tissue-resident cells, they also display characteristics as self-renewal and long-term maintenance.

As mentioned before, these innate-like $\gamma\delta$ T cells acquire their effector function already during development in the thymus. In the periphery, they can trigger a rapid and massive proinflammatory cytokine release after recognition of pathogen pattern recognition receptors (PRRs) and/or by inflammatory cytokine receptors.

The immature "inducible" $\gamma\delta$ T cells are CD24⁺ while the mature cells are CD24⁻, and they show characteristics of IL17 and IFN γ producing cells, but differ from their fetal counterparts.

They need to be activated in the secondary lymphoid organs to produce cytokines¹²⁶. Further scRNA-seq assays revealed a large percentage of $\gamma\delta$ T cells in lymph nodes that show characteristics of naïve T cells egressing from the thymus. They correspond to CD44⁻, Ccr9⁺ and S1Pr1⁺ cells¹⁰⁵. They don't go through a massive clonal expansion after activation.

$\gamma\delta$ T cells can produce several cytokines. In addition to IFN γ and IL17, when stimulated they can express TNF, granzymes, IL13, IL2, and IL4¹⁴³.

In mice, they have been shown to play a role in pathogen clearance, such as of *Escherichia coli*, *Listeria*, *Mycobacterium*, *Salmonella*, *Pseudomonas*, and CMV, and also control tumor surveillance, tissue repair, autoimmunity, and allergy^{144, 145}.

4.6 Nuclear Factor of Activated T Cells (NFAT)

The Nuclear Factor of Activated T cell (NFAT) family of transcription factors consists of five members: NFATc1 (NFAT2 or NFATc), NFATc2 (NFAT1 or NFATp), NFATc3 (NFAT4 or NFATx), NFATc4 (NFAT3), and NFAT5^{146, 147}.

The 'genuine' NFATc1, c2, c3, and c4 factors are activated via calcium signaling, while NFAT5 is activated upon osmotic stress¹⁴⁸. As shown in figure 4.4, the four calcium-dependent NFAT family members share approximately 80% of homology in their DNA-binding domain of 300 amino acids, designated as the Rel similarity domain (RSD). Their N-terminal transactivation domain (TAD-N), and the regulatory domain, known as NFAT-homology region (NHR) show also sequence similarities¹⁴⁹. The regulatory domain harbors several phosphorylation sites organized in the serine-rich domain (SRD), which acts as substrates for protein kinases and phosphatases. In addition, the nuclear localization signals (NLS) and nuclear export signals (NES) are located in the regulatory domain.

NFAT members are expressed in a large variety of cells comprising the hematopoietic system, in cardiomyocytes, muscles, bone, and brain, and are involved in numerous functions. In lymphocytes, the three members NFATc1, NFATc2, and NFATc3 are highly expressed. Inactivation of the *Nfatc1* gene leads to a lethal embryonic phenotype, due to a defect in the development of embryonic heart^{150, 151}.

Nfatc2 ko mice are born normally but develop with age a hyper-proliferative syndrome and elevated immune responses^{152, 153}. Mice deficient for both *Nfatc2* and *Nfatc3* show increased characteristics, similar but accelerated as in *Nfatc2* ko mice, i.e. hyperproliferation of peripheral T and B cells with subsequent splenomegaly and a tendency to generate Th2 type cells. Additionally, lymphocytes double ko for *Nfatc2* and *Nfatc3* show a marked decrease in Fas ligand expression, and, therefore, resistance to apoptosis¹⁵⁴.

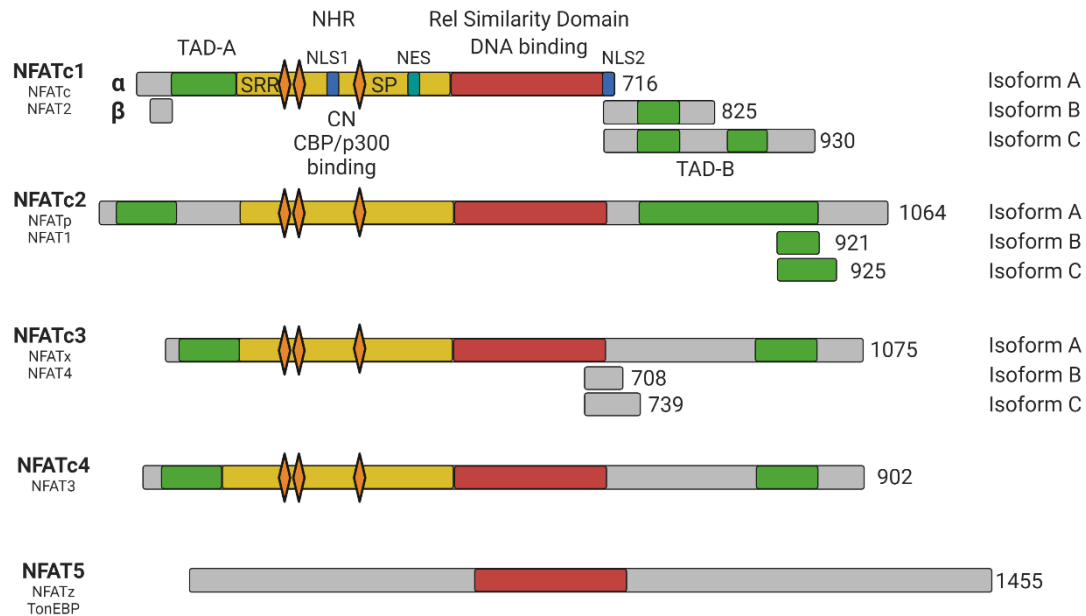


Figure 4.4 Schematic diagram of the NFAT family members.

The five NFAT transcription family members are listed with their alternative names (on the left) and the amino acid length of each isoform (on the right).

All the five NFAT transcription family members share the most conserved Rel Similarity-DNA binding domain (RSD, in red).

Only NFATc1, c2, c3, and c4 share a common regulatory domain (NHR, in yellow) and the two transactivation domains (TAD-A and TAD-B, in green). The regulatory domain contains the serine-threonine residues that are targets for phosphorylation and de-phosphorylation, the NLS1 and the NES are shown. The NHR is also the site for CN and co-activator CBP/p300 bindings.

NFATc1, c2, and c3 express three isoforms indicated as A, B, and C. Only NFATc1 express additional isoforms indicated with α and β that are differentiated by the presence of α - or the β - peptides, at their N-termini.

Calcium signal-dependent activation of the four NFAT members is triggered by TCR activation and signaling. This leads to activation of downstream components as mentioned previously in the section pre-TCR signaling. In brief, the binding of TCR or BCR with cognate antigen induces the activation of phospholipase C (PLC) and the generation of the second messenger inositol-1,4,5-trisphosphate (IP_3) and diacylglycerol (DAG). IP_3 , with stromal interaction molecules 1 and 2 (STIM1 and STIM2), and the Ca^{2+} release-activated Ca^{2+} channels (CRAC) activation, induces the influx of Ca^{2+} into the cytosol. Ca^{2+} binds to calmodulin, which activates the serine/threonine phosphatase calcineurin. Calcineurin-mediated dephosphorylation of SRD unmask the NLSs of NFAT factors, leading to the import of NFAT/calcineurin complexes translocation into the nucleus. In the nucleus, the RHD mediates the binding of NFAT to its consensus sequence 5'-GGAAA-3' located within the promoter of target genes. In resting cells, the NFAT homology region (NHR) is highly phosphorylated and the nuclear localization

signals are hidden, whereas the nuclear export signal is exposed, keeping NFAT in an inactive state in the cytoplasm.

With different kinetics, all members of the NFAT family, once in the nucleus, are re-phosphorylated by several kinases, such as glycogen synthase kinase (GSK3), casein kinase I (CKI), Erk1, c-Jun N-terminal kinase 3 (JNK3), and MAP/SAP kinases. The phosphorylation induces the inactivation of transcriptional activity of NFATs and their export back to the cytoplasm.

The promoters of several genes involved in the development and activation of T and B cells contain the NFAT consensus motif. Well known NFAT target genes are the genes encoding: IL-2, IL-4, IL-5, IL-3, IFN γ , GM-SCF, TNF α , IL2R α (CD25), Fas ligand, CD40 ligand, EGR2 and EGR3, p57^{lck} and others¹⁴⁹.

NFAT members control the differentiation and effector function of T cells and their cytokine production^{155, 156}. NFATc1 is required for the differentiation and activation of T follicular helper (Tfh) cells, through the control of IRF4 and BATF factors expression. Different from the ablation of NFATc2 and the specific ablation of NFATc1 in B cells, which affected mildly the germinal center (GC) formation, the ablation of NFATc1 and NFATc2 in T cells impaired the humoral immune response¹⁵⁷. In Tfh cells, NFATc1 and NFATc2 control the expression of ICOS, PD-1, CXCR5, and CD40L, and cytokines such as IL-4 and IL-21 essential for Tfh cell differentiation, GC formation, and B-cell affinity maturation^{158, 159, 160, 161, 162}.

It was reported that NFAT members control the expression of the *Foxp3* gene that orchestrates the Treg function. However, in mice deficient for NFATc1 and NFATc2, nTreg development is normal, indicating a minor role of NFAT factors in Treg function^{158, 163, 164, 165, 166}. In T follicular regulatory (Tfr) cells, NFATc1 induces the expression of CXCR5, necessary for their homing to GCs¹⁵⁸, and the expression of the inhibitory receptor CTLA-4^{163, 167}. In CD4⁺ T cells, TCR activation, without co-stimulatory signals, leads to T cell anergy, and the cells become hyporesponsive. In this scenario, NFATc2 is activated but forms either homodimers or complexes with other transcription factors than AP-1, such as with EGR2 and EGR3 factors. It is assumed that this activates the transcription of the “anergy-inducing genes”, such as E3 ubiquitin ligases and proteases, Itch, Cbl-b, Grail, diacylglycerol kinase α (DGK α), and caspase 3^{168, 169, 170}. In contrast, NFATc1- in particular its short isoform NFATc1/ α A- plays an opposite role in anergy induction and is not induced in anergic T cells¹⁷¹.

During T cell exhaustion, a process induced by chronic TCR stimulation, such as in chronic infections or cancer, T cells became unresponsive as well. Likely, NFATs are also involved in this process, where their association with AP-1 factors is impaired^{172, 173}.

4.6.1 The transcription factor NFATc1

In mice, the gene encoding NFATc1 in mouse is located on chromosome 18. Both in mouse and human, the *Nfatc1* genes consist of 11 exons and span approximately 110 and 134 kb DNA, respectively¹⁷⁴. Due to the presence of two promoters, the inducible P1 (distal) and the constitutive P2 (proximal) promoter, two poly-A sites, pA1 and pA2, and alternative splicing events, several isoforms of the *Nfatc1* gene are generated (Figure 4.5). In our laboratory, Chuvpilo *et al.* identified and described six NFATc1 isoforms in T cells (Figure 4.5)^{175, 176}. Three isoforms are generated under the control of the P1 promoter, indicated as *Nfatc1αA*, *Nfatc1αB*, and *Nfatc1αC*, and the other three are directed by the P2 promoter, *Nfatc1βA*, *Nfatc1βB*, and *Nfatc1βC*^{174, 177}. The α and β forms differ from each other by the presence of the α- or β-peptide, respectively. The 42aa α-peptide is coded by exon 1, the 27aa β-peptide by exon 2.

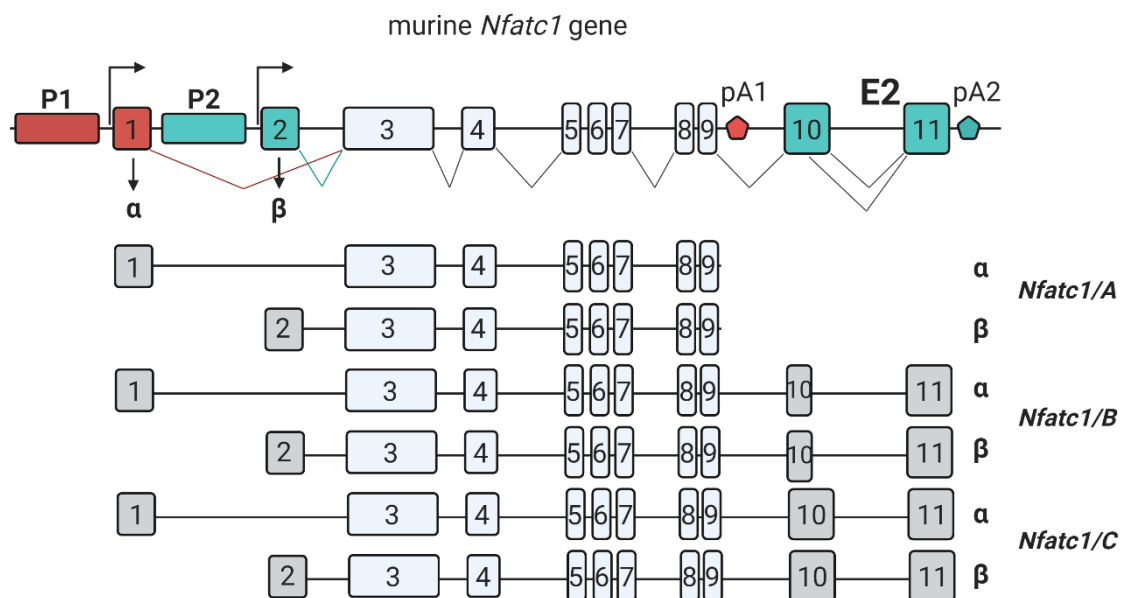


Figure 4.5 Structure of the murine *Nfatc1* gene.

Due to the usage of the two promoters, P1 and P2, two polyA sites, pA1 and pA2, and alternative splicing events, six isoforms are generated in lymphocytes. The isoforms *Nfatc1/αA*, *αB*, and *αC* are generated by the usage of the P1 promoter. The transcription of the other isoforms, *Nfatc1/βA*, *βB*, and *βC* is directed by the promoter P2. The α-forms contain the so-called α-peptide, expressed by exon1, and the β-forms harbor the β-peptide, expressed by exon 2.

NFATc1/A is the shortest isoform and lacks the long C-terminal transactivation domain that is characteristic for NFATc1/B and NFATc1/C and conserved between NFATc1 and NFATc2 proteins.

The transcription of the short isoform NFATc1/αA is strongly regulated by the activity of the Enhancer 2 (E2), located within the intron 10, in combination with the P1 promoter.

Picture was generated with Biorender.com and adapted from Rudolf R. *et al.*, *Frontiers in immunology*, 2014 and Serfling E. *et al.*, *Cell Communication and Signaling*, 2012.

Conventional inactivation of the *Nfatc1* gene causes embryonic death, due to a defect in the development of cardiac valve and septa. In the periphery, this inactivation induces a defect in lymphocyte proliferation^{150, 178}. *Nfatc1* has been shown to control Th1 and Th2 generation and proliferation, cell cycle, and immune response after cell stimulation via the activation of the transcription of genes, such as the *Il2* and *Ifng* genes, and many of other genes^{155, 156}. NFATc1 is involved in the activation of genes associated with cell cycle progression, such as genes encoding cyclin A2, D3, c-myc, and also with the cell cycle inhibitors p21 and p15. In addition, NFATc1, differently from NFATc2, acts as an anti-apoptotic factor, inducing the expression of *Bcl2* and other *Bcl2* family members^{5, 179}.

Among all the isoforms, the transcription of the inducible isoform *Nfatc1αA* is directed by the P1 promoter and terminates at the pA1 site, located downstream of exon 9 (Figure 4.5). The transcription of the two longer isoforms, *Nfatc1B* and *Nfatc1C*, is controlled by both the P1 and P2 promoters, but it ends at the pA2 site, downstream of exon 11 (Figure 4.5). In naïve and resting effector T cells, the P2 promoter controls the constitutive transcription of the *Nfatc1* gene, generating the β-isoforms of long NFATc1/βB and NFATc1/βC.

Primary stimulation of the TCR complex promotes the differentiation and proliferation of Th1 and Th2 cells. During this phase, the activity of the P2 promoter is suppressed, and the P1 promoter becomes active and starts to transcribe the short, inducible isoform NFATc1/αA (of 716aa residues).

The activity of P1 and the transcription of the inducible isoform NFATc1/αA is autoregulated by the binding of NFAT proteins within the P1 promoter that contains NFAT binding sites as well as binding sites for other factors, such as NF-κB, CREB, Fos, ATF proteins, SP1, and SP3 factors^{174, 177}. The enhancer 2 (E2), located within intron 10 of the *Nfatc1* locus, is another important regulatory element that contributes to the full transcriptional activity of the P1 promoter (Figure 4.5). It has been shown in luciferase reporter experiments that the combination of P1 and E2 enhances the expression of NFATc1/αA 10 fold, compared to the combination of other regulatory elements⁵. Furthermore, the E2 region of the *Nfatc1* gene along the locus shows the typical signs of an enhancer, i.e. DNase I hypersensitive chromatin sites, H3K4me3 marks, and further modifications that indicate its transcriptional activity¹⁷⁴. The short isoform, acting in an autocrine loop of regulation, keeps the P1 activity and the transcription of itself and genes involved in the immune response. Without further stimulation, the P1 promoter activity is suppressed again. Upon the secondary stimulation, Th1 and Th2 cells are rapidly activated and start to produce NFATc1/αA directed by promoter P1 activity^{177, 180, 181}. During an immune response, NFATc1/αA appears to be the main isoform in supporting the proliferation of activated T cells in the periphery. Differently from the other isoforms, NFATc1/αA possesses a shorter C-terminal peptide, therefore it lacks a second transactivation domain (TAD-B, in Figure 4.4). The lack of TAD-B changes the potential

collaboration with other transcription factors, thus, the functions of the different NFATc1 isoforms. The C-terminal of the long isoform NFATc1/C is a target for SUMOylation. This post-translational modification converts NFATc1 into an *I/2* gene suppressor¹⁸².

NFATc1/ α A also protects lymphocytes from the Activation Induced Cell Death (AICD)¹⁷⁷.

4.6.1.1 NFATc1 in T cell development

While the role of NFATc1 in peripheral T cell function and differentiation has been well established, little attention was paid to the role of NFATc1 during thymocyte development. It has been previously observed that the DN population bears a strong basal expression of NFATc1, compared to DP and SP populations. Among the DN populations, the pre-TCR negative population of DN3 thymocytes showed the highest NFATc1 expression level¹⁸⁰.

For all other members of the NFAT transcription factor family, the importance of NFATc1 in thymocyte development is reflected in the studies of ko mouse models. Indeed, in *Nfatc2*^{-/-}, *Nfatc3*^{-/-} or *Nfatc2*^{-/-}*Nfatc3*^{-/-} mice, the development of DN thymocytes is normal, which suggests that NFATc1 can compensate for this lack^{153, 154}. However, in the *VavCre-Nfatc1*^{fl/fl} mouse model analyzed by Patra *et al.*, the hematopoietic deficiency of *Nfatc1* induced a significant decrease of thymic cellularity, together with a decrease in the thymic size, and a developmental block at the DN1 stage⁴.

The essential role of IL-7/IL-7R signaling during thymocyte development is well established¹⁸³. IL-7 signaling is essential during the earliest phases of thymocyte development and for supporting the cells during β -selection. Mice deficient in IL-7 or IL-7R α (the alpha chain of the IL-7 receptor) have a very small thymus and a block of T cell development during DN1 cell differentiation into DN2^{184, 185}. Patra *et al.* showed that during thymocyte development the activation of NFATc1 occurs via a calcineurin-independent alternative pathway. In DN thymocytes, the IL-7–Jak3 signals activated the transcription factor NFATc1 by phosphorylating the Tyr 371 residue in the regulatory region of NFATc1. Moreover, in response to IL7 signals, NFATc1, in cooperation with STAT5, induced the upregulation of the anti-apoptotic gene *Bcl2*⁴.

In pre-TCR negative thymocytes, the only *Nfatc1* promoter activity detected was the P2 promoter activity and, therefore, the *Nfatc1* β -forms are the only *Nfatc1* isoforms that are expressed at that stage. The pre-TCR signaling leads to the induction of P1 promoter activity, the transcription of the inducible α -*Nfatc1* isoforms, and the autoregulation of the P1 promoter activity by the short inducible NFATc1/ α A isoform.

Nevertheless, *Nfatc1* over-expression, as induced in the *VavCre-R26-caNfatc1aA-Stop*^{fl/fl} and in Δ Cam mouse models, caused a decrease in thymic cellularity, a reduction in thymus size, a stop in thymocyte development during the DN3 stage, and a reduction of cellular plasticity.

This block in thymocyte development might be due to a less rearrangement of the β chain and, therefore, a defect in pre-TCR formation^{5, 186}.

4.7 Aim of the study and outcome

The present research aims to understand the role of NFATc1 during thymocyte development at the molecular level, particularly during the early stages of T cell development. During the DN stages, several delicate and coordinated steps lead the early thymocytes to a proper differentiation and a phenotypical fate.

Previous studies have demonstrated the importance of a certain level of NFATc1 expression during thymocyte development. Improper expression and activity of NFATc1 could have detrimental effects on T cell development in the thymus.

One of the first objectives of this research is the identification of genes, essential for thymocyte development in the thymus, which are the direct target of NFATc1-mediated regulation. This first goal is achieved through ChIP-seq and RNA-seq assays, by the use of the newly generated mouse model *Nfatc1/A-Bio.BirA*, optimized for more specific chromatin precipitation and purification.

The aberrant expression of NFATc1 in different mouse models, such as *Rag1Cre-Nfatc1^{fl/fl}* (*Nfatc1* conditional gene ko), and Δ Cam (NFATc1 over-activation) aims to confirm the misregulation of these target genes, in gene expression assays, such as real-time assays. Besides, FACS analysis confirms that in NFATc1-deficient mice, an increase of $\gamma\delta$ T cells occurs, suggesting a role for NFATc1 in controlling the thymocyte choice between $\alpha\beta$ and $\gamma\delta$ lineage.

Furthermore, similar observations emerge also from the *Rag1Cre-E2^{fl/fl}* mouse model, in which the regulatory element, Enhancer 2 (E2) is depleted, leading to a specific ablation of the NFATc1/ α inducible isoforms.

These findings have significant implications for the understanding of the role of NFATc1 in the thymocyte lineage fate and suggest the importance of the optimal expression of NFATc1 for a normal $\alpha\beta$ T cell development.

5 Materials and Methods

5.1 Materials

5.2 Chemicals and reagents

Reagent	Company
KCl	Roth
Na ₂ HPO ₄	Roth
NaOH	Roth
CaCl ₂	Roth
HCl	Roth
LiCl	Roth
NaCl	Roth
MgCl ₂	Roth
Ethanol	Roth
Isopropanol	Roth
Methanol	Roth
Agarose	Roth
Tris-HCl	Roth
Acetic Acid	Roth
6x DNA Loading Dye	Thermo Fisher Scientific
Midori Green	Nippon Genetics
GeneRuler 1kb and 100bp	Thermo Fisher Scientific
Ethylenediaminetetraacetic acid (EDTA)	Roth
NP-40	Roth
Dimethyl-sulfoxide (DMSO)	Roth, Gibco
Sodium Deoxycholate	Roth
β-Mercaptoethanol	Roth
Phenylmethylsulfonyl Fluoride (PMSF)	Roth
Sephadex G50	Sigma-Aldrich
Bradford Reagent	Bio Rad
Pierce™ ECL Western Blotting Substrate	Thermo Fisher Scientific
Acrylamide	Roth
Ammonium Persulfate (APS)	Roth
Tetramethylethylenediamine (TEMED)	Roth

Tween-20	Roth
Sodium Lauryl Sulfate (SDS)	Roth
Glycine	Roth
Non-fat Dried Milk Powder	Roth
Ponceau S	Sigma-Aldrich
Bromophenol Blue	Sigma-Aldrich
Agar	Roth
LB Medium	Roth
Ampicillin	Roth
Formaldehyde 37%	Roth
Trypan Blue Solution	Sigma-Aldrich
Triton-X 100	Roth
Polyethyleneimine (PEI)	Sigma-Aldrich
TurboFect TransfectionReagent™	Thermo Fisher Scientific
Bovine Serum Albumin (BSA)	Miltenyi Biotech
SYBR Green 2X	Thermo Fisher Scientific
Glycerol	Roth
1,4-Dithiothreitol (DTT)	Sigma-Aldrich

dH₂O was taken from the “Biocel MilliQ system” (Millipore).

5.2.1 Consumables

Item	Company
Centrifuge tubes 15ml and 50ml	GBO
Centrifuge tubes 1,5ml	Sarstedt
Safe-Lock centrifuge tube 1,5ml	Eppendorf
Pipette tips/Filtered pipette tips 1000µl, 200µl, 100µl, 10µl	Sarstedt
Pasteur glass pipettes	Scheller
PCR strips of 8 tubes and domed caps	Scheller
Cuvettes (quarz)	Hellma
Cuvettes (plastic)	Braun
Cell separation LD columns	Miltenyi Biotech
Cell separation MS columns	Miltenyi Biotech
Cell Strainer 70µm Nylon filter	Falcon

Cryo tubes 2ml	Greiner
Petri dishes 10cm diameter	GBO
Serological pipettes 5ml, 10ml, 25ml	GBO
Sterile filter 0,2 µm and 0,45µm	ROTH
Syringes 1ml, 5ml, 10ml	Omnifix-F, Braun
Syringe needles 21Gx1 ½”	Neobject®
Well-plates 6, 12, 24, 48-well	GBO
Cell culture dishes 6cm	GBO
Cell culture dishes 10cm	GBO
Cell culture flasks 75cm ²	GBO
5ml Polystyrene round-bottom tubes	Falcon
96 Well cell culture plates V-bottom	Cellstar
LightCycler®v480 multiwell plate 96	Roche
Forceps and scissors for the preparation of mice organs	Hartenstein
Parafilm	Pechiney Plastic Packaging

5.2.2 Instruments

Machine	Company
Autoclave systec DX-45	Systec
Autoclave systec V-75	Systec
Ice machine Scotsmen AF100	Genheimer
BD FACSCANTO™ II	BD
Fusion SL	Vilbert Lourmat
Gel Doc™ XR+	BioRad
Electrophoresis chamber	PeqLab
Electrophoresis power supply	Micro-Bio-Tec-Brand
Real-time PCR machine	Roche
Centrifuge J2-HS & J221	Beckman
Balance FCB	Kern
Fridges 4 °C	Liebherr, Siemens, BOSH
Freezer -20 °C	Liebherr, Siemens, BOSH
Freezer -70 °C	Liebherr, Siemens

Centrifuge 5420	Eppendorf
Centrifuge 5418	Eppendorf
Centrifuge 5415	Eppendorf
Centrifuge Rotina 420R	Hettich Laborapparate
Varifuge 3.0 R	Heraeus Sepatech
Biofuge 15R	Heraeus Sepatech
LUMIstar Omega	BMG labtech
Tank Blotting	Biometra
Power PAC 200	BioRad
Electrophoresis power supply 3000 Xi	BioRad
Heating block	Liebisch
Incubator Hera Cell	Heraeus Sepatech
Vortex mixer	Hartenstein
Shaker	Hartenstein
Light microscope CK2	Olympus
Ph meter	WTW
GeneQuant pro	Amersham Biosciences
Photometer nanodrop	PeqLab
Sterile work bench	kötterman
UV Stratalinker™ 1800	Stratagene
SimpliAmp thermocycler	Thermo Fisher Scientific
Waterbath 1083	GFL
Bachofer	Edelstahl
Rotary mixer	Hartenstein
Rotary mixer 4°C	Hartenstein
Vibra Cell	SONICS
Incubator shaker	Innova®43
Platform mixer	Ratek
Laminar Flow Biological Hood	BIOHAZARD

5.2.3 Buffers

Buffers	Components	Concentration/Quantity
TAE 50X	Tris HCl Acetic Acid	242g 57,1ml

	0,5M EDTA pH 8.0	100ml
	dH ₂ O	up to 1l
RIPA Buffer	Tris HCl, pH 7.5	50mM
	NaCl	150mM
	Triton-X 100	1%
	Na-deoxychololat	1%
	SDS	0,1%
	EDTA, pH 8.0	1mM
PAGE Running Buffer 10X	Tris HCl, pH 8.5	25mM
	Glycine	192mM
	SDS	0,1%
Tris Buffered Saline-0,5%	Tris HCl, pH 7.5	25mM
Tween (TBS-T)	Glycine	150mM
	Tween-20	0,05%
4X Laemmli Buffer	1M Tris HCl, pH 6.8	250mM
	SDS	5%
	Glycerol	40%
	Bromophenol blue	0,005%
	β-mercaptoethanol	10%
PAGE Transfer Buffer 10X	Tris HCl, pH 8.5	25 mM
	glycine	192 mM
	methanol	10%
Lysis Buffer	Tris pH 7,9	50mM
	EDTA pH 8	10mM
	SDS	1%
IP Buffer	Tris pH 7.9	30mM
	EDTA pH 8	2mM
	NaCl	165mM
	SDS	0,3%
	Triton X-100	1%
1 st Wash for ChIP	SDS	2%
2 nd Wash for ChIP	Tris pH 7,9	10mM
	EDTA pH 8	1mM
	LiCl	250mM
	NP-40	1%
	Sodium deoxycholate	1%
3 rd Wash for ChIP	Tris pH 7,9	20mM
	EDTA pH 8	1mM
	NaCl	50mM
	SDS	0,1%
Elution Buffer	Tris HCl pH 7,9	10mM
	EDTA pH 8	5mM
	SDS	1%
	NaCl	300mM
MACS Buffer	NaCl pH 7.4	137mM
	Na ₂ HPO ₄	10mM
	KCl	2,6mM

	KH ₂ PO ₄	1,8mM
	BSA	0,5% (w/v)
	NaN ₃	0,1% (w/v)
	EDTA	2 mM
FACS Buffer	NaCl pH 7,4	137 mM
	Na ₂ HPO ₄	10 mM
	KCl	2,6 mM
	KH ₂ PO ₄	1,8 mM
	BSA	0,1 % (w/v)
	NaN ₃	0,1 % (w/v)
Blocking Buffer	BSA	5g
	GCWSF	5g
	Triton-X 100	1,5ml
	PBS	500ml
TE Buffer	EDTA 0.5 M, pH 8.0	1mM
	Tris-Cl 1 M, pH 8.0	10mM
	dH ₂ O	Up to volume

5.2.4 Kits

Item	Company
ChIP DNA Clean & Concentration	ZYMO RESEARCH
RNeasy® Plus Mini kit (50)	QIAGEN
CD4 (L3T4) MicroBeads + LD columns	Miltenyi Biotech
CD8a (Ly-2) MicroBeads + LD Columns	Miltenyi Biotech
TCRγ/δ ⁺ T Cell Isolation kit + MS Columns	Miltenyi Biotech
First Strand cDNA Synthesis kit	Thermo Fisher Scientific
SuperScript® IV Reverse Transcriptase	Invitrogen® Thermo Fisher Scientific
Superscript™ IV VILO	Invitrogen® Thermo Fisher Scientific
Extracta® DNA Prep for PCR and AccuStart II	WWV
GelTrack PCR SuperMix	
DreamTaq Hot Start DNA Polymerase	Thermo Fisher Scientific
Q5® High-Fidelity 2X Master Mix	New England BioLab

5.2.5 Oligonucleotides

All the oligonucleotides were obtained from Sigma-Aldrich. Lyophilized primers were dissolved in an indicated amount of 10mM Tris HCl, pH 7.6, to reach a concentration of 100μM. The primer stock was diluted to a final concentration of 20μM with dH₂O.

5.2.5.1 Genotyping

Gene mouse name	Primers
<i>Nfatc1/A-Bio</i>	fw 5'-TGGGACTCGACTCTACCGAA-3' rev 5'-GTTTGAGCGCCACTCCATCT-3' fw 5'-TTTTACCAATTGGGCGGTGG-3' rev 5'-TCGGTAGAGTCGAGTCCCAG-3'
<i>BirA</i>	fw 5'-GTGTAAGTGTGGACAGAGGAG-3' rev WT 5'-GAACTTGATGTGTAGACCAGG-3' rev tg 5'-GCCAGCCAGAATTTATATGCAG-3'
Δ Cam	fw 5'-AGTATCGAATGTGTGCTGTA-3' rev 5'-TTGAATCGGTCTAATTTTCTGATGT-3'
<i>Rag1-Cre</i>	fw 5'-ATGGTGCAAGTTGAATAACC-3' rev 5'-TTATAAGCAATCCCCAGAAA-3'
<i>Nfatc1^{fl/fl}</i>	fw 5'- AACATTTGGCCTGCTTGATAGAG-3' rev 5'-CAACAGAAGCCAGCTTTCACAG-3'
<i>Nfatc1 E2^{fl/fl}</i>	fw 5'-G TTCAGAGGCCGAGCTAGAG-3' rev 5'-TTTCAGGTGCCCAAGAGAGC-3'
<i>Nfatc1Ex3-Gfp</i>	fw 5'-GGAGGTAAGTCAAGCTATTGGGT-3' rev 5'-TGTGGCCGTTTACGTCG-3'

5.2.5.2 ChIP

Target	Primers
NFATc1 Enhancer 2	fw 5'-CCACTTTCTTTTCCATGAGGTC-3' rev 5'-ACCTGCAGTTCAAAACACCTCT-3'
NFATc1 +7.5kb	fw 5'-GCCCTGTAAAATACGCCTCAAT-3' Rev 5'-CCTCAAGCCTTCCTTCCCTATT -3'

5.2.5.3 Real-time PCR

Gene	Primers
<i>Actb</i>	fw 5'-TGTCCACCTTCCAGCAGATGT-3' rev 5'-AGCTCAGTAACAGTCCGCCTAG-3'
<i>Nfatc1 E1-E3</i>	fw 5'-GGGAGCGGAGAACTTTGC-3' rev 5'-CAGGGTTCGAGGTGACACTAGG-3'
<i>Nfatc1 E2-E3</i>	fw 5'-AGGACCCGGAGTTCGACTTC-3' rev 5'-GCAGGGTTCGAGGTGACACTAGG-3'

<i>Bcl2</i>	fw 5'-GGCGCCCCTGGGGGCTGCCC-3' rev 5'-ACCTGCAGTTCAAAACACCTCT-3'
<i>Bcl2a1a</i>	fw 5'-GATACGGCAGAATGGAGGTT-3' rev 5'-GAAAGAGCATTTCACAGATC -3'
<i>Bcl2a1b</i>	fw 5'-GTATGTGCTACAGGTACCCG-3' rev 5'-AGATTCTTTTCAACTTCCTTC-3'
<i>Bcl2a1d</i>	fw 5'-TACGAGTTCATGTATATCCA-3' rev 5'-ATTATTCTGGCGGTATCTAT-3'
<i>Tcf7</i>	fw 5'-GGCAGCATCCGCAGCCTCAA-3' rev 5'-CAGTGGGGGCAGGGAAGTGC-3'
<i>Ccr9</i>	fw 5'-CAATCTGGGATGAGCCTAAACAAC -3' rev 5'-ACCAAAAACCAACTGCTGCG-3'
<i>1810009J06Rik</i>	fw 5'-CTCTCCCAGCTAACAGTGAT-3' rev 5'-TCAATTTAATCAGCATGATG-3'
<i>Gm2663</i>	fw 5'-TCAATGATCAGTGGGTACTG-3' rev 5'-ACTGTGGATACTTGGGAGTT-3'
<i>Cd24a</i>	fw 5'-CTTCTGGCACTGCTCCTACC-3' rev 5'-AACAGCCAATTTCGAGGTGGAC-3'
<i>Tcrg</i>	fw 5'-AGCTATACATTGGTACCGGC-3' rev 5'-TTTTTTGTTCTTCCCTCCTA-3'
<i>Egr2</i>	fw 5'-CTACCCGGTGGGAAGACCTC-3' rev 5'-AATGTTGATCATGCCATCTCC-3'
<i>Egr3</i>	fw 5'-TGCCCCAACCGCCGCTTACTCTC-3' rev 5'-GGCGCACCCCCTTTCTCCGACTT-3'
<i>Sox13</i>	fw 5'-CGGAACAGCAGCCACATCAAGAGA-3' rev 5'-ATGGTGTAGCTTTGGCGAGCAC -3'
<i>Nr4a1</i>	fw 5'-TGTGAGGGCTGCAAGGGCTTC-3' rev 5'-AAGCGGCAGAACTGGCAGCGG-3'
<i>Nr4a3</i>	fw 5'-AGGGCTTCTTCAAGAGAACGG-3' rev 5'-CCATCCCGACACTGAGACAC-3'

5.2.6 Cells

Primary murine total thymocytes

Isolated thymocyte subpopulations (DN, DP, and SP, $\gamma\delta$ T cells)

5.2.6.1 Media and cell culture supplements

β-Mercaptoethanol

BSS/BSA

PBS/BSA

Dulbecco's Modified Eagle Medium,
(DMEM)

RPMI 1640

Fetal Bovine Serum

L-Glutamine

Penicillin/Streptomycin

Sodium pyruvate

All media and cell culture supplements were supplied by GIBCO, except BSS/BSA which we received from the Institute of Virology and Immunobiology, University of Würzburg.

5.2.6.2 Ligands and chemicals for cell stimulation

Reagent	Company
12-O-Tetradecanoylphorbol-13-acetate (TPA)	Merck
Ionomycin	Invitrogen®Thermo Fisher Scientific
Cyclosporin A (CsA)	Calbiochem
Recombinant human IL-7	Peprotech

5.2.7 Antibodies and conjugates

5.2.7.1 ChIP

Streptavidin Dynabeads M-280, Thermo Fisher Scientific

5.2.7.2 Antibody-conjugates for flow cytometry

*Antibody-Conjugated	Clone	Supplier	Dilution
Anti-CD16/anti-CD32	93	Biologend	1:200
Anti-CD4-Pacific Blue	GK1.5	Biologend	1:300
Anti-CD8-Amcyan	53-6.7	Biologend	1:300
Anti-CD8-APC/Cy7			
Anti-CD8-APC			

Anti-CD3-APC	145-2C11	Biolegend	1:300
Anti-CD3-PE			
Anti-CD25- APC/Cy7	PC61	Biolegend	1:300
Anti-CD25-APC			
Anti-CD25-PE			
Anti-CD44-APC	IM7	Biolegend	1:300
Anti-CD44-PE/Cy7			
Anti-CD44-FITC			
Anti-TCR $\gamma\delta$ -FITC	GL3	Biolegend	1:100
Anti-TCR $\gamma\delta$ -PE/Cy7			
Anti-TCR $\gamma\delta$ -biotin	GL3	Biolegend	1:100
Anti-TCR β -PE	H57-597	Biolegend	1:100
Anti-TCR β -PerCP			
Anti-CD24	M1/69	Biolegend	1:300
Zombie Aqua™	-	Biolegend	1:1000
Zombie NIR™			

*anti-mouse Antibodies

5.2.7.3 Primary and Secondary Antibodies for Western Blots

Antibody	Clone	Supplier	Dilution
Anti- β Actin	BA3R	Invitrogen®Thermo Fisher Scientific	1:2000
Streptavidin-Peroxidase Polymer-Ultrasensitive	-	Sigma-Aldrich	1:1000
Anti-NFATc1	7A6	BD Pharmigen™	1:000
Goat anti-mouse IgG HRP		Invitrogen®Thermo Fisher Scientific	1:20000
Goat anti-rabbit IgG HRP		Invitrogen®Thermo Fisher Scientific	1:20000

5.2.8 Data analysis software and online tools

Software	Website
Galaxy ¹⁸⁷	https://usegalaxy.org/
MACS2 ^{188, 189}	

GREAT 3.0.0 ¹⁹⁰	http://great.stanford.edu/public/html/
Integrative Genome Viewer (IGV)	http://www.broadinstitute.org/software/igv/download
NCBI GEO DataSets	http://www.ncbi.nlm.nih.gov/gds
NCBI Primer-Blast	http://www.ncbi.nlm.nih.gov/tools/primer-blast/
Reverse Complement	http://www.bioinformatics.org/sms/rev_comp.html
FANTOM5_SSTAR	http://fantom.gsc.riken.jp/5/sstar/Main_Page
e!Ensembl	http://www.ensembl.org/index.html
GORilla ^{191, 192}	http://cbl-gorilla.cs.technion.ac.il/
VISTA Gateway	http://pipeline.lbl.gov/cgi-bin/gateway2
Morpheus-Broad Institute	https://software.broadinstitute.org/morpheus/
Biorender	https://app.biorender.com/
HOMER ¹⁹³	http://homer.ucsd.edu/homer/motif/
BD FACSDiva 5.0 (BD)	
FlowJo™ 10 software	
Citavi 6.4	
Endnote X9.3.2	
GraphPad Prism 5	
ImageJ	
Microsoft®Word for Microsoft	
Microsoft®Excel for Microsoft	
Microsoft®PowerPoint for Microsoft	
R software	
DESeq	
Venn Diagram Plotter	

5.2.9 Mice

The mice investigated in this thesis were bred and kept in the “Zentrum für Experimentelle Molekulare Medizin” (ZEMM) of the University of Würzburg following the guidelines of the German Animal Welfare Laws for Experimental Animals.

The mice had ad libitum access to water and standard rodent chow.

Genotyping was performed regularly with the tail or the ear biopsies collected at 4th week after birth.

All the animals used in this project were at C57B/6 background and were used at 4 weeks of age unless mentioned otherwise. Siblings animals of both genders were used throughout.

The following genetically modified mice lines were used:

Designated Line	Line according to reference	Reference
B6. <i>Nfatc1/A-Bio.BirA</i>	<i>Nfatc1/A-Bio.BirA</i> tg	Klein-Hessling <i>et al.</i> , 2017
Calcineurin tg B6.ΔCam	ΔCam tg	Patra <i>et al.</i> , 2006
B6. <i>Rag1Cre-Nfatc1^{fl/fl}</i>	<i>Rag1^{tm1(cre)Thr}</i>	McCormack MP <i>et al.</i> , 2003
	B6(Cg)- <i>Nfatc1^{tm3Glm/AoaJ}</i>	Aliprantis AO, <i>et al.</i> , 2008
B6. <i>Rag1Cre-E2^{fl/fl}</i>	<i>Rag1Cre-E2^{fl/fl}</i>	Established in our lab
B6. <i>Nfatc1-eGfp-Bac</i>	C57/BL/6 tg <i>Nfatc1-Egfp</i>	Hock <i>et al.</i> , 2013

5.3 Methods

5.3.1 Generation of transgenic mice lines

The generation of B6. *Nfatc1/A-Bio BirA* mice has been described previously¹⁵⁵.

The truncated murine CN-A mutant (ΔCam) construct was described previously¹⁹⁴ and provided by R. Kincaid (Department of Pharmacology, Pennsylvania State University College of Medicine, Hershey, PA). The ΔCam mice line was generated in our laboratory as described previously^{5, 194}.

Double mutants of *Rag1Cre-Nfatc1^{fl/fl}* and *Rag1Cre-E2^{fl/fl}* mice were generated by breeding the mice with loxP-flanked exon 3 of *Nfatc1* alleles (*Nfatc1^{fl/fl}* mice) or mice with loxP-flanked *Nfatc1*-Enhancer 2 (*E2^{fl/fl}* mice) with mice that express Cre recombinase under the control of the *Rag1* gene expression (*Rag1Cre* mice).

The *Nfatc1-eGfp-Bac* mouse model has been described previously¹⁸⁰.

5.3.1.1 Genotyping and Polymerase Chain Reaction (PCR)

The genomic DNA of mice was extracted from 3mm ear or tail biopsies using Extracta® DNA Prep for PCR according to the manufacturer's instructions. Briefly, biopsies were incubated for 40min, at 95°C with 50μl of extraction buffer. Afterward, samples were cooled down and 50μl of stabilization buffer was added. Samples were stored at 4°C or immediately used for PCR reactions. PCR reactions were performed using AccuStart II GelTrack PCR SuperMix, DreamTaq PCR Polymerase, or Q5 High-Fidelity DNA Polymerase, according to the expected genotype of mice.

The oligonucleotides used as primers for PCR amplification are indicated in the section "Oligonucleotides, Genotyping" 5.2.5.1.

PCR cycle programs were optimized according to the mouse line.

The general cycle program is as following:

- initial denaturation 95°C for 3min,
- denaturation 98°C for 15sec,
- annealing (variable) 57°- 62°C for 30sec,
- elongation 72°C for 40-45sec,
- final elongation 72°C for 5min,
- incubation 4°C

x 35-38 cycles (steps 2-4)

AccuStart II GelTrack PCR SuperMix	22.5µl final volume/each sample
AccuStart Mastermix	12.5µl
20µM forward primer	2µl
20µM reverse primer	2µl
dH ₂ O	up to volume
Genomic DNA	2.5µl

DreamTaq PCR Polymerase mix	50µl final volume/each sample
10X DreamTaq buffer	5µl
10mM dNTPs	1µl
20µM forward primer	0.5µl
20µM reverse primer	0.5µl
25mM Mg ²⁺	2µl
5U/µl DreamTaq Pol	0.3µl
dH ₂ O	up to volume
Genomic DNA	2µl

Q5 High- Fidelity DNA Polymerase mix	20µl final volume/each sample
5X Q5 Reaction Buffer	4µl
10 mM dNTPs	0.5µl
20µM forward primer	0.5µl
20µM reverse primer	0.5µl
25mM Mg ²⁺	1.7µl
Q5 High-Fidelity DNA Polymerase	0.2µl
dH ₂ O	Up to volume

Genomic DNA

2 μ l

5.3.1.2 Gel electrophoresis of DNA

The amplicons of PCR reactions were run in agarose gels. The optimal percentage of the agarose matrix depends on the size of the DNA. For DNA fragments \geq 1kb, 1% agarose gels, and for fragments \leq 500bp, 2% agarose gels were used. The agarose powder was dissolved in 1X TAE buffer, and 3 μ l/100ml (of gel) Midori Green was added to the gel to visualize the DNA under UV-light. DNA molecules were separated according to their size in an electric field, in a proper electrophoretic chamber.

The size of the amplified DNA bands was estimated by adding Gene ruler marker DNA in one of the gel lanes. The Gels were visualized using the Gel DocTM XR⁺ system.

5.3.2 Cell culture

5.3.2.1 Cell counting

Cell counting was performed using the Trypan blue staining method. Trypan blue stains dead cells whilst leaving viable cells unstained. A 1:10 or 1:20 dilution of the cell suspension was prepared in Trypan blue. 10 μ l of the cell dilution was used for counting using a hemocytometer. Cell number was calculated following the formula; $n \times \text{dilution factor} \times 10^4$ cells/ml, where n is the number of cells counted in the hemocytometer.

5.3.2.2 Cell culture media

Cells were cultured at 37 °C and 5% of CO₂ in an incubator.

Primary murine cells were cultured in a complete RPMI (cRPMI) medium supplemented with 10% FBS.

RPMI supplemented with

10% FBS (v/v)

2mM L-glutamine

1mM Sodium pyruvate

0,5% Penicillin/Streptomycin (v/v)

0,1mM 2-mercaptoethanol

MEM non-essential amino-acids

5.3.2.3 Preparation of single-cell suspension of murine thymocytes

Mice were sacrificed by euthanasia with inhalation of CO₂ in a proper chamber.

Thymi were collected and immediately placed on a petri dish containing 5ml of BSA/BSS solution.

Subsequently, thymi were mashed through a 70 μ m cell strainer placed in a petri dish containing 5ml of BSA/BSS to prepare a single-cell suspension.

Cells were centrifuged at 1500rpm for 5min at 4°C and washed twice with cold BSA/BSS. The supernatant was discarded and the cells were resuspended in cRPMI medium and counted as described previously. A 4 to 12 weeks young thymus contains $>1 \times 10^8$ thymocytes on average.

5.3.2.4 Isolation of DN, DP thymocytes, and $\gamma\delta$ T Cells

For isolation of DN or DP cells, single-cell suspensions of thymocytes were generated as previously described (section 5.3.2.3). DN thymocyte selection was carried out using MACS magnetic separation with anti-CD4 (L3T4) and anti-CD8 (Ly-2) microbeads from Miltenyi Biotec according to the manufacturer's protocol. In brief, total thymocytes were counted, 10^8 total cells were centrifuged at 1500rpm for 5min at 4°C and resuspended in 900 μ l of MACS buffer. 100 μ l of anti-CD4 and anti-CD8 microbeads were added to the cell suspension and mixed well. Thymocyte suspensions were incubated with the Microbeads for 10min at 4°C and afterward loaded onto LD columns that were pre-washed with 2ml of MACS buffer.

DN thymocytes were isolated applying a "negative selection" strategy: CD8⁺ and CD4⁺ SP cells and CD4⁺CD8⁺ DP cells were retained into the column matrix, whereas DN thymocytes were collected as the flow-through.

A "positive selection" strategy was applied for DP and SP cell enrichment. DP and SP thymocytes were flushed out from the column matrix using 3ml of MACS buffer.

$\gamma\delta$ thymocytes were isolated using the TCR $\gamma\delta$ ⁺ T Cell Isolation Kit, from Miltenyi Biotec according to the manufacturer's protocol. In brief, a sequential cell isolation system was carried out: in the first step, a mixture of anti-CD11b and anti-CD45R (B220) micro beads was added to the cell suspension for the depletion of non-T cells. In addition, this mixture contained anti-TCR $\gamma\delta$ T cells-biotin microbeads for the labeling of $\gamma\delta$ T cells. Subsequently, anti-biotin microbeads were added to the isolated T cell suspension for the positive selection of TCR $\gamma\delta$ T cells. In the end, the $\gamma\delta$ T cells retained in the column matrix were flushed out and collected.

5.3.2.5 Cultivation and stimulation of thymocytes

For cell stimulation, total thymocytes or isolated DN cells were resuspended in a complete RPMI-1640 medium supplemented with 10% FBS. The thymocytes were cultured at a final concentration of $3-5 \times 10^6$ /ml in 6- or 12-well plates and were stimulated for 4h in the presence of 12-O-tetradecanoylphorbol-13-acetate (TPA; 100ng/ml) and ionomycin calcium salt (I;

100ng/ml). For the inhibition of NFATc1 activity, the immunosuppressant cyclosporin A (CsA) (100ng/ml) was also added to the medium.

Both the stimulated and unstimulated control cells were incubated at 37°C with 5% CO₂ saturation for 4h.

5.3.3 Molecular methods

5.3.3.1 Purification by affinity-based chromatin immunoprecipitation and sequencing (ChIP-seq)

Total thymocytes from control *BirA* or *Nfatc1/A-Bio.BirA* mice stimulated with TPA and ionomycin, and unstimulated *Nfatc1/A-Bio.BirA* thymocytes were used for purification affinity-based Chromatin Immunoprecipitation and sequencing (ChIP-seq) experiments. The system, in contrast to the standard chromatin immunoprecipitation assays, is a purification affinity-based ChIP. This system makes use of Streptavidin-coupled magnetic beads (Dynabeads M-280). The Streptavidin-coupled beads bind specifically NFATc1/A proteins expressed together with a biotin-tag in *Nfatc1/A-Bio.BirA* mice. *Nfatc1/A-Bio.BirA* express, additionally, an *E.coli* biotin ligase, which couples biotin molecules to the NFATc1/A-biotin-tag.

10⁷ total thymocytes were used for each ChIP assay. The cells were cultured in a cRPMI-1640 medium at the final concentration of 5x10⁶/ml, and left unstimulated or stimulated with TPA and I (each 100ng/ml) at 37°C, for 4h.

Afterward, thymocytes were collected, transferred into a new 15ml falcon tube, centrifuged at 1500rpm, for 5min, at 4°C, and then washed once with cold PBS. The thymocytes were fixed with the addition of formaldehyde at the final concentration of 1%, whirling the 15ml tube at RT for 10min. The fixation reaction was quenched with the addition of 125mM glycine keeping the tubes in rotation at RT for 5min.

Cells were washed twice with 10ml cold PBS and centrifuged at 1500rpm, for 5min, at 4°C. Aliquots of 10⁷ cells were transferred to an Eppendorf tube, and centrifuged at 9500rpm, for 5min, at 4°C.

The cell pellet was resuspended in 1% SDS-containing lysis buffer and serine protease inhibitor, PMSF at 1:100 dilution. The lysis of cells was further carried out by passing the thymocytes through a 21GA2 needle using a 1ml syringe for 10 times.

The cells were then left on ice for at least 30min.

To obtain chromosomal DNA fragments of length between 200-800 bp, sonication was performed for 10min at 35% of amplitude alternating 30sec of pulse and 30sec of pause, with a Vibra-Cell VCX 130 sonicator.

Chromatin fragments were collected by centrifugation at 14000rpm, for 15min, at 4°C.

Samples of chromatin in each sample were measured by spectrometry and the chromatin concentration was adjusted in all samples to the final volume of 520µl of lysis buffer, according to the formula $520x \frac{Abs\ sample}{Abs\ lowest\ sample}$.

10% or 20% input DNA was taken aside from previously generated fragmented chromatin and stored at -20°C for subsequent analyses.

100µl or 200µl of fragmented chromatin were mixed with 900µl or 800µl of IP buffer containing PMSF.

50µl of Streptavidin-coupled Dynabeads M-280 were washed with 900µl of IP buffer and 100µl of lysis buffer and placed on a roller shaker for 10min at RT.

The chromatin fragments were then incubated with the beads and kept on a roller shaker first, at RT for 4h and after, at +4°C o/n.

The beads were magnetically harvested and washed 2x with 1ml of IP buffer, and 2x with each of the 3 washing solutions (section 5.2.3).

To revert cross-links between proteins and chromatin fragments, the DNA fragment-bead complexes, in parallel with the input DNA, were incubated at 65°C, o/n, with 200µl of elution buffer supplemented with 200mM of NaCl.

For a complete deproteination and RNA depletion, proteinase K (20mg/ml for 1,5h at 42°C and RNase (10mg/ml for 1h at 37°C) treatments were performed.

DNA fragments were purified using the ChIP DNA Clean & Concentrator kit and were used for amplification of *Nfatc1* enhancer region as a positive control or “target”, and a region +7.5kb downstream of TSS of *Nfatc1* gene, as a negative control, or “no target”.

The protocol for Taq-Polymerase PCR assays was as follows:

Master Mix (per sample) 20µl

10mM NTPs	0,8µl
20µM forward primer	0,8µl
20µM reverse primer	0,8µl
H ₂ O	Up to volume
DNA	2µl

Enzyme Master Mix (per sample) 20µl

10x Taq polymerase Buffer	4µl
25mM MgCl ₂	3µl
Taq Polymerase	2U
H ₂ O	Up to volume

The initial denaturation of 95°C for 3min was followed by 35 cycles at 95°C, for 30sec, 55°C for 35sec, 72°C for 45sec. The final elongation step was for 5min at 72°C before cooling down to 4°C.

The primers used are indicated in section 5.2.5.2.

Experiments in triplicates were used for ChIP-seq analysis: 3ng of precipitated DNA from each sample was used for library preparation. The library was prepared using NEBNext® Ultra™ II DNA Library Prep Kit for Illumina® according to the manufacturer's protocol, with a final amplification of 13 cycles for the PCR enrichment reaction.

The quantity of library was assessed by Qubit 2.0, and the quality was determined on a Bioanalyzer 2100 using a high sensitivity DNA chip.

5.3.3.1.1 ChIP-seq analysis

The FASTQ files of the sequencing analysis were converted into BAM files with the software Galaxy. The raw reads were aligned with Galaxy software, using the function Map with Bowtie for Illumina (Galaxy Version 1.1.2). MACS2^{188, 189} package tool was used for the function "call peak". Call peak is the main function of the MACS2 package. MACS identifies enriched binding sites in ChIP-seq experiments. Based on the genome complexity, MACS2 evaluated the significance of enriched ChIP regions and improves the spatial resolution of binding sites by combining the information of both sequencing tag position and orientation. MACS2 generated an output file containing a list of peaks associated with a specific chromosomal region.

The 5000 top peaks (MACS2 assigned a score to each peak) were associated with nearby genes by using the software GREAT (Genomic Regions Enrichment of Annotations Tool)¹⁹⁰. GREAT defines the biological meaning of a set of non-coding genomic regions by analyzing the annotations of the nearby genes. GREAT can properly include also distal binding sites to genes, and false positives can be excluded by a binomial test over the input genomic regions.

5.3.3.2 RNA isolation from thymocytes and cDNA synthesis

RNA was extracted either from thymocytes cultured as previously reported or from freshly isolated thymocytes.

Thymocytes were washed once with 10ml of BSA/PBS and centrifuged at 1500rpm, for 5min, at 4°C. The supernatant was removed, and cells were transferred to a new Eppendorf tube (RNase-free plastic), washed again with PBS, and centrifuged at 9500rpm, for 5min, at 4°C. Cells were lysed in 350µl or 600µl of RLT buffer supplemented with β-mercaptoethanol (10µl/ml) from RNeasy Plus Mini Kit (QIAGEN) and homogenized by both vortexing and passing through a 21GA needle before freezing at -70°C. Further steps were proceeded according to the manufacturer's protocol. The RNA was eluted in 30µl of RNase-free water.

RNA concentration was measured using a Nanodrop spectrophotometer, and an RNA amount between 100ng and 2.5µg was used to generate cDNA.

Complementary DNA was generated using the Superscript™ IV VILO kit from Thermo Fisher Scientific combining 4µl of Superscript master mix, a specific amount of template RNA, and the provided water up to 20µl of total volume, for each sample. The cycle program was as follows:

- 25°C for 10min
- 50°C for 10min
- 85°C for 5min

The resulting cDNA was used immediately for real-time PCR or was stored at -20°C.

5.3.3.3 Real-time PCR (qRT-PCR)

Real-time PCR was performed to check the level of expression of indicated genes.

In real-time PCRs, the amount of amplified copies is quantified with a fluorescent dye, SYBR Green, which can intercalate into DNA.

The used PCR conditions were as follows:

Pre-incubation 95°C for 5min

amplification 95°C for 10sec, 60°C for 30sec, 72°C for 30sec

Melting-curve 95°C for 5sec, 65°C for 1min, 97°C continuous

Cooling 40°C for 10sec

The quantification cycle (Cq) values were used to calculate the fold induction of the amplified gene in comparison with a reference gene. All values were normalized against the housekeeping gene *Actb* (encoding β-actin), which was used as a control and indicator of cDNA quality.

According to the quality of cDNA, a dilution of 1:2, 1:3, or 1:5 of cDNA samples was used to run a real-time PCR.

A final volume of 18.5µl of the master mix was prepared for each sample as follows:

SYBR Green 2X	10µl
Forward Primers	0.4µl
Reverse Primers	0.4µl
H ₂ O	Up to volume
diluted cDNA	1.5µl

The master mix containing cDNA was loaded into the LightCycler® Multiwell Plate 96 and the real-time PCR reaction was performed in the real-time PCR machine.

The expression levels of the genes of interest were calculated as follows:

$$Cq_{\text{gene}} - Cq_{\beta\text{actin}} = \Delta Cq$$

$$\Delta Cq_{\text{gene}} - \Delta Cq_{\beta\text{actin}} = \Delta\Delta Cq_{\text{gene}}$$

$$2^{(-\Delta\Delta Cq_{\text{gene}})} = \text{Relative fold change gene}$$

5.3.3.4 Preparation of cDNA libraries and NGS-RNA-sequencing

For RNA-sequencing, total thymocytes from *BirA* tg or *Nfatc1-Bio.BirA* tg mice stimulated with TPA and ionomycin, and unstimulated thymocytes from the *Nfatc1-Bio.BirA* tg mice or isolated DN thymocytes from control *BirA* tg and *Nfatc1-Bio.BirA* tg mice either unstimulated or stimulated with TPA and ionomycin, all in triplicates, were used. The RNA was purified with the RNeasy Plus Micro kit from QIAGEN according to the manufacturer's protocol. The RNA was quantified with a Qubit 2.0 fluorometer from Invitrogen and the quality was assessed on a Bioanalyzer 2100 using an RNA 6000 Pico chip, both from Agilent.

For the cDNA library preparation, only samples with an RNA integrity number (RIN) of > 8 were used.

Barcoded mRNA-seq cDNA libraries were prepared from 50ng of total RNA using the NEBNext® Poly(A) mRNA Magnetic Isolation Module and NEBNext® Ultra™ II RNA Library Prep Kit for Illumina® according to the manual. The quantity was assessed using Invitrogen's Qubit HS assay Kit, and library size was determined using Agilent's 2100 Bioanalyzer HS DNA assay.

Barcoded RNA-Seq libraries were onboard clustered using HiSeq® Rapid SR Cluster Kit v2 using 8pM and 59bps were sequenced on the Illumina HiSeq2500 using HiSeq® Rapid SBS Kit v2 (59 Cycle). The raw output data of the HiSeq was pre-processed according to the Illumina standard protocol. Sequence reads were trimmed for adapter sequences and further processed using the software CLC Genomics Workbench (v11 with CLC's default settings for RNA-Seq analysis. Reads were aligned to the GRCm38 mouse genome.

For the DN RNA-seq analysis, the obtained FASTQ files were controlled for quality with FastQC and were aligned using STAR (version 2.7) to the GRCm38.98 reference genome using standard settings. The aligned data were counted using the feature Counts function of the R subread package in R (Version 1.2.5001). Differential expression analysis based on the raw count-matrix was performed using the DESeq2 algorithm. Significant differentially expressed genes were defined as having a p-value < 0.05 and log₂ fold change > 1 and log₂ fold change < -1.

All significant differentially expressed genes were visualized using the pHeatmap package in R <https://CRAN.R-project.org/package=pheatmap> .

5.3.3.5 Protein extraction and quantification

Cells were harvested and washed twice with PBS and centrifuged at 1500rpm for 5min, at 4°C. The cell pellet was resuspended in RIPA buffer supplemented with protease inhibitor (PMSF, 10µl/ml). The volume of added RIPA buffer was 10 times the volume of the cell pellet. Cells were chilled on ice for 30min. To achieve complete lysis, cells were sonicated for 30sec with a 50% amplitude. Protein extracts were collected in the supernatant after centrifugation at max speed, for 30min at 4°C.

All protein extracts from different samples were normalized on the lowest protein concentration sample with the addition of RIPA buffer and Laemmli buffer, using the formula $90\mu\text{l} \times [(\text{Abs sample}) / (\text{Abs lowest sample})]$, where 90µl is a chosen final volume. Laemmli buffer contains β-mercaptoethanol that keeps the protein in an unfolded conformation so that proteins are separated according to their size, in SDS-PAGE.

The protein concentration of the samples was determined using the Bradford assay. This assay is based on complexes built between the Bradford reagent (Coomassie-Brilliant-Blue G-250) and proteins under acidic conditions, leading to different absorption characteristics (465nm without and 596nm with proteins).

Protein Assay Dye Reagent Concentrate was diluted 1:5. 1ml of the dilution was mixed with 3µl of protein sample in a plastic cuvette, and the absorption was measured using a spectrometer at 595nm.

5.3.3.6 Western Blot

Proteins can be analyzed by Western Blot methodology, which consists of three steps, (1) separation of proteins according to their size on a Polyacryl Amide Gel Electrophoresis (SDS-PAGE), (2) transfer of the proteins to a nitrocellulose membrane, (3) detection of specific proteins using antibodies.

Proteins are extracted as described in section 5.3.3.5.

- The protein extracts were mixed with 4x Tris-glycine buffer, Laemmli buffer. Laemmli buffer contains SDS and β-mercaptoethanol. SDS is a detergent and induces denaturation of proteins. The protein extracts were boiled at 99°C, for 5min and loaded onto a 10% acrylamide gel. The acrylamide gel is divided into stacking gel and running gel, the stacking gel leads the proteins to line up and enter the running gel at the same time. The running gel leads to the separation of proteins according to their size.

Stacking gel	Running gel 10% Acry	components
6.8ml	4.9ml	H ₂ O
1.7ml	4.2ml	Acrylamide
1.25ml	3.125ml	Tris pH 6.8/8.8
100µl	125µl	SDS 10%
100µl	125µl	APS 10%
10µl	5µl	TEMED

(1) The gel was loaded in an appropriate SDS-PAGE chamber containing 1X of running buffer and a current of 20mA was applied.

(2) After separation, the proteins were transferred to a nitrocellulose membrane in a 1X transfer buffer at 300mA for 1,5h. The transfer efficiency was verified upon staining of the membrane by a Ponceau S.

The membrane was washed with TBS containing 0,5% Tween 20 (TBS-T). The membrane was blocked for 1h in 4% non-fat dry milk dissolved in 1X TBS-T, to avoid unspecific binding of antibodies.

The membranes were subsequently probed with the primary antibody, o/n, at 4°C with moderate shaking. On the next day, the membranes were washed three times for 15min, with 1X TBS-T with shaking.

(3) The membranes were incubated with appropriate secondary antibody for 1h, at RT. This second incubation was followed by additional three washings, 10min each with TBS-T, before the addition of the substrate Pierce™ ECL Western Blotting Substrate. The signal was detected with the Fusion SL camera.

5.3.4 Flow cytometry (FACS)

2x10⁶ total thymocytes were washed with cold FACS buffer and resuspended in 90µl of 1:200 diluted anti-CD16/anti-CD32-antibody mix. After 20min of incubation at 4°C, thymocytes were centrifuged at 1500rpm, for 5min, at 4°C, and the supernatant was removed. Thymocytes were resuspended in 100µl of PBS containing 1:1000 dilution of Viability staining Zombie and incubated for 20min, at RT, in the dark. Zombie Aqua™ or Zombie NIR™ is an amine-reactive fluorescent dye that is non-permeant to live cells but permeant to cells with compromised membranes. Thus, it can be used to assess the live vs. dead status of mammalian cells. After washing the cells with FACS buffer, 10µl of a 10X mix of antibodies were added to the thymocytes to stain the surface markers. The final concentration of the antibodies used varied due to manufacturers' recommendations and titration upon arrival of the antibodies. Individual

dilutions are indicated in the materials section 5.2.7.2. Cells were mixed with Abs solution by vortexing and incubated for 15min, at RT, in the dark.

Thymocytes were washed with FACS buffer to remove the excess antibodies and centrifuged at 1500rpm, for 5min, at 4°C.

Subsequently, cells were resuspended in 200µl FACS buffer and acquired at flow cytometer or fixed with 4% of formaldehyde in PBS and stored at 4°C until acquisition.

For intracellular staining, after the surface staining, described above, the thymocytes were incubated for 20min with 100µl of fixation buffer (1:2 in dH₂O, eBioscience) at 4°C. After fixation, the cells were washed with 100µl of 1X permeabilization buffer (1:10 in dH₂O, eBioscience) and centrifuged at 1800rpm, for 5min, at 4°C. Thymocyte pellets were resuspended in 100µl of antibodies mix prepared in 1X permeabilization buffer, and incubated o/n, at 4°C, in the dark. The day after, thymocytes were washed with 100µl of 1X permeabilization buffer, centrifuged at 1800rpm, for 5min, at 4°C. The cell pellets were resuspended in FACS buffer and acquired using a FACS Canto flow cytometer and analyzed with FlowJo™ Software.

5.3.5 Statistical analysis

Statistical analyses were performed using GraphPad 5.0 (Prism) software. All the results are indicated as the mean ± SEM. A confidence level of 95% level was used, and the statistical significance was determined by unpaired student's t-tests. Significant differences between data were indicated with *p-value < 0.05, **p-value < 0.005, ***p-value < 0.001, ****p-value <0.0001.

6 Results

6.1 The *Nfatc1/A-Bio.BirA* mouse model, an excellent tool for more specific ChIP-seq assays

To identify NFATc1/A binding sites and potential target genes during thymocyte development, we performed affinity-based ChIP-seq experiments. Due to the lack of a specific antibody against the inducible *Nfatc1* isoform, *Nfatc1A*, a transgenic mouse model recently generated was used, *Nfatc1/A-Bio.BirA*. This mouse model has been previously described¹⁵⁵. Briefly, a bacterial artificial chromosome (BAC) vector containing 200kb of the *Nfatc1* gene locus modified with an artificial biotinylation acceptor site at the C-terminal end of the short isoform NFATc1/A (Figure 6.1 A) was used to generate the transgenic (tg) mouse line. *Nfatc1/A-Bio* mice were crossed to *BirA* tg mice that express the bacterial BirA ligase from the ROSA26 locus. In this mice line, the tagged short isoform NFATc1/A expressed from the BAC locus will be biotinylated *in vivo*. In ChIP experiments, this model allowed us to precipitate specifically chromatin fragments bound by NFATc1/A, using streptavidin beads.

To check any transgene-induced artifact in thymocyte differentiation, we analyzed the distribution of thymic subpopulations in *Nfatc1/A-Bio.BirA* and control *BirA* mice. FACS analysis of thymocytes, stained with anti-CD4 and anti-CD8, revealed comparable distribution and cell numbers in the thymocyte subpopulations in the control and *Nfatc1/A-Bio.BirA* mice (Figure 6.1 B). In peripheral naïve T and B cells from WT mice, *Nfatc1* induction with the phorbol-ester TPA and the Ca²⁺ ionophore ionomycin reaches the highest level after 24h of stimulation, and after 2h in effector T cells. Surprisingly, in *Nfatc1/A-Bio.BirA* thymocytes, the induction of *Nfatc1* occurred already after 2h of stimulation, and it reached a plateau at 4h of stimulation (Supplementary figure S1). Therefore, we set 4 hours as the optimal time for stimulation of thymocytes with TPA and ionomycin for maximum NFATc1/A-Bio expression, nuclear accumulation, and DNA binding to identify all potential NFATc1/A binding sites.

Due to the presence of a third *Nfatc1* allele in *Nfatc1/A-Bio.BirA* mice, we checked the level of *Nfatc1* RNA expression in isolated DN and DP+CD4⁺+CD8⁺ populations. In both populations, upon stimulation with TPA and ionomycin (T+I), *Nfatc1* expression increased by two-fold compared to that in *BirA* control mice. *Nfatc1* induction was impaired by the addition of 100ng/ml of the calcineurin inhibitor Cyclosporin A (CsA) (Figure 6.1 C and D). Western blot experiments confirmed the expression of sufficient amounts of biotinylated NFATc1/A proteins after T+I stimulation in thymocytes from these mice to perform ChIP experiments (Figure 6.1E).

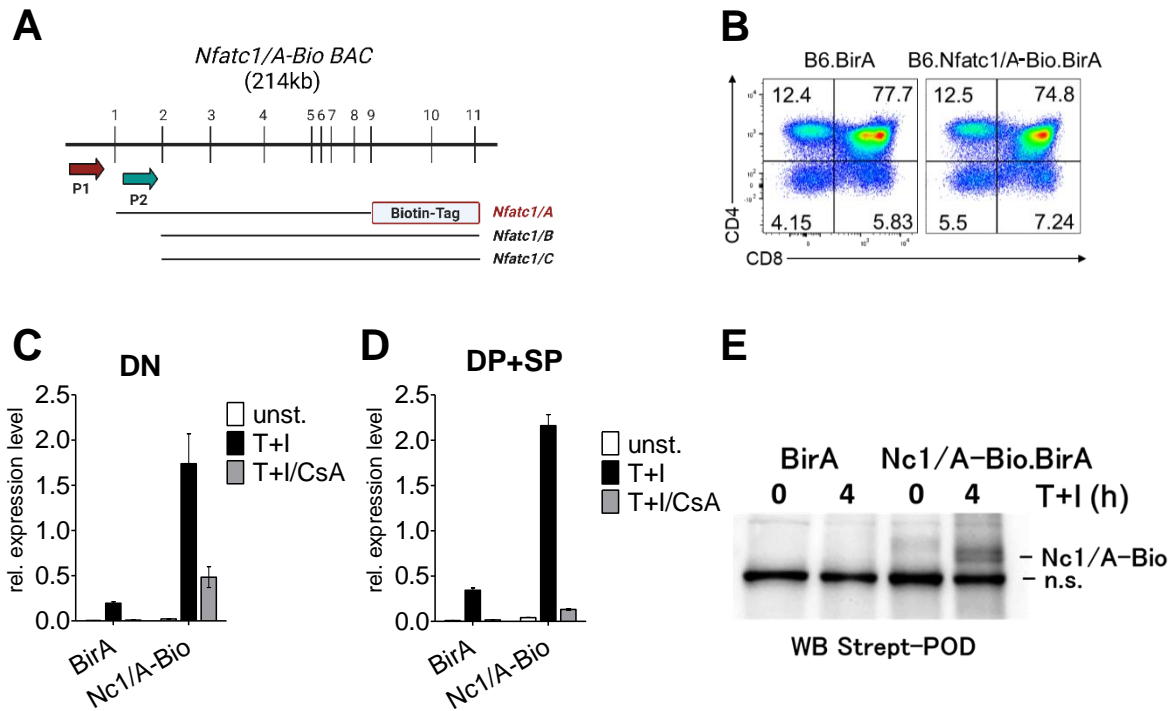


Figure 6.1 *Nfatc1/A-Bio.BirA* tg mice are ideal tools for ChIP experiments to identify NFATc1 target genes.

(A) Structure of the BAC transgene to express NFATc1/A-Bio protein. The biotin-tag is linked to exon 9 and expressed only as a part of the short isoform NFATc1/A. The promoters P1 (red arrow) and P2 (green arrow) are indicated. (B) Flow cytometry of freshly isolated thymocytes from *BirA* control and *Nfatc1/A-Bio.BirA* mice, stained with anti-CD4 and anti-CD8 Abs. The percentages of the four developmental populations are indicated in the corresponding quadrants. (C) qRT-PCR assays showing *Nfatc1* expression levels in isolated *BirA* and *Nfatc1/A-Bio.BirA* (Nc1/A-Bio) DN thymocytes. Thymocytes were cultured for 4h in the presence of T+I (100ng/ml each), in presence or absence of CsA (100ng/ml), or were left unstimulated. The total RNA was extracted and reverse-transcribed to cDNA. The qRT-PCR reactions were conducted with specific primers for *Nfatc1* and normalized to the house keeping gene *Actb*. (D) qRT-PCR assays for *Nfatc1* expression level in isolated *BirA* and *Nfatc1/A-Bio.BirA* DP, CD4⁺ and CD8⁺ thymocytes. Thymocytes treated as described in C. (E) Western Blot analysis of protein extracts from total thymocytes of *BirA* and *Nfatc1/A-Bio.BirA* mice stimulated with T+I (100ng/ml) for 4h, or left unstimulated. Biotinylated NFATc1/A proteins (Nc1/A-Bio) were detected with Streptavidin-POD. The position of NFATc1/A-Bio in the gel is indicated.


All data are representative of at least three independent experiments and are shown as mean \pm SEM.

6.2 Identification of NFATc1/A binding sites

In the first set of experiments, we performed NFATc1/A ChIP-seq assays with preparations of total thymocytes from double-transgenic *Nfatc1/A-Bio.BirA* and control *BirA* mice. Western blots assays demonstrated that culturing thymocytes with TPA and ionomycin for 4h, there was a substantial upregulation of biotinylated NFATc1/A in *Nfatc1/A-Bio.BirA* thymocytes (Figure 6.1 E). We precipitated cross-linked DNA fragments from stimulated *BirA* control and stimulated and unstimulated *Nfatc1/A-Bio.BirA* thymocytes, using streptavidin-linked beads. Purified DNA was used to generate DNA libraries for NGS sequencing of 50bp in length. The sequencing reads from *BirA* control and *Nfatc1/A-Bio.BirA* samples were aligned to the mm9 mouse genome. Using the program MACS2 for peak calling^{188, 189}, we identified 23.694 peaks for NFATc1/A binding. These peaks showed high enrichment in NFAT binding motif, TTTCCA, compared to stimulated *BirA* control thymocytes (Figure 6.2 A). This result confirmed that the immunoprecipitated fragments consisted of NFAT consensus binding motifs that were bound by NFATc1/A-Bio proteins.

Klein-Hessling et al.¹⁵⁵ have identified NFATc1/A target genes in activated effector CD8⁺ cytotoxic cells (CTL⁺) making use of *Nfatc1/A-Bio.BirA* mouse model¹⁹⁵. We compared the 23.694 NFAT binding sites identified in activated thymocytes (Thy⁺) to the 17.923 sites observed in activated CTLs. Among all, we selected 11535 peaks with a cut-off score > 200 in at least one set and calculated the peaks log₂ score ratio (Thy⁺/CTL⁺). The highest values are associated with an enriched binding in thymocytes and the lowest with strong binding observed in CTLs. Figure 6.2 B shows the number of peaks correlated to different values of score ratio. We then sorted the peaks into three different groups according to the score ratios named CTL-specific (CTL⁺, log₂ score ratio <-4, 1.615), common (3>log₂ score ratio>-3, 5623), and thymocyte-specific (Thy⁺, log₂ score ratio >5, 3.602). Examples of NFATc1/A binding for each group are shown in figure 6.2 C.

A

Name	p-value	log p-value	Binding motif
NFAT	1e ⁻⁹³⁹	-2.143e ⁺⁰³	

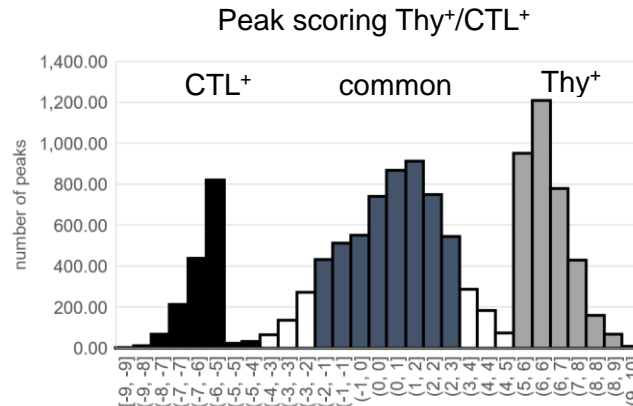
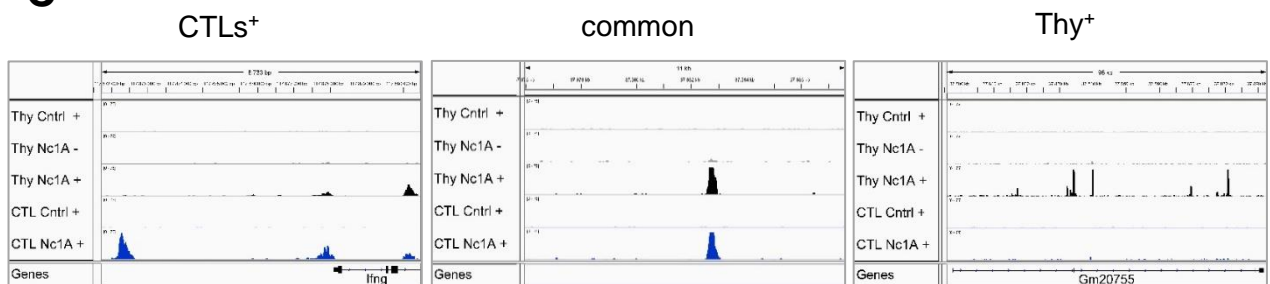
B**C**

Figure 6.2 Thymocytes and CTLs contain specific and shared NFATc1 binding sites.

(A) NFAT motif enrichment in stimulated *Nfatc1/A-Bio.BirA* compared to stimulated *BirA* thymocytes. The motif enrichment analysis was obtained with HOMER software. (B) Comparison between thymocytes and CTLs peaks, obtained from ChIP-seq assays. The log₂ of the score ratio is indicated on the x axis and the number of peaks with a specific score ratio, in each population, is indicated on the y axis. According to the distribution of peaks numbers, three groups were generated (CTLs⁺/common/Thy⁺). (C) Visualization of example chromosomal regions-containing peaks specific for thymocytes, for CTLs, as the *lfn3* gene, and peaks shared between thymocytes and CTLs. The NFATc1/A binding sites are visualized with IGV software.

We performed a motif enrichment analysis on each of the three groups, using the software HOMER. HOMER uses an algorithm that identifies transcription factor binding motifs that are enriched compared to the mouse genome background. As expected, in all groups, the NFAT and NFAT:AP1 motifs are the most abundant. Figure 6.3 A shows the list of the binding motifs for TFs that are the most significantly enriched in NFAT-bound sequences for thymocytes. They are the binding motif of well-known factors involved in thymocyte development like E2A, HEB, or ETS. The binding motifs statistically enriched in the CTL⁺ (Figure 6.3 B) and common peaks are especially for factors from the AP-1 transcription factor family. Overall, these results

indicate that the binding of NFATc1/A is in close vicinity to the binding of factors involved specifically in T cell activation or T cell development when CTL enriched and thymocyte enriched peaks are compared.

A

Rank	Name	p-value	log p-value	Binding Motif
1	NFAT (RHD)	1e-930	-2.143e+03	
5	E2A (bHLH)	1e-190	-4.388e+02	
6	HEB (bHLH)	1e-189	-4.373e+02	
12	EGR (ETS)	1e-149	-3.436e+02	
15	Tcf12 (bHLH)	1e-139	-3.222e+02	
16	Tcf21 (bHLH)	1e-137	-3.173e+02	
36	Jun-AP-1 (bZIP)	1e-110	-2.543e+02	
44	ETS1 (ETS)	1e-101	-2.341e+02	

B

Rank	Name	p-value	log p-value	Binding Motif
1	NFAT (RHD)	1e-240	-5.535e+02	
3	BATF (bZIP)	1e-190	-4.388e+02	
4	Atf3 (bZIP)	1e-212	-4.889e+02	
5	AP-1 (bZIP)	1e-189	-4.373e+02	
6	Fos (bZIP)	1e-110	-2.543e+02	
11	Jun-AP-1 (bZIP)	1e-101	-2.341e+02	

Figure 6.3 Transcription factor binding motifs are specifically and differentially enriched near the NFATc1 binding sites in thymocytes and CTLs.

(A) Motif enrichment of transcription factors involved in thymocyte development. (B) Motif enrichment of transcription factors involved in T cell activation and function¹⁷⁶.

The analysis was generated with HOMER software²¹¹. Some selected factors of the most significant are ranked in respect of their p-value and log p-value.

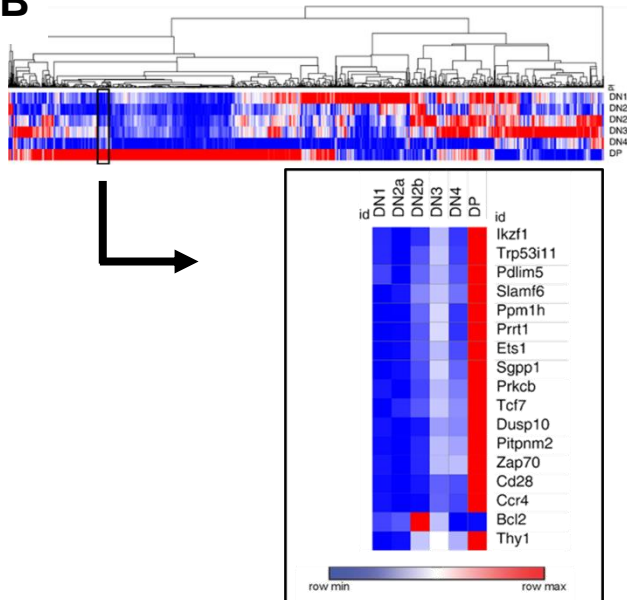
6.3 Identification of NFATc1/A binding sites in thymocytes *in vivo*

We further focused on detecting NFATc1/A binding in developing thymocytes in a more physiological situation, without the “artificial” TPA and ionomycin stimulation of cells *in vitro*. We performed ChIP-seq assays with freshly isolated *BirA* and *Nfatc1/A-Bio.BirA* thymocytes. Precipitated chromatin fragments showed the enrichment of the NFAT binding motif (Figure 6.4 A) The MACS2 program allowed us to identify 1635 peaks bound by NFATc1/A *in vivo* with 2321 genes in 500kb vicinity. We associated genes-containing peaks in freshly isolated thymocytes with publicly available RNA-seq data (from the “The Immunological Genome Project”¹⁹⁶) differently expressed during the stages of thymocyte development. We obtained a list of 1734 genes naturally involved in thymocyte development with NFATc1/A binding sites nearby. Some of these genes are known to regulate thymocyte development and survival, as the *Tcf7* (encoding TCF-1), *Bcl2*, *Ikzf1*, *Ets1*, *Rorc* (encoding ROR γ t), and *Ccr9* genes. Others are important mediators of pre-TCR and TCR signaling, as the *Zap70*, *Lck*, and *Cd28* genes. However, the majority of those genes are expressed at a low level in the early stages of thymocyte development, i.e. DN stages. This is shown in figure 6.4 B where a clustered view on the expression of potential NFATc1/A target genes in individual thymocyte subsets is presented. The binding of NFATc1/A along the genetic loci of *Ccr9*, *Tcf7*, *Bcl2*, and other genes important in thymocytes is shown in figure 6.4 C and supplementary S3. NFATc1-dependent regulation of *Bcl2*, *Tcf7*, and *Ccr9* transcription was further analyzed in qRT-PCR with RNA from total thymocytes stimulated for 4h with TPA and ionomycin without or with CsA or left unstimulated. The NFATc1-dependent upregulation or downregulation of the genes was sensitive to the calcineurin inhibitor, CsA (Figure 6.4 D).

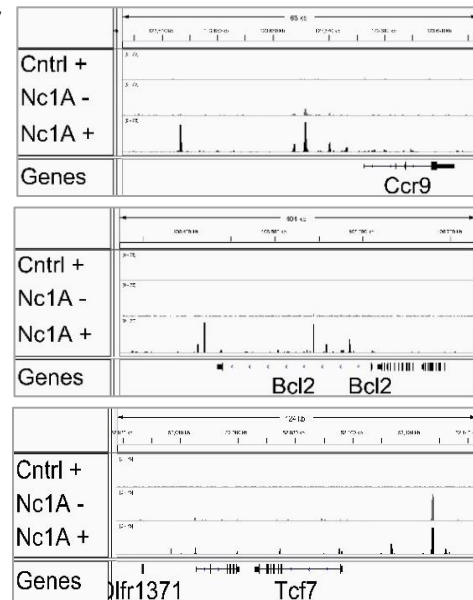
A

Name	p-value	log p-value	Binding motif
NFAT	1e ⁻⁴⁷⁹	-1.104e ⁺⁰³	

B



C



D

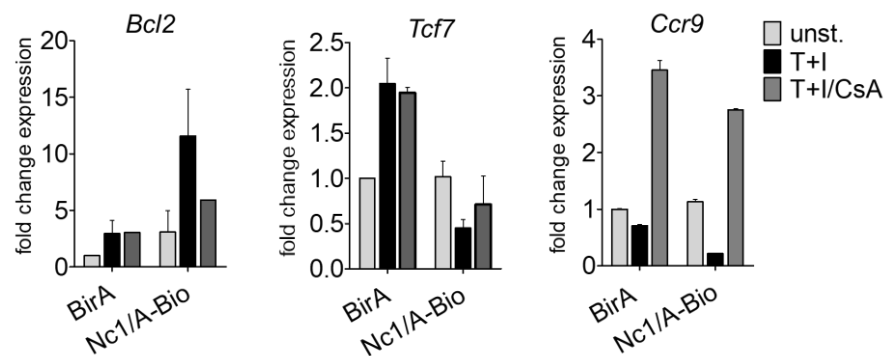


Figure 6.4 NFATc1/A regulates genes in DN and DP thymocytes.

(A) NFAT binding motif enriched in precipitated chromatin fragments from *Nfatc1/A-Bio.BirA* unstimulated thymocytes. (B) Heat-map of genes with NFATc1/A binding sites differentially expressed during thymocyte development (from “The Immunological Genome Project”²¹⁵). Heat-map generated by the on-line tool Morpheus Broad Institute. (C) NFATc1/A binding sites at the loci of the indicated genes. The bindings are visualized with IGV software. (D) Expression level of genes indicated in C. qRT-PCR was performed on total *BirA* and *Nfatc1/A-Bio.BirA* (Nc1/A-Bio) thymocytes stimulated for 4h with T+I, with T+I+CsA, or left unstimulated. Gene expression in T+I and T+I+CsA thymocytes was normalized to that of *Actb* gene and expressed as fold induction relative to the gene expression in unstimulated *BirA* thymocytes.

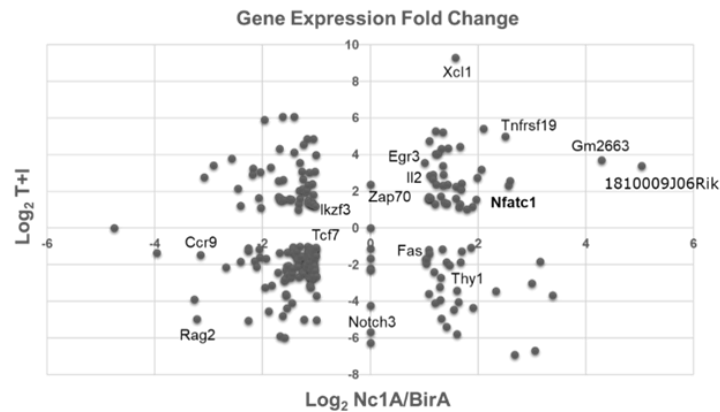
Data are representative of at least three independent experiments and are shown as mean \pm SEM.

6.4 NFATc1/A binding sites and gene expression in thymocytes

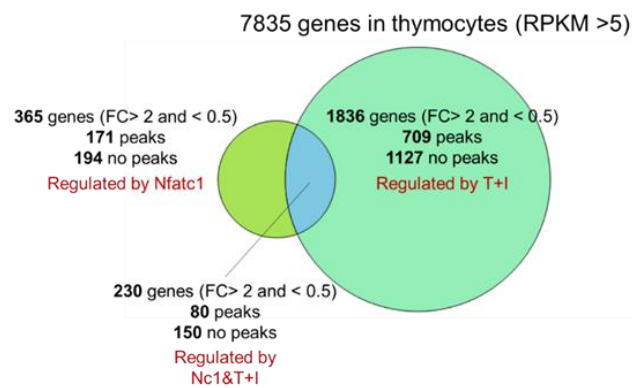
We also isolated the RNA from *BirA* and *Nfatc1/A-Bio.BirA* total thymocytes and performed NGS assays (performed kindly by Dr. Matthias Klein, Institute of Immunology, University of Mainz). We calculated the fold change of gene expression, comparing stimulated and non-stimulated *BirA* control thymocytes. This comparison indicated which genes were regulated predominantly by TPA and ionomycin stimulation in thymocytes. We also calculated the fold change of gene expression comparing *Nfatc1/A-Bio.BirA* and *BirA* control thymocytes, both stimulated. This last comparison indicated the transcriptional changes introduced by overexpression of NFATc1 due to the transgene. Thereby we identified genes upregulated or downregulated exclusively by NFATc1, by TPA and ionomycin induction, or by the influence of both (Figure 6.5 A). The plot in figure 6.5 A shows the distribution of genes with a fold change (FC) spanning between ≥ 2 and ≤ 0.5 .

The genes identified in RNA-seq assays (7835 genes with RPKM more than 5), which changed their expression either by stimulation with TPA and ionomycin (1836) and/or by the higher NFATc1 levels (365) in the BAC transgenic mice, were also associated with NFATc1/A binding determined in ChIP-seq assays. In each group of genes regulated differently by NFATc1, TPA, and ionomycin, or both, we further discriminated which genes contained NFATc1 binding sites (Figure 6.5 B). We concentrated on the 5000 strongest NFATc1/A peaks and identified 2399 genuine genes in a distance of 500kb using the GREAT tool (Genomic Regions Enrichment of Annotations Tool)¹⁹⁰. Among these genes were numerous known NFATc1-targets genes, as the *Nfatc1* gene itself and the *Ifng*, *Cd40lg*, and *Bcl2* genes, as well as new NFATc1 targets, such as the *Tcf7* (encoding TCF-1) and *Nr4a1* and *Nr4a3* genes (encoding Nurr-77 and Nor-1). We wondered whether the more than 7000 genes, identified by the NGS-RNA- and ChIP-seq assays shared similar or identical functions. We made use of the online tool GOrilla^{191, 192}. We searched for enriched GO terms in the list of the 365 genes regulated by NFATc1, compared to the total list of 7835 genes as background. The results show that the genes regulated by NFATc1 have functions associated with immune response and regulation of cell activation (Figure 6.5 C).

A



B



C

GO term	Description	FDR q-value	Enrichment (N, B, n, b)
GO:0002337	immune system process	1.07E-16	2.98 (7481,621,336,83)
GO:0006955	immune response	4.77E-10	3.36 (7481,311,336,47)
GO:0002682	regulation of immune system process	2.45E-7	2.35 (7481,597,336,63)
GO:0002684	positive regulation of immune system process	1.81E-6	2.63 (7481,398,336,47)
GO:0050865	regulation of cell activation	2.36E-6	3.03 (7481,272,336,37)
GO:0006952	defense response	1E-5	2.68 (7481,341,336,41)
GO:0050776	regulation of immune response	9.35E-6	2.67 (7481,342,336,41)

Figure 6.5 NFATc1/A binds to and regulates the expression of target genes in thymocytes and CTLs.

(A) RNA-seq analysis on total *BirA* and *Nfatc1/A-Bio.BirA* thymocytes. The xy plot represents the log₂ fold change of gene expression regulated exclusively by NFATc1 (on the x axis), by T+I (on the y axis), and by both conditions. (B) The Venn diagram represents the number of genes regulated only by NFATc1, only by T+I stimulation, or by both, selected by the FC ≥ 2 and/or FC ≤ 0.5 (identified in the RNA-seq analysis) that contain or not NFATc1 binding sites (identified in ChIP-seq analysis). (C) Gene Ontology analysis of the genes regulated by NFATc1. The data are generated with GOrilla software^{209,210}.

6.5 The NFATc1/A binding at the *Tcrb* and *Tcra* loci

NFATc1 is involved in the regulation of several genes important for thymocyte development. During the DN stages, the recombination and transcription of the *Tcrb* locus is an essential step for pre-TCR signaling and, later, for proper T cell functioning. Among several genes regulated by NFATc1, in our RNA-seq analysis on total *BirA* control and *Nfatc1/A-Bio.BirA* thymocytes, we detected a group of genes located along the *Tcrb* locus that was greatly upregulated in *Nfatc1/A-Bio.BirA* thymocytes. The genes are referred to as *trypsinogen genes* and are located in a repressed chromatin region^{197, 198} along the *Tcrb* locus (Figure 6.6 A).

A

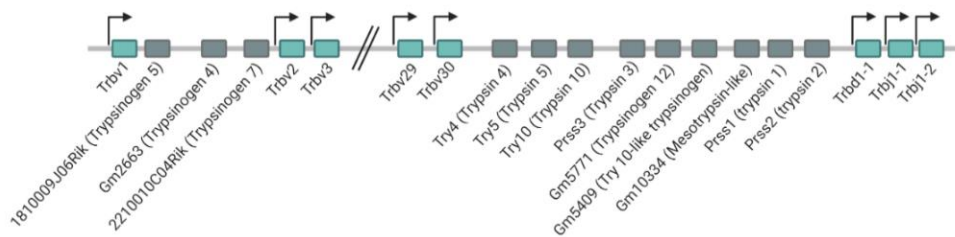


Figure 6.6 Trypsinogen genes are located into the *Tcrb* locus.

(A) Location of the trypsinogen genes interspersed among the gene segments of the *Tcrb* locus. Picture created with BioRender.com.

The heat-maps of the expression levels of these genes in total thymocytes and isolated DN thymocytes from *BirA* and *Nfatc1/A-Bio.BirA* mice stimulated and unstimulated, revealed the upregulation of some of the trypsinogen genes (Figure 6.7 A and B, see also section 6.12). Interestingly, the gene *Try10* appears to be upregulated only in DN thymocytes. This observation is in line with the previous observation that during DN developmental stages, the chromatin assumes a different configuration along the *Tcrb* locus, compared to later stages¹⁹⁷. Real-time PCR analysis also confirmed that the strong induction of NFATc1 upon stimulation leads to the fold change expression of these genes (Figure 6.7 C). Intriguingly, some of these genes, as the *Prss2*, *Gm2663*, and *1810009J06Rik* genes showed also NFATc1/A binding along their loci, suggesting that under these conditions, the chromatin status at this region changes from transcriptionally inactive to accessible and prone to be transcribed (Figure 6.7 D)

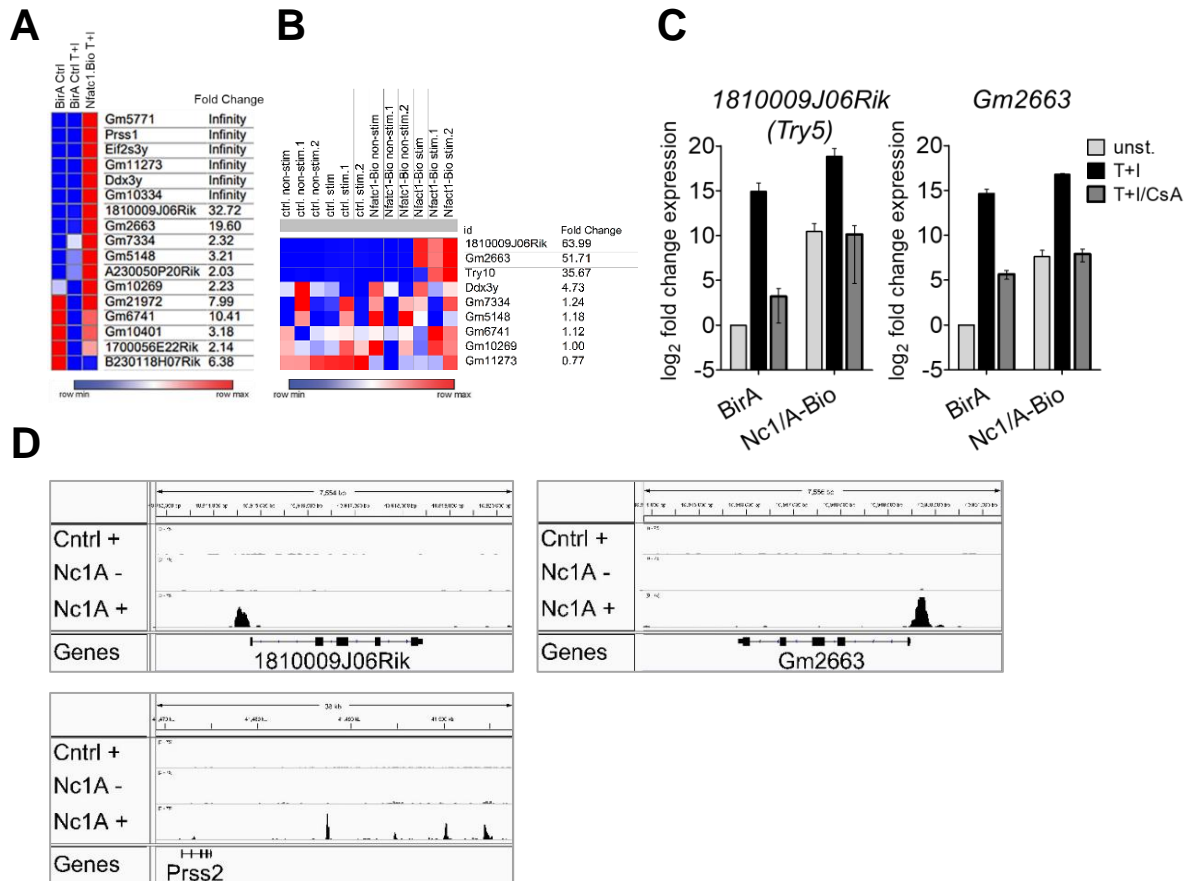


Figure 6.7 Upregulation of the trypsinogen genes is dependent on strong NFATc1 induction.

(A) Heat-map of trypsinogen genes upregulated by NFATc1 overexpression in total thymocytes from *BirA* and *Nfatc1/A-Bio.BirA* mice. Heat-map generated by the on-line tool Morpheus Broad Institute. (B) Heat-map of trypsinogen genes upregulated by NFATc1 induction in DN thymocytes from *BirA* and *Nfatc1/A-Bio.BirA* mice. Heat-map generated with the on-line tool Morpheus Broad Institute, (see also section 6.12). (C) qRT-PCR analysis confirmed that the upregulation of the trypsinogen genes was induced by the strong NFATc1 induction. Total *BirA* and *Nfatc1/A-Bio.BirA* thymocytes were stimulated for 4h with T+I, T+I+CsA or left unstimulated. Gene expression was normalized to that of *Actb* gene and expressed as a fold induction relative to expression in unstimulated *BirA* control thymocytes. Data from at least three independent experiments are shown as mean \pm SEM. (D) NFATc1/A binding sites at some indicated trypsinogen genes in *BirA* stimulated, *Nfatc1/A-Bio.BirA* freshly isolated and stimulated *Nfatc1/A-Bio.BirA* total thymocytes. The binding sites are visualized with IGV software.

Our ChIP-seq analysis showed that NFATc1/A binds at the 3' side of the *Tcrb* locus, where the Enhancer β (E β) and the Promoter of one D gene segment (PD β 1) are located (Figure 6.8 A). This result leads to speculation about the possible role of NFATc1 in recruiting histone-modifiers enzymes at this site, inducing a shift of the open chromatin toward the trypsinogen genes.

In addition, our ChIP-seq analysis showed that NFATc1/A binds at the Enhancer α (E α) in the *Tcra* locus either in freshly isolated and stimulated thymocytes from *Nfatc1/A-Bio.BirA* mice

(Figure 6.8 B). $E\alpha$ is a *Tcra* locus regulatory element located downstream of $C\alpha$. In the *Tcra* locus, the $E\alpha$ controls the initial germinal transcription and the V(D)J recombination of the overlapping *Tcra/Tcrd* locus. Taken together, these data suggest the involvement of NFATc1 in the regulation of the *Tcrb* and *Tcra* loci, coding for the TCR components, the TCR β and TCR α chains.

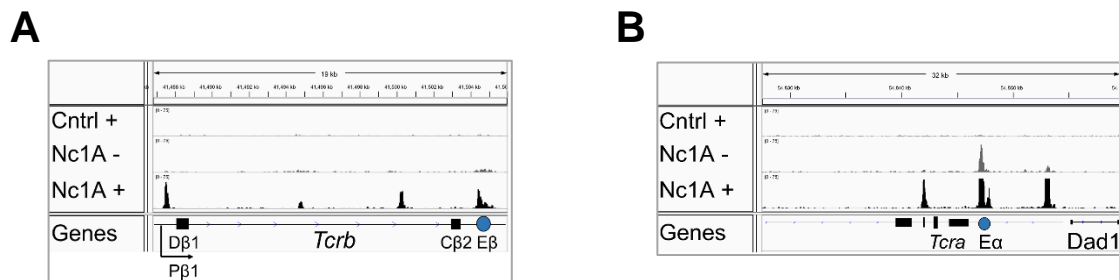


Figure 6.8 NFATc1/A binding at the murine *Tcrb* and *Tcra* loci.

(A) NFATc1/A binding at the *Tcrb* locus. The peaks are located in correspondence of the PD β 1 and the E β motifs in stimulated thymocytes from *Nfatc1/A-Bio.BirA* mice. (B) NFATc1/A binding at the *Tcra* locus from *Nfatc1/A-Bio.BirA* mice. The peaks are located in correspondence of the $E\alpha$ in stimulated and freshly isolated thymocytes. The NFATc1/A binding is visualized with IGV software.

6.6 Lack of NFATc1 expression in DN thymocytes leads to a moderate decrease in thymic cellularity

It has been shown that NFATc1 plays an essential role during thymocyte development. NFATc1 expression and activity are essential either during the DN stages of thymocyte development, in the pre-TCR negative (before the pre-TCR formation), and pre-TCR positive thymocytes¹⁹⁹. In the *VavCre-Nfatc1^{fl/fl}* mouse model, the ablation of NFATc1 in hematopoietic T cell progenitors leads to the shrinking of lymphatic organs, a dramatic decrease of thymic cellularity, and a block in thymocyte development at the DN1 stage⁵. In our studies, we made use of a different mouse model for abolishing the *Nfatc1* gene expression, the *Rag1Cre-Nfatc1^{fl/fl}* mouse model. In this mouse model, the Cre recombinase is expressed under the control of the *Rag1* gene locus and deletion of *Nfatc1* exon 3 starts at the DN2 stage resulting in the loss of NFATc1 protein.

We checked the expression level of the *Nfatc1* gene by real-time PCR in freshly isolated DN, DP, and SP thymocytes from *Nfatc1^{fl/fl}*, *Rag1Cre-Nfatc1^{fl/+}*, and *Rag1Cre-Nfatc1^{fl/fl}* mice. We performed real-time PCR analysis using both primers specific for the inducible α and the constitutive β *Nfatc1* isoforms. *Ex vivo* DN thymocytes from *Rag1Cre-Nfatc1^{fl/fl}* mice showed a dramatic reduction in the relative and fold change expression of *Nfatc1* compared to control animals, confirming that the Cre system has worked properly (Figure 6.9 A and S2). We

obtained similar results in freshly isolated DP and SP thymocytes from *Rag1Cre-Nfatc1^{fl/fl}* mice, in which the relative and fold change expression of the *Nfatc1* gene resulted in a dramatic reduction in *Rag1Cre-Nfatc1^{fl/fl}* thymocytes and less dramatically in *Rag1Cre-Nfatc1^{fl/+}* compared to *Nfatc1^{fl/fl}* control thymocytes (Figure 6.9 B and S2).

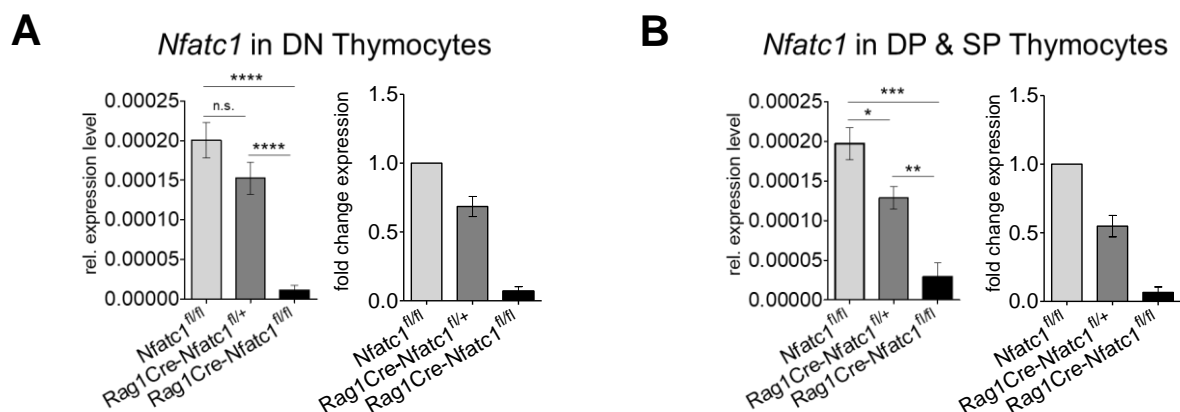


Figure 6.9 NFATc1 expression in *Rag1Cre-Nfatc1^{fl/fl}* mice is abolished.

(A) qRT-PCR of *Nfatc1* gene relative expression (on the left) and fold change expression (on the right) in freshly isolated DN subset from *Nfatc1^{fl/fl}* control, *Rag1Cre-Nfatc1^{fl/+}*, and *Rag1Cre-Nfatc1^{fl/fl}* thymocytes. (B) qRT-PCR of the *Nfatc1* gene relative expression (on the left) and fold change expression in freshly isolated DP and SP subsets from *Nfatc1^{fl/fl}* control, *Rag1Cre-Nfatc1^{fl/+}* and *Rag1Cre-Nfatc1^{fl/fl}* thymocytes. *Nfatc1* gene expression in the three genotypes was normalized to that of *Actb* and in fold change analysis, it was expressed as fold induction relative to *Nfatc1^{fl/fl}* control thymocytes. Data are representative of at least three independent experiments and are shown as mean \pm SEM. Unpaired student's t-test was performed. *p-value < 0.05, **p-value < 0.005, ***p-value < 0.001, ****p-value < 0.0001, n.s. is non-significant.

The depletion of NFATc1 in thymocytes did not affect dramatically the cellularity of the thymus, in contrast to the NFATc1-hematopoietic depletion in *VavCre-Nfatc1^{fl/fl}* mice. However, in *Rag1Cre-Nfatc1^{fl/fl}* mice compared to control littermates, we observed a moderate but statistically significant decrease in cell number (Figure 6.10 A). Despite the cellularity in *Nfatc1* ko thymus was not tremendously affected in *Rag1Cre-Nfatc1^{fl/fl}* mice, we wondered if the ratio between the thymocyte populations changed, due to the ablation of NFATc1. Flow cytometry analysis on total thymocytes, stained with anti-CD4 and anti-CD8 Abs, showed slight differences in the percentages of population distribution between the different genotypes (Figure 6.10 B). We observed a statistically significant difference in the absolute number of the DP and CD4⁺ thymocyte populations in the *Rag1Cre-Nfatc1^{fl/fl}* mice, compared to the control mice. However, we detected an overall decrease in the absolute cell number in all four thymocyte populations (Figure 6.10 C). When thymocytes were stained also for the DN subpopulation markers CD25 and CD44, we did not observe abnormalities in the DN subpopulations in *Rag1Cre-Nfatc1^{fl/+}* and *Rag1Cre-Nfatc1^{fl/fl}* compared to *Nfatc1^{fl/fl}* thymocytes

(Figure 6.10 D). The absolute cell number of each DN subpopulation did not show significant differences (Figure 6.10 E).

These results show that despite a strongly reduced NFATc1 expression, the thymic cellularity and the distribution of thymocyte populations in a 4 weeks-old thymus are not dramatically affected. NFATc1-deficient thymocytes are moderately reduced at the DN stage.

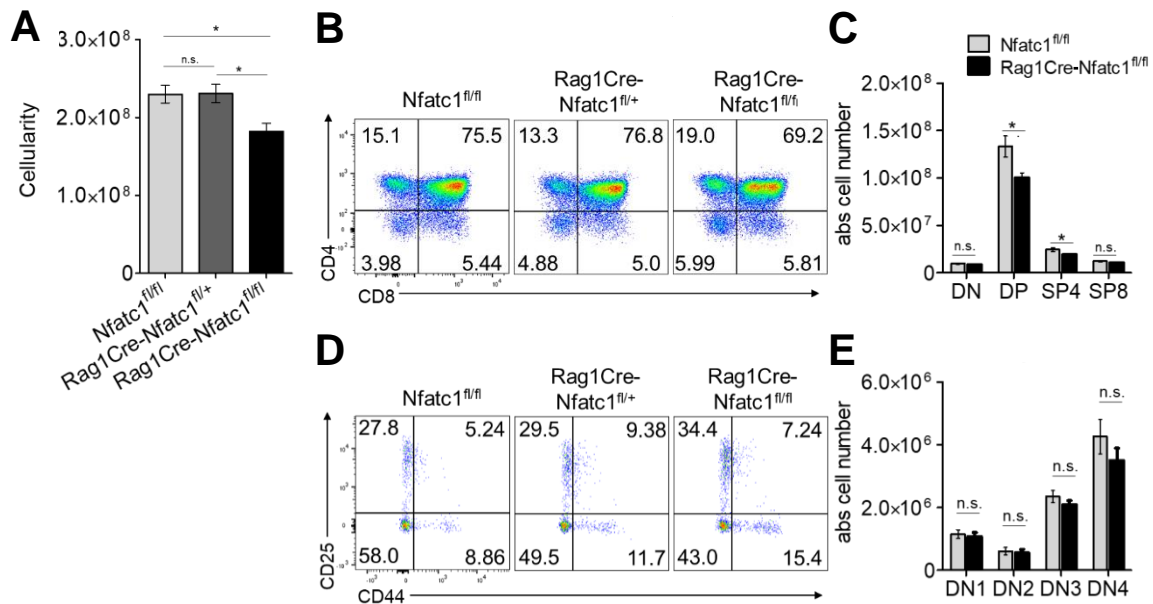


Figure 6.10 Lack of NFATc1 activity leads to a moderate decrease in the number of thymocytes.

(A) Thymic cellularity in the *Nfatc1^{fl/fl}*, *Rag1Cre-Nfatc1^{fl/+}* and *Rag1Cre-Nfatc1^{fl/fl}* mice. (B) FACS analysis on total thymocytes from *Nfatc1^{fl/fl}*, *Rag1Cre-Nfatc1^{fl/+}* and *Rag1Cre-Nfatc1^{fl/fl}* mice. To visualize the four developmental stages in the thymus (DN, DP, CD4⁺ and CD8⁺), cells were stained with mouse anti-CD4 and anti-CD8 Abs. The percentage of each population is indicated in the corresponding quadrants. (C) Absolute cell numbers of DN, DP, CD4⁺ and CD8⁺ thymic populations from *Nfatc1^{fl/fl}* and *Rag1Cre-Nfatc1^{fl/fl}* mice. (D) FACS analysis on total thymocytes from *Nfatc1^{fl/fl}*, *Rag1Cre-Nfatc1^{fl/+}* and *Rag1Cre-Nfatc1^{fl/fl}* mice. The thymocytes were stained with anti-CD4, anti-CD8, anti-CD25 and anti-CD44 Abs to visualize the four DN subpopulations (DN1, DN2, DN3 and DN4). The percentage of each population is indicated in the corresponding quadrants. DN subpopulations were analysed gating on DN thymocytes. (E) Absolute cell numbers of the DN subpopulations from *Nfatc1^{fl/fl}* and *Rag1Cre-Nfatc1^{fl/fl}* mice. Data are indicative of at least six independent experiments and are shown as mean \pm SEM. Unpaired student's t-test was performed. *p-value < 0.05, n.s. is non-significant.

6.7 Lack of expression of the NFATc1/ α inducible isoforms during DN stages leads to a moderate reduction in thymic cellularity

The inducible expression of NFATc1/ α isoforms is mediated by the *Nfatc1* P1 promoter and the expression of exon 1 encoding the α peptide at the N-terminus. Our lab described previously that the inducible *Nfatc1 α* gene expression, regulated by the P1 promoter, is controlled by a regulatory element of app. 1000bp in size, located in intron 10 of the *Nfatc1*

gene locus, and designed as enhancer E2⁵. We wondered whether the E2 enhancer exerts a marked effect on thymocyte development when the inducible NFATc1/α isoforms are missing in thymocytes. We used a newly generated mouse model from our lab in which the E2 enhancer segment is flanked by two Loxp sequences, in combination with the Cre recombinase under the control of the *Rag1* gene expression. This mouse model was designed as *Rag1Cre-E2^{fl/fl}*. We checked if the deletion of the enhancer E2, in the *Rag1Cre-E2^{fl/fl}* thymocytes, prevents the expression of the inducible isoforms. We assessed the *Nfatc1α* expression, generated from the inducible P1 promoter, by real-time PCR in freshly isolated DN, DP, and SP thymocytes from *E2^{fl/fl}* and *Rag1Cre-E2^{fl/fl}* mice. *Ex vivo* DN thymocytes from *Rag1Cre-E2^{fl/fl}* showed a dramatic reduction in the relative expression of the inducible *Nfatc1α* isoforms compared to *E2^{fl/fl}* control, confirming that E2, together with the P1 promoter, regulates specifically the expression of the *Nfatc1α* isoforms in thymocytes (Figure 6.11 A). In freshly isolated DP and SP thymocytes, the relative expression of the *Nfatc1α* isoforms was also diminished in *Rag1Cre-E2^{fl/fl}* mice compared to *E2^{fl/fl}* control mice (Figure 6.11 B).

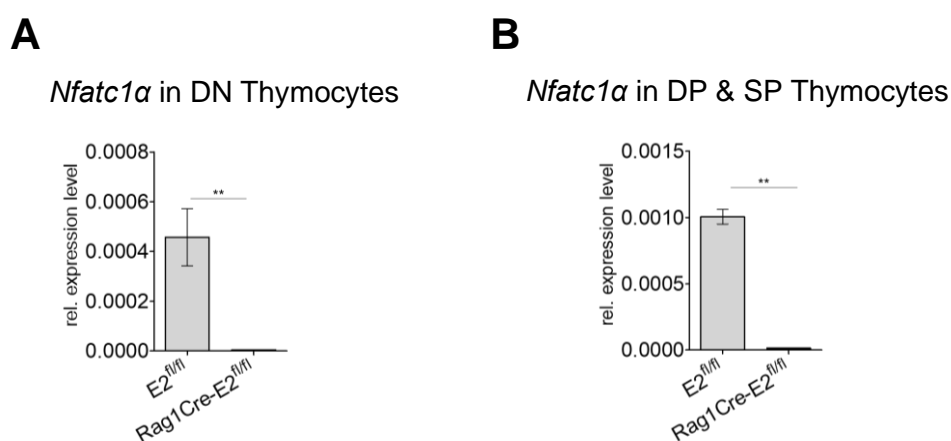


Figure 6.11 The expression of the NFATc1/α isoforms in *Rag1Cre-E2^{fl/fl}* mouse is abolished.

(A) Relative expression of exon 1-containing *Nfatc1α* isoforms in freshly isolated DN subset from *E2^{fl/fl}* control and *Rag1Cre-E2^{fl/fl}* thymocytes, assessed by qRT-PCR. (B) Relative expression of exon 1-containing *Nfatc1α* isoforms in freshly isolated DP and SP subsets from *E2^{fl/fl}* control and *Rag1Cre-E2^{fl/fl}* thymocytes, assessed by qRT-PCR. Gene expression of the two genotypes was normalized to that of *Actb* gene. Data are from at least three independent experiments and are shown as mean ± SEM. Unpaired student's t-test was performed. **p-value < 0.005.

Similar to NFATc1-deficient thymocytes, the lack of the inducible isoforms in thymocytes did not affect dramatically the cellularity of the thymi. However, in *Rag1Cre-E2^{fl/fl}* compared to control littermates, a statistically significant moderate decrease in cell number was observed (Figure 6.12 A).

The FACS analysis on total thymocytes, stained with anti-CD4 and anti-CD8 Abs, showed the normal thymocyte population distribution between the two genotypes (Figure 6.12 B). We observed a statistically significant difference in the absolute number of the DP thymocyte populations, comparing control and *Rag1Cre-E2^{fl/fl}* thymocytes (Figure 6.12 C). The FACS staining for the DN subpopulation markers, CD25 and CD44, showed no abnormalities in the DN subpopulations in *Rag1Cre-E2^{fl/fl}* compared to *E2^{fl/fl}* thymocytes (Figure 6.12 D). The absolute cell number of each DN subpopulation did not show significant differences (Figure 6.12 E).

These results show that the lack of the expression of the NFATc1/α isoforms does not affect dramatically the thymic cellularity and the distribution of thymocyte populations in the thymus.

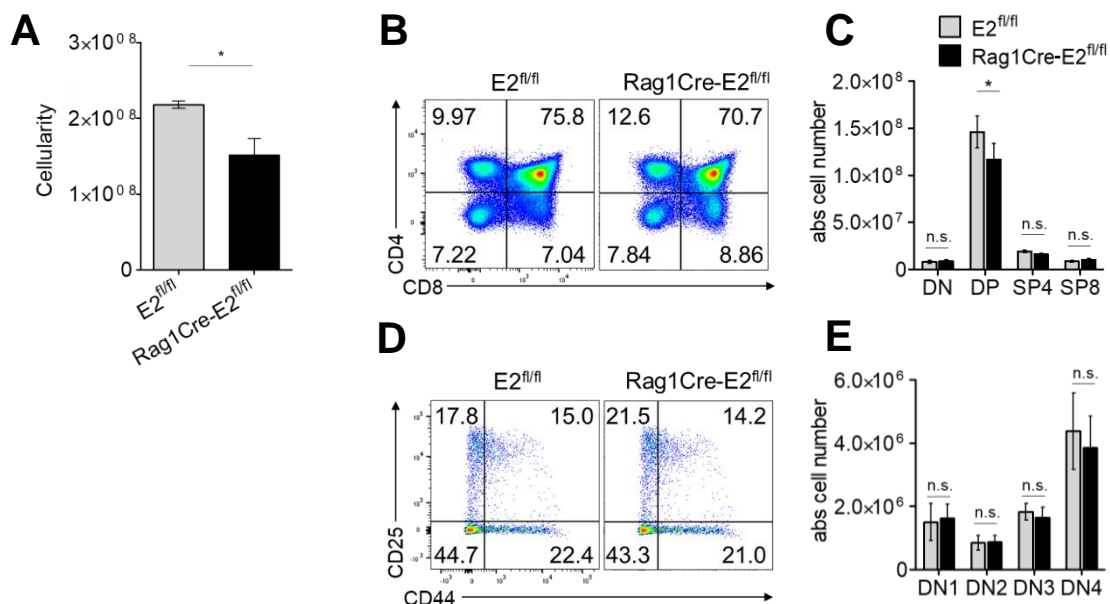


Figure 6.12 Depletion of NFATc1/α isoforms leads to a decrease in the number of thymocytes.

(A) Cellularity of the *E2^{fl/fl}* control and *Rag1Cre-E2^{fl/fl}* mice. (B) FACS analysis on total thymocytes from *E2^{fl/fl}* control and *Rag1Cre-E2^{fl/fl}* mice. To visualize the four developmental stages in the thymus (DN, DP, CD4⁺ and CD8⁺) cells were stained with anti-CD4 and anti-CD8 Abs. The percentage of each population is indicated in the corresponding quadrants. (C) Absolute cell numbers of thymic populations, DN, DP, CD4⁺ and CD8⁺ cells. (D) FACS analysis on total thymocytes from *E2^{fl/fl}* control and *Rag1Cre-E2^{fl/fl}* mice. The thymocytes were stained with anti-CD25 and anti-CD44 Abs to visualize the four DN subpopulations (DN1, DN2, DN3 and DN4). The percentage of each population is indicated in the corresponding quadrants. DN subpopulations were analysed gating on DN thymocytes. (E) Absolute cell numbers of the DN subpopulation.

Data are indicative of at least 6 independent experiments and are shown as mean ± SEM. Unpaired student's t-test was performed. *p-value < 0.05., n.s. is non-significant.

6.8 Lack of NFATc1 activity leads to an increase of $\gamma\delta$ thymocytes in the thymus

Patra *et al.*⁴ have reported that during the early stages of thymocyte development (in DN stages), NFATc1 localizes in the nucleus of pre-TCR negative thymocytes already during the DN2 stage, and reaches the highest nuclear concentration during the DN3 stage. The DN2-DN3 stages represent the bifurcation point between $\alpha\beta$ and $\gamma\delta$ T cells. To assess whether NFATc1 plays a role in determining the $\alpha\beta$ or $\gamma\delta$ lineage fate of the developing thymocytes, we performed a flow cytometry analysis of *ex vivo* thymocytes from *Nfatc1^{fl/fl}*, *Rag1Cre-Nfatc1^{fl/+}*, and *Rag1Cre-Nfatc1^{fl/fl}* mice. We stained the thymocytes with Abs against TCR δ^+ and TCR β^+ . In FACS analysis, we gated thymocytes for TCR β^+ , indicating TCR β^+ thymocytes, and for TCR δ^+ , indicating $\gamma\delta$ thymocytes. FACS analysis showed a slight decrease in the percentage of TCR $\alpha\beta$ thymocytes either in *Rag1Cre-Nfatc1^{fl/+}* and *Rag1Cre-Nfatc1^{fl/fl}* compared to *Nfatc1^{fl/fl}* control mice (Figure 6.13 A). However, the decrease of the $\alpha\beta$ thymocytes was statistically non-significant (Figure 6.13 B). The absolute cell number of $\alpha\beta$ thymocytes showed only a tendency in cell number reduction, which was also non-significant (Figure 6.13 C). Both analyses reflected only a slight propensity for cell reduction. On the other hand, FACS analysis showed an NFATc1 dose-dependent increase in the percentage of $\gamma\delta$ thymocytes either in the *Rag1Cre-Nfatc1^{fl/+}* (0,6% *Rag1Cre-Nfatc1^{fl/+}* vs 0,4% *Nfatc1^{fl/fl}* control) and more than two-fold in the *Rag1Cre-Nfatc1^{fl/fl}* thymocytes, compared to control littermates (1% *Rag1Cre-Nfatc1^{fl/fl}* vs 0,4% *Nfatc1^{fl/fl}* control) (Figure 6.13 A and D). The summary of several experiments is shown in figure 6.13 E. The accumulation of $\gamma\delta$ thymocytes, induced by the partial or complete loss of NFATc1, was also observed for the absolute cell number with a three-fold increase in *Rag1Cre-Nfatc1^{fl/fl}* mice, and a two-fold increase in *Rag1Cre-Nfatc1^{fl/+}* mice compared to control thymocytes (Figure 6.13 F). To exclude the possibility that the increase in TCR δ^+ thymocytes number was influenced by a difficulty in detecting surface TCR β expression on DN thymocytes, we performed an intracellular staining for TCR β^+ and TCR δ^+ T cell receptor chains. FACS analysis confirmed the accumulation of the TCR δ^+ receptor in *Rag1Cre-Nfatc1^{fl/fl}* total and DN gated thymocytes, whereas the proportion of TCR β^+ cells was comparable both in total and in DN thymocytes (Figure 6.14 A and D). The relative and absolute TCR δ^+ cell number confirmed the increase of TCR $\gamma\delta$ cells in both gated populations (Figure 6.14 B, C, E, and F). Of notice, we observed a significant increase in the population of thymocytes expressing both the intracellular TCR β^+ and TCR δ^+ chains in NFATc1-deficient mice, either in total and DN thymocytes (0.18% in total *Nfatc1^{fl/fl}* vs 0.35% in *Rag1Cre-Nfatc1^{fl/fl}*, and 1.48% in DN *Nfatc1^{fl/fl}* vs 3.05% in *Rag1Cre-Nfatc1^{fl/fl}*) (Figure 6.14 A and 6.14 D). These results suggest a positive influence of the lack of NFATc1 activity on the number of $\gamma\delta$ T cells in the thymus.

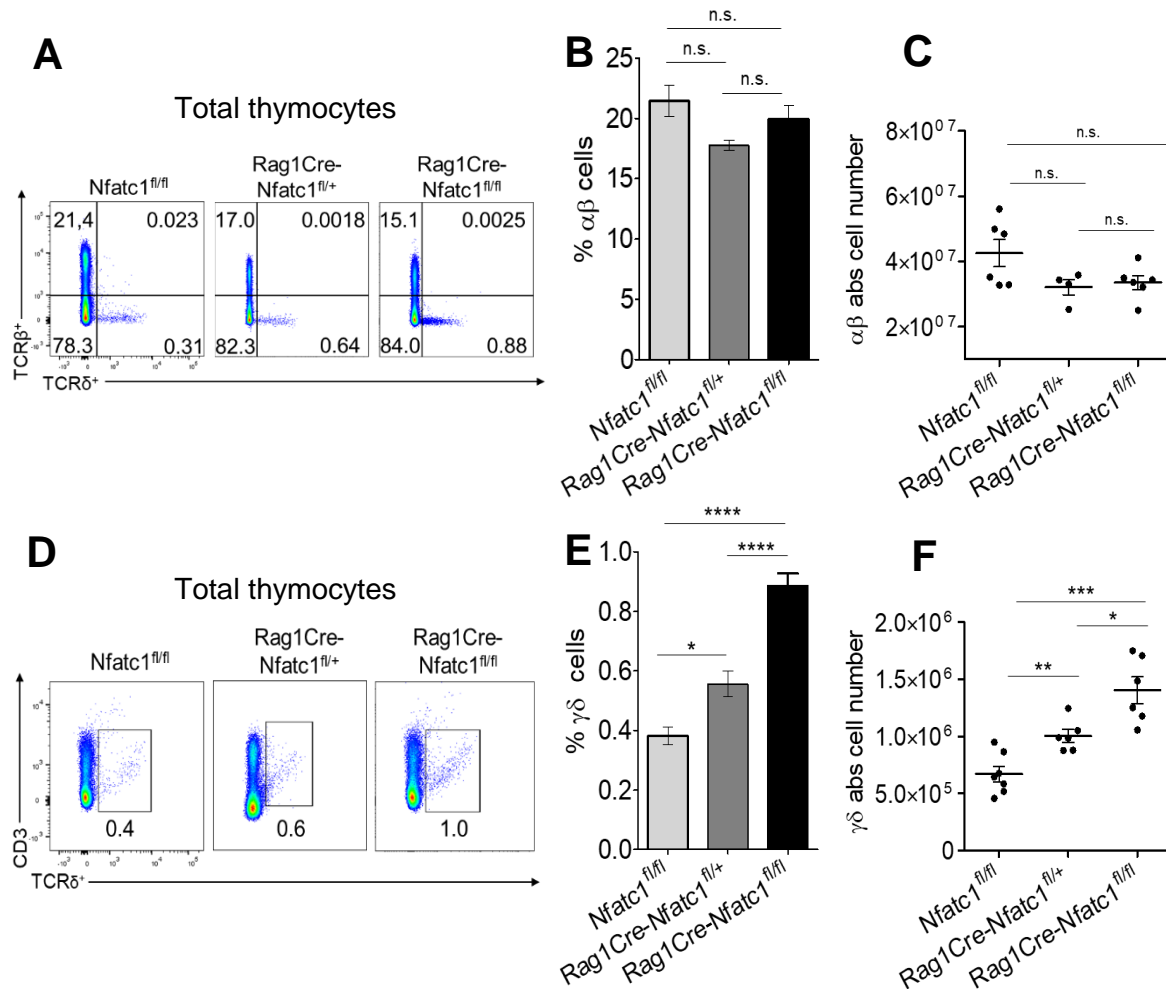


Figure 6.13 Increase in $\gamma\delta$ T cell number in *Rag1Cre-Nfatc1^{fl/fl}* mice.

(A) FACS analysis of thymocytes from *Nfatc1^{fl/fl}* control, *Rag1Cre-Nfatc1^{fl/+}* and *Rag1Cre-Nfatc1^{fl/fl}* mice. Total thymocytes were stained with anti-TCR δ^+ and anti-TCR β^+ Abs. The percentage of each population is indicated in the respective quadrant. (B) Percentage of $\alpha\beta$ T cells in thymi from *Nfatc1^{fl/fl}* control, *Rag1Cre-Nfatc1^{fl/+}* and *Rag1Cre-Nfatc1^{fl/fl}* mice. (C) Absolute cell numbers of $\alpha\beta$ T cells in thymi from *Nfatc1^{fl/fl}* control, *Rag1Cre-Nfatc1^{fl/+}* and *Rag1Cre-Nfatc1^{fl/fl}* mice. Each black dot represents one mouse. (D) Thymocytes as in (A) were stained with anti-TCR δ^+ chain and anti-CD3 Abs. Gated on live cells. The percentage of each population is indicated in the respective quadrants. (E) Distribution of percent of $\gamma\delta$ T cells in *Nfatc1^{fl/fl}* control, *Rag1Cre-Nfatc1^{fl/+}* and *Rag1Cre-Nfatc1^{fl/fl}* mice. (F) Absolute cell numbers of $\gamma\delta$ T cells from *Nfatc1^{fl/fl}* control, *Rag1Cre-Nfatc1^{fl/+}* and *Rag1Cre-Nfatc1^{fl/fl}* mice. Each black dot represents one mouse.

Data are indicative of at least 6 independent experiments and are shown as mean \pm SEM. Unpaired student's t-test was performed. *p-value < 0.05, **p-value < 0.005, ***p-value < 0.001, ****p-value < 0.0001, n.s. non-significant.

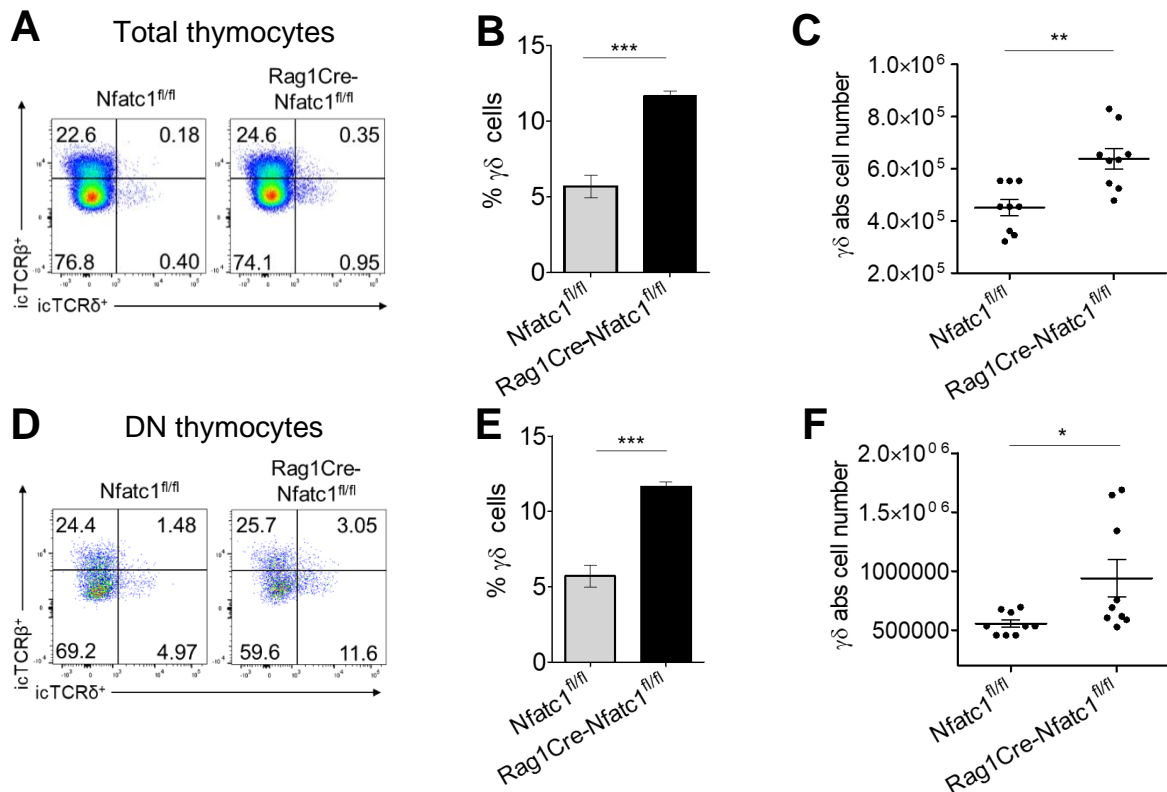


Figure 6.14 Increase of intracellular TCRδ⁺ T cells upon ablation of NFATc1 in thymus.

(A) *Nfatc1*^{fl/fl} and *Rag1Cre-Nfatc1*^{fl/fl} thymocytes were stained with anti-TCRδ⁺ and anti-TCRβ⁺ intracellularly. The percentage of each population is indicated in the respective quadrants. (B) Quantification of the percent intracellular TCRδ⁺ T cells in *Nfatc1*^{fl/fl} control and *Rag1Cre-Nfatc1*^{fl/fl} mice. (C) Quantification of the absolute cell numbers of intracellular TCRδ⁺ T cells in *Nfatc1*^{fl/fl} control and *Rag1Cre-Nfatc1*^{fl/fl} mice. Each black dot represents one mouse. (D) Thymocytes were stained as in A and analysed by flow cytometry gated for DN thymocytes. (E) Quantification of the percent intracellular TCRδ⁺ T cells among DN thymocytes in *Nfatc1*^{fl/fl} control and *Rag1Cre-Nfatc1*^{fl/fl} mice. (F) Quantification of the absolute cell numbers of intracellular TCRδ⁺ T cells in *Nfatc1*^{fl/fl} control and *Rag1Cre-Nfatc1*^{fl/fl} mice. Each black dot represents one mouse. Data are representative of at least six mice from every genotype and are shown as mean ± SEM. Unpaired student's t-test was performed. *p-value < 0.05, **p-value < 0.005, ***p-value < 0.001, ****p-value < 0.0001.

Since the lack of NFATc1 induces an increase in γδ thymocytes, we checked the NFATc1 expression level in αβ and γδ T cells, specifically. We used the *Nfatc1-eGfp-Bac* mouse model, in which *eGfp* is linked to the exon 3 of *Nfatc1* to report the transcriptional activity of the *Nfatc1* gene²⁰⁰.

We analyzed GFP expression by FACS analysis in TCRβ⁺ and TCRδ⁺ thymocytes from these mice. FACS analysis revealed that a similar percentage of γδ T cells and αβ T cells expressed GFP and therefore showed NFATc1 activity. Surprisingly, GFP expression, indicated by the MFI, was higher in γδ T cells compared to αβ T cells (Figure 6.15 A).

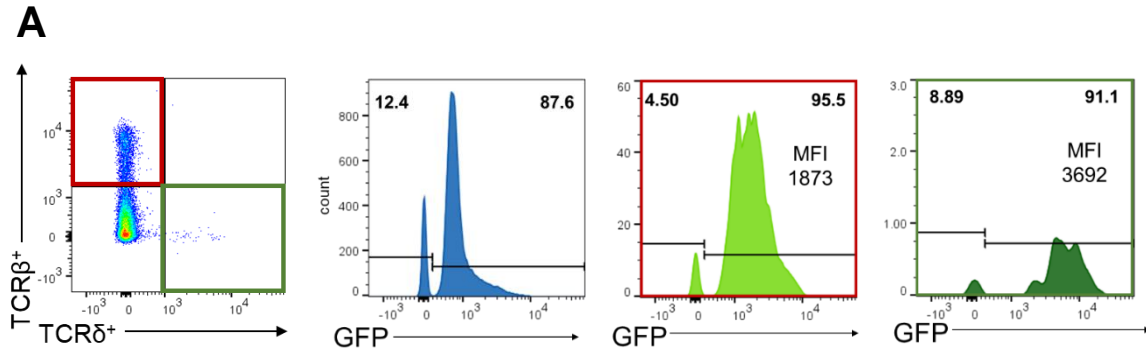


Figure 6.15 $\gamma\delta$ T cells express higher levels of NFATc1 compared to $\alpha\beta$ T cells.

(A) Total thymocytes from *Nfatc1-eGfp-Bac* mice were isolated and stained with anti-TCR β^+ and anti-TCR δ^+ Abs. The level of GFP was evaluated in each population, as indicated by the gates.

The red square indicates the gate of TCR β^+ and green square indicates the gate of TCR δ^+ thymocytes with the corresponding percentage of GFP $^-$ and GFP $^+$ thymocytes. Percentages are indicated in the respective gates. MFI, mean fluorescence intensity.

While the lack of NFATc1 leads to an increase of $\gamma\delta$ T cells, we then asked whether the maximum NFAT activity could reverse our observation regarding increased $\gamma\delta$ T cells in the *Rag1Cre-Nfatc1^{fl/fl}* mice. We made use of a different mouse model, the Δ Cam mice¹⁸⁶. These transgenic mice express a truncated version of the phosphatase calcineurin driven by the proximal *Lck* promoter and the human CD2 enhancer located downstream. Deletion of the regulatory domain of calcineurin results in constitutive activity and, therefore, an over-activation of all NFAT factors, including NFATc1. The FACS analysis showed that in Δ Cam mice, the percentage (Figure 6.16 A and B) and the absolute number of $\gamma\delta$ thymocytes was strongly reduced compared to the littermate control mice (Figure 6.16 C).

Taken together, these data suggest that NFATc1 plays a role in deciding the fate of developing thymocytes between $\alpha\beta$ and $\gamma\delta$ lineages.

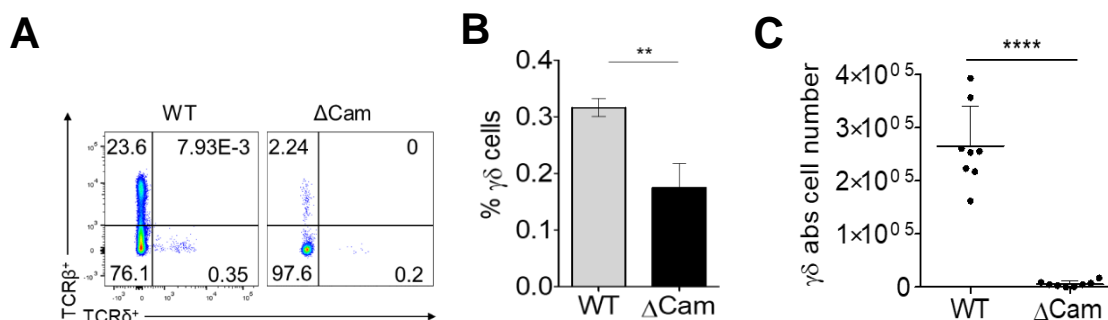


Figure 6.16 Decreased $\gamma\delta$ cells in Δ Cam mice.

(A) FACS analysis on total thymocytes from B6 WT and Δ Cam mice, stained with mouse anti-TCR β ⁺ and anti-TCR δ ⁺ Abs. The percentage of the respective thymocyte populations are indicated in each quadrant. (B) Quantification of the percent of $\gamma\delta$ T cells among total thymocytes from WT and Δ Cam mice. (C) Quantification of the absolute cell numbers of $\gamma\delta$ T cells among total thymocytes from WT and Δ Cam mice.

Data are representative of at least six mice from every genotype and are shown as mean \pm SEM. Unpaired student's t-test was performed. **p-value < 0.005, ****p-value < 0.0001.

6.9 The deficiency of the NFATc1/ α isoforms leads to an increase of $\gamma\delta$ T cells in the thymus

To assess whether the NFATc1/ α isoforms play a role in the lineage fate of developing thymocytes, we performed a flow cytometry analysis of thymocytes from $E2^{fl/fl}$ control and $Rag1Cre-E2^{fl/fl}$ mice. We stained the thymocytes with Abs for TCR δ ⁺ and TCR β ⁺.

In FACS analysis, we gated thymocytes for TCR β ⁺, indicating TCR $\alpha\beta$ thymocytes, and for TCR δ ⁺, indicating $\gamma\delta$ thymocytes. The analysis showed a seven-fold increase in the percentage of $\gamma\delta$ thymocytes in the $Rag1Cre-E2^{fl/fl}$ compared to control littermates (1.17% $Rag1Cre-E2^{fl/fl}$ vs 0.16% $E2^{fl/fl}$ control) (Figure 6.17 A).

On the other hand, also in this mouse model, the increase of $\gamma\delta$ T cells induced by the loss of the inducible NFATc1/ α was not counterbalanced by a decrease in $\alpha\beta$ T cells, confirmed in FACS analysis (Figure 6.17 A). The percentage and the absolute cell number of $\alpha\beta$ T cells were statistically non-significant, although the absolute cell number showed a slight tendency to decrease (Figure 6.17 B and C). The percentage and the absolute cell number calculation of $\gamma\delta$ thymocytes, instead, revealed a four-fold increase in $Rag1Cre-E2^{fl/fl}$ compared to $E2^{fl/fl}$ control thymocytes (Figure 6.17 D and E). The increment of $\gamma\delta$ T cells in this mouse model was greater than that observed upon the complete loss of NFATc1 (Figure 6.13 D, E, and F).

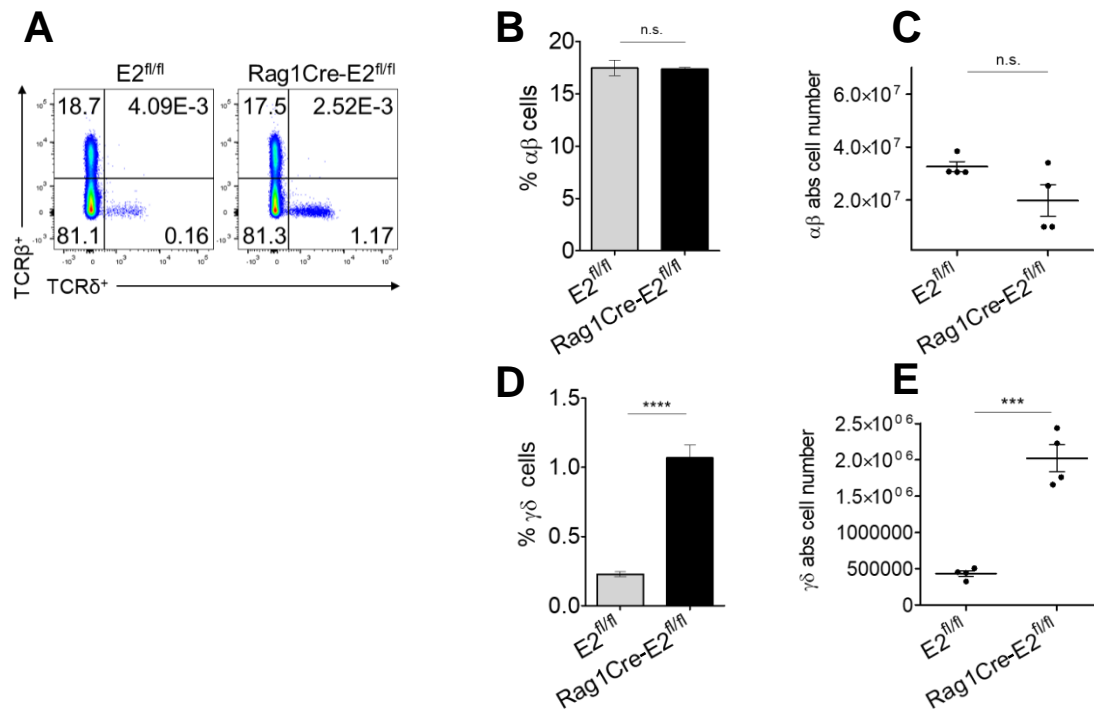


Figure 6.17 $\gamma\delta$ T cell number increases upon ablation of NFATc1/ α isoforms in the thymus.

(A) FACS analysis of thymocytes from *E2^{fl/fl}* control and *Rag1Cre-E2^{fl/fl}* mice. Total thymocytes were stained with anti-TCR δ^+ and anti-TCR β^+ Abs. The percentage of each population is indicated into the respective quadrants. (B) Percentage of $\alpha\beta$ T cells from *E2^{fl/fl}* control and *Rag1Cre-E2^{fl/fl}* mice. (C) Absolute cell numbers of $\alpha\beta$ T cells from *E2^{fl/fl}* control and *Rag1Cre-E2^{fl/fl}* mice. Each black dot represents one mouse. (D) Quantification of the percentage of $\gamma\delta$ T cells from *E2^{fl/fl}* control and *Rag1Cre-E2^{fl/fl}* mice. (E) Absolute cell numbers of $\gamma\delta$ T cells from *E2^{fl/fl}* control and *Rag1Cre-E2^{fl/fl}* mice. Each black dot represents one mouse.

Data are representative of four mice for every genotype and shown as mean \pm SEM. Unpaired student's t-test was performed. ***p-value < 0.001, ****p-value < 0.0001, n.s. non-significant.

To exclude that the increased positive signal of the TCR δ^+ thymocytes was influenced by a difficulty in detecting surface TCR β expression on DN thymocytes, we performed intracellular staining with anti-TCR β^+ and anti-TCR δ^+ antibodies. FACS analysis confirmed the increased transcription and translation of the TCR $\gamma\delta$ receptor in *Rag1Cre-E2^{fl/fl}* total and DN gated thymocytes (Figure 6.18 A and D). The relative and absolute TCR $\gamma\delta$ cell number confirmed the increase of TCR $\gamma\delta$ cells in both gated populations (Figure 6.18 B, C, E, and F). Again, the intracellular staining showed an increase in the population of thymocytes expressing both the intracellular TCR β^+ and the TCR δ^+ chains in NFATc1/ α -deficient mice, in both total and DN thymocytes (0.037% in total *E2^{fl/fl}* vs 0.59% in *Rag1Cre-E2^{fl/fl}*, and 0.62% in DN *E2^{fl/fl}* vs 4.84% in *Rag1Cre-E2^{fl/fl}*) (Figure 6.18 A and 6.18 D).

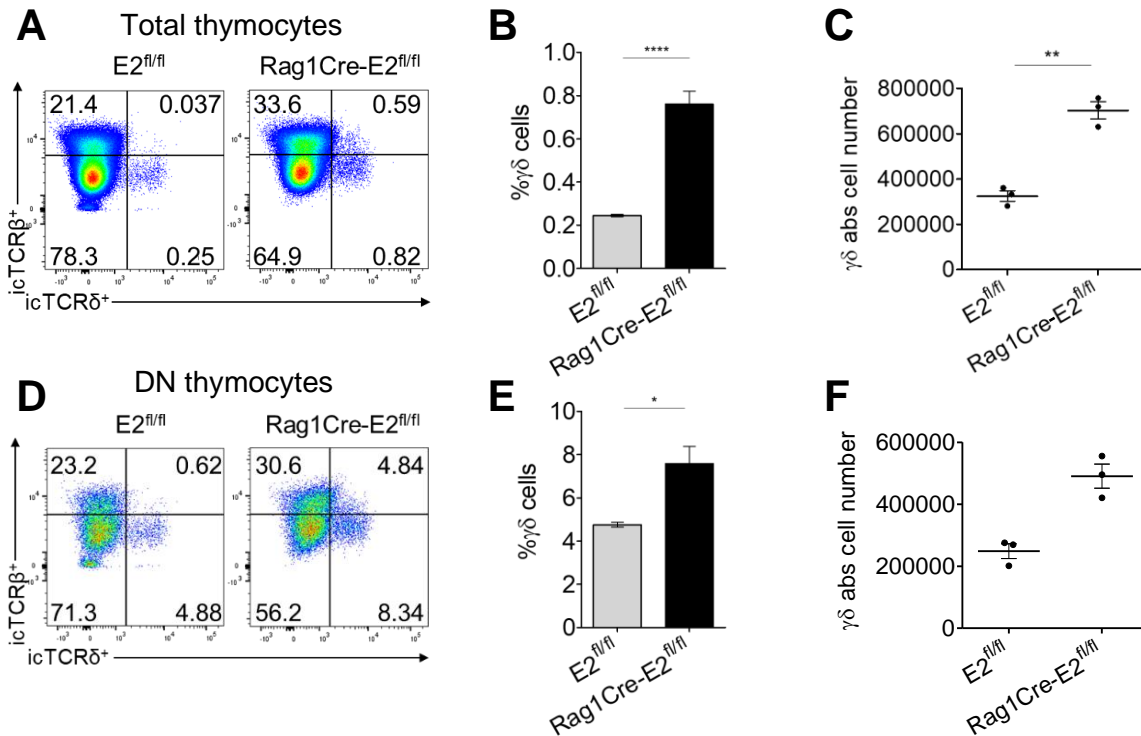


Figure 6.18 $\gamma\delta$ T cell number increases upon ablation of NFATc1/ α isoforms in the thymus.

(A) Intracellular staining was performed with $E2^{fl/fl}$ and $Rag1Cre-E2^{fl/fl}$ thymocytes with anti-TCR δ^+ and anti-TCR β^+ Abs. The percentage of each population is indicated adjacent to the respective gate. Gate applied on living thymocytes. (B) Percentage of intracellular δ^+ T cells in $E2^{fl/fl}$ control and $Rag1Cre-E2^{fl/fl}$ mice. (C) Absolute cell numbers of $\gamma\delta$ T cells in thymi from $E2^{fl/fl}$ control and $Rag1Cre-E2^{fl/fl}$ mice. Each black dot represents one single mouse. (D) Thymocytes as in A gated for DN thymocytes. (E) Percentage of intracellular δ^+ T cells in $E2^{fl/fl}$ control and $Rag1Cre-E2^{fl/fl}$ DN thymocytes. (F) Absolute cell numbers of $\gamma\delta$ T cells in DN thymocytes from $E2^{fl/fl}$ control and $Rag1Cre-E2^{fl/fl}$ mice. Each black dot represents one single mouse.

Data are representative of three mice for every genotype and shown as mean \pm SEM. Unpaired student's t-test was performed. *p-value < 0.05, **p-value < 0.005, ****p-value < 0.0001.

6.10 NFATc1 deficiency increases the level of CD4 $^+$ $\gamma\delta$ T cells

We showed above that the increase of $\gamma\delta$ T cell population in $Rag1Cre-Nfatc1^{fl/fl}$ thymocytes occurred together with a slight decrease of $\alpha\beta$ T cells. However this decrease was though, non-significant (Figure 6.13 B and C). It is known that thymic $\gamma\delta$ T cells are enriched in the CD4 $^-$ and CD8 $^-$ thymocyte population, as they do not express any of these co-receptors. Some $\gamma\delta$ T cell populations can express CD8 in the murine thymus^{200, 201}. In human, the population of $\gamma\delta$ CD8 $\alpha\alpha^+$ T cells is predominantly enriched in the gut²⁰².

We wanted to characterize the $\gamma\delta$ thymocyte population in $Rag1Cre-Nfatc1^{fl/fl}$ mice, checking for the expression of surface markers. The analysis of some classic $\alpha\beta$ thymocyte markers, such as CD4 and CD8, revealed that the $\gamma\delta$ population in $Rag1Cre-Nfatc1^{fl/fl}$ mice expressed a higher level of CD4 co-receptor, in a dose-dependent manner, compared to $Nfatc1^{fl/fl}$ control

and *Rag1Cre-Nfatc1^{fl/+}* thymocytes (9.05% *Nfatc1^{fl/fl}*, 17.3% *Rag1Cre-Nfatc1^{fl/+}* and 41.7% *Rag1Cre-Nfatc1^{fl/fl}*) (Figure 6.19 A). An increase of four-fold was evident in the percentage of CD4⁺ γδ cells in NFATc1 ko compared to *Nfatc1^{fl/fl}* control thymocytes, and this increase was statistically significant (Figure 6.19 B).

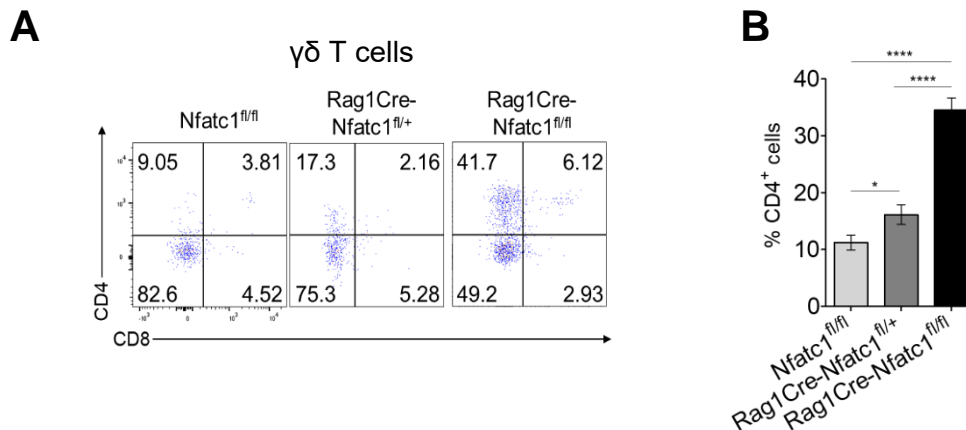


Figure 6.19 γδ T cells express high levels of CD4 co-receptor in mice bearing NFATc1-deficient thymocytes.

(A) FACS analysis of freshly isolated *Nfatc1^{fl/fl}*, *Rag1Cre-Nfatc1^{fl/+}* and *RagCre-Nfatc1^{fl/fl}* thymocytes. The thymocytes were stained with anti-CD4, anti-CD8, anti-CD3, anti-TCRδ⁺ and anti-TCRβ⁺ Abs. Thymocytes analysed by flow cytometry gated for γδ T cells and analysed for the expression of CD4 and CD8 markers. (B) Percentage of CD4⁺ γδ T cells from *Nfatc1^{fl/fl}*, *Rag1Cre-Nfatc1^{fl/+}* and *RagCre-Nfatc1^{fl/fl}* mice.

Data are representative of at least six mice from every genotype and are shown as mean ± SEM. Unpaired student's t-test was performed *p-value < 0.05, ****p-value < 0.0001.

The same analysis was carried out using thymocytes from the *Rag1Cre-E2^{fl/fl}* mice to understand if only the lack of the inducible *Nfatc1α* isoforms led to a higher expression of the co-receptor CD4 on the cell surface of γδ thymocytes. FACS analysis revealed that the γδ population in *Rag1Cre-E2^{fl/fl}* mice expressed a higher level of CD4 co-receptors compared to *E2^{fl/fl}* control thymocytes (8.5% *E2^{fl/fl}* and 42% *Rag1Cre-Nfatc1fl/fl*) (Figure 6.20 A). The percentage of γδ CD4⁺ cells in *Rag1Cre-E2^{fl/fl}* mice increased significantly by four-fold compared to *E2^{fl/fl}* control thymocytes (Figure 6.20 B). The increase of the percentage of CD4⁺ γδ T cells in *Rag1Cre-E2^{fl/fl}* was the same as in *Rag1Cre-Nfatc1^{fl/fl}* (Figure 6.19 A and 6.20 A).

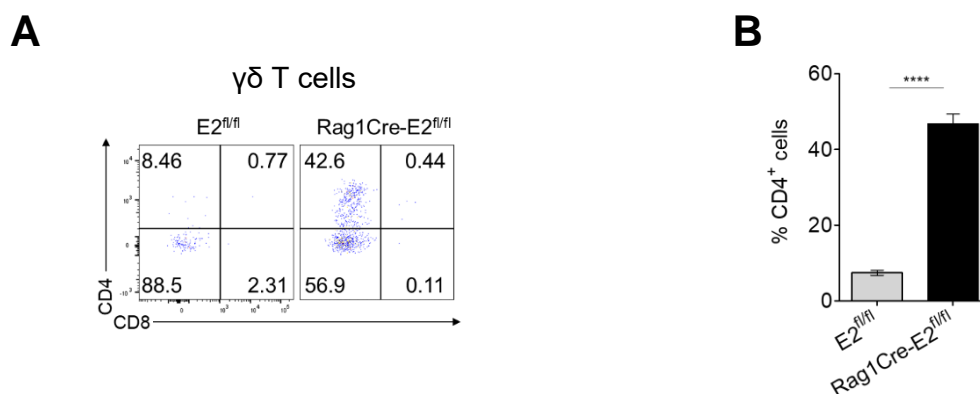


Figure 6.20 $\gamma\delta$ T cells express a high level of CD4 co-receptor in the absence of NFATc1/ α isoforms.

(A) FACS analysis of freshly isolated E2^{fl/fl} and Rag1Cre-E2^{fl/fl} thymocytes. The thymocytes were stained with anti-CD4, anti-CD8, anti-CD3, anti-TCR δ ⁺ and anti-TCR β ⁺ Abs. Thymocytes gated for $\gamma\delta$ and analysed for the expression of CD4 and CD8 markers. (B) Percentage of CD4⁺ $\gamma\delta$ T cells in E2^{fl/fl} and Rag1Cre-E2^{fl/fl} mice.

Data are representative of at least six mice from every genotype and are shown as mean \pm SEM. Unpaired student's t-test was performed *p-value < 0.05, ****p-value < 0.0001.

6.11 CD24^{low/-} $\gamma\delta$ T cells increase upon loss of NFATc1

Among the surface markers that characterize the developmental stages of $\gamma\delta$ T cells, as well as thymocyte development¹⁸, CD24 expression is an indicator for the differentiation status of the thymocytes. While CD24⁺ indicates more immature $\gamma\delta$ T cells, low expression or no expression of CD24 on their cell surface marks cells that have acquired their effector potential of IFN- γ or IL17-A secretion, respectively¹²⁷.

Control *Nfatc1*^{fl/fl}, *Rag1Cre-Nfatc1*^{fl/+} and *Rag1Cre-Nfatc1*^{fl/fl} thymocytes were stained with Abs for TCR δ ⁺ and CD24. FACS analysis showed a gradual increase in the percentage of $\gamma\delta$ thymocytes with no expression of the CD24 surface marker on *Rag1Cre-Nfatc1*^{fl/+} and *Rag1Cre-Nfatc1*^{fl/fl} thymocytes (11.5% in *Nfatc1*^{fl/fl} control, 27.6% in *Rag1Cre-Nfatc1*^{fl/+} and 51.5% in *Rag1Cre-Nfatc1*^{fl/fl} thymocytes). In parallel, a gradual decrease of the percentage of $\gamma\delta$ thymocytes that express CD24 surface marker in *Rag1Cre-Nfatc1*^{fl/+} and *Rag1Cre-Nfatc1*^{fl/fl} mice was also observed (88.5% in *Nfatc1*^{fl/fl} control, 72.0% in *Rag1Cre-Nfatc1*^{fl/+} and 48.5% in *Rag1Cre-Nfatc1*^{fl/fl} thymocytes) (Figure 6.21 A). The percentage of CD24⁻ and CD24⁺ $\gamma\delta$ thymocytes for each genotype is indicated in figure 6.21 B. The absolute cell number calculated from the FACS analysis confirmed the decrease of CD24⁺ cells and the increase of CD24⁻ $\gamma\delta$ thymocytes in *Nfatc1* ko mice (Figure 6.21 C).

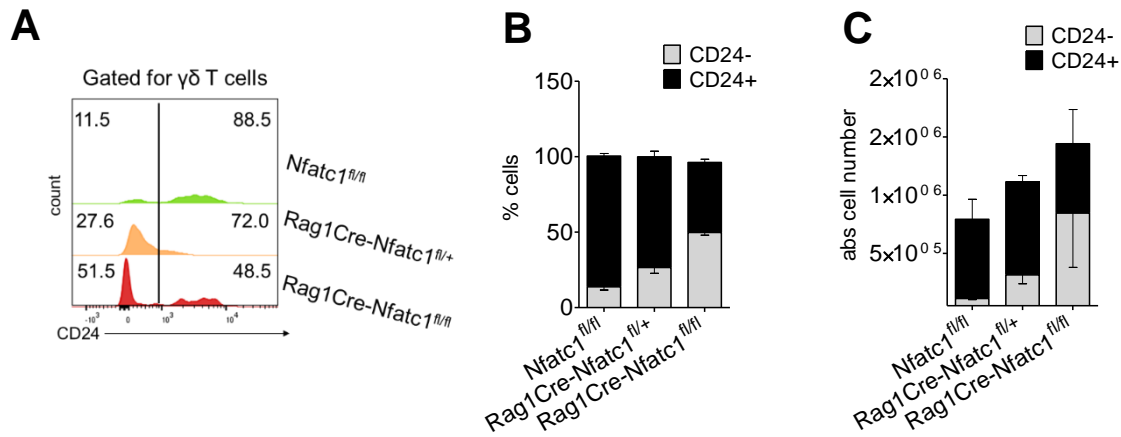


Figure 6.21 NFATc1 deficient γδ thymocytes express a low level of the differentiation marker CD24.

(A) FACS analysis of *Nfatc1^{fl/fl}* control, *Rag1Cre-Nfatc1^{fl/+}* and *Rag1Cre-Nfatc1^{fl/fl}* total thymocytes stained with anti-TCRδ⁺ and anti-CD24 Abs. The histogram shows the percentage of γδ T cells expressing CD24 (on the x axis) in each genotype. The percentage of CD24^{low/-} and CD24⁺ cells is indicated adjacent to the respective gate. (B) Percentage of CD24^{low/-} and CD24⁺ γδ T cells from *Nfatc1^{fl/fl}* control, *Rag1Cre-Nfatc1^{fl/+}* and *Rag1Cre-Nfatc1^{fl/fl}* mice, calculated in A. (C) Absolute numbers of CD24^{low/-} and CD24⁺ γδ T cells calculated from A, from *Nfatc1^{fl/fl}* control, *Rag1Cre-Nfatc1^{fl/+}* and *Rag1Cre-Nfatc1^{fl/fl}* mice.

Similar analyses were performed with the *Rag1Cre-E2^{fl/fl}* mice. FACS staining of thymocytes with anti-TCRδ⁺ and anti-CD24 showed a drastic increase of CD24⁺ thymocytes in *Rag1Cre-E2^{fl/fl}* compared to *E2^{fl/fl}* mice (14.6% in *E2^{fl/fl}* and 70.2% in *Rag1Cre-E2^{fl/fl}* thymocytes) together with a great decrease of γδ T cells expressing CD24 surface marker (83.0% in *E2^{fl/fl}* and 29.2% in *Rag1Cre-E2^{fl/fl}* thymocytes) (Figure 6.22 A). The percentage and the absolute cell number of γδ T cells CD24⁻ and CD24⁺ are indicated (Figure 6.22 B and C).

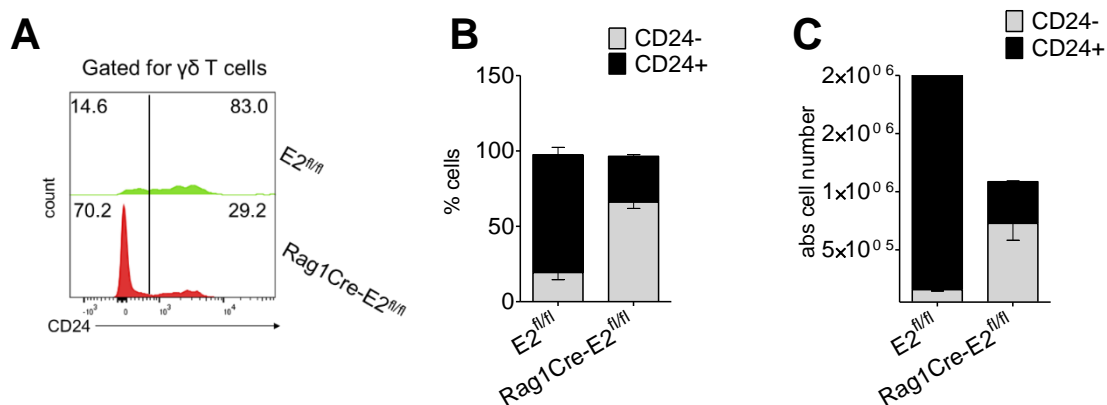


Figure 6.22 NFATc1/α-deficient γδ thymocytes express a low level of the differentiation marker CD24.

(A) FACS analysis of *E2^{fl/fl}* control and *Rag1Cre-E2^{fl/fl}* total thymocytes stained with mouse anti-CD24. The histogram shows the percentage of γδ T cells expressing CD24 (on the x axis) in each genotype. The percentage of CD24^{low/-} and CD24⁺ cells is indicated adjacent to the respective gate. (B) Percentage of CD24^{low/-} and CD24⁺ γδ T cells from *E2^{fl/fl}* control and *Rag1Cre-E2^{fl/fl}* mice, calculated in A. (C) Absolute number of CD24^{low/-} and CD24⁺ γδ T cells from *E2^{fl/fl}* control and *Rag1Cre-E2^{fl/fl}* mice.

These results suggest that in NFATc1-deficient $\gamma\delta$ thymocytes CD24 surface marker is not expressed.

Our CHIP-seq assays showed the binding of NFATc1/A at the *Cd24a* gene locus, in a region located upstream of the TSS. This region corresponds to the promoter of the *Cd24a* gene. Our observation suggests that NFATc1/A binds to the promoter of the *Cd24a* locus and thereby controls its activity (Figure 6.23 A).

To confirm the regulation of the *Cd24a* gene by NFATc1, we performed real-time PCR analysis on isolated $\gamma\delta$ thymocytes. Figure 6.23 B shows that in both *Nfatc1* ko and *Nfatc1 α* ko $\gamma\delta$ thymocytes, *Cd24a* expression is reduced by ~50% or more compared to control $\gamma\delta$ thymocytes.

These results indicate that NFATc1 controls positively the expression of the *Cd24a* gene. Therefore, in *Rag1Cre-Nfatc1^{fl/fl}* and *Rag1Cre-E2^{fl/fl}* mice, a large number of $\gamma\delta$ thymocytes do not express the CD24 surface marker.

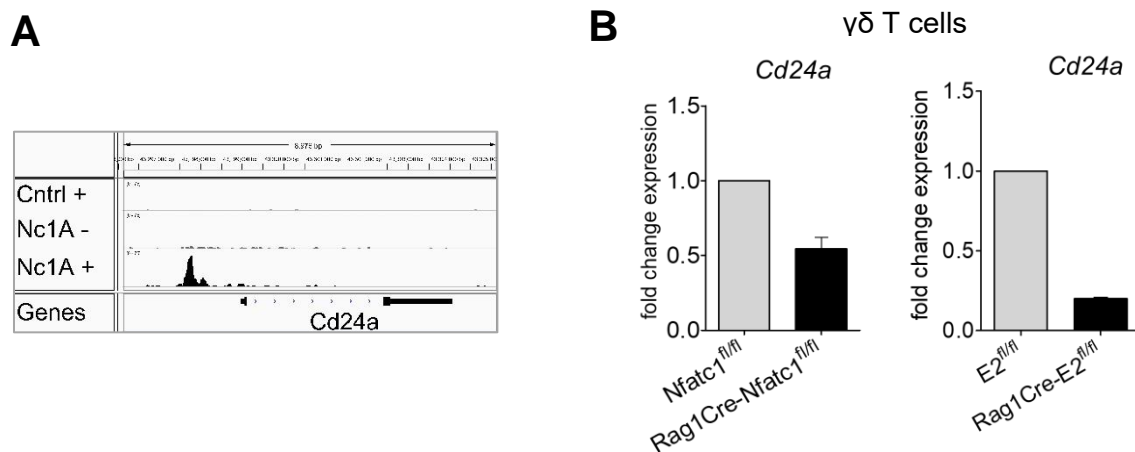


Figure 6.23 *Cd24a* is a potential NFATc1 target gene.

(A) NFATc1/A binding at the *Cd24a* locus. Visualized with IGV software. (B) Fold change expression of the *Cd24a* gene assessed by qRT-PCR in $\gamma\delta$ T cells isolated from *Nfatc1^{fl/fl}* and *Rag1Cre-Nfatc1^{fl/fl}* mice (on the left) and from *E2^{fl/fl}* and *Rag1Cre-E2^{fl/fl}* (on the right). Data are from at least two independent experiments and are shown as mean \pm SEM. Gene expression was normalized to that of *Actb* gene and expressed as fold induction relative to the gene expression in control *Nfatc1^{fl/fl}* and *E2^{fl/fl}* $\gamma\delta$ T cells.

6.12 NFATc1 regulates important genes for $\gamma\delta$ T cells development

The fate decision between $\alpha\beta$ and $\gamma\delta$ T cell occurs at the DN2 stage during the thymocyte development. Due to the increase in $\gamma\delta$ T cells in *Rag1Cre-Nfatc1^{f/f}* mice, we speculated that NFATc1 could play a role in determining the $\alpha\beta$ and $\gamma\delta$ T cell fate. Therefore, we asked whether some genes involved in $\gamma\delta$ T cell development are also NFATc1 target genes. We performed RNA-seq analysis of isolated DN thymocytes from *Nfatc1/A-Bio.BirA* and *BirA* control littermates that were either stimulated with TPA and ionomycin or left unstimulated. The resulting reads were aligned with the mm9 genome and processed by using the software R. Among the resulting genes, we selected the ones with a $\log_2FC \geq 1$ or ≤ -1 , and with a p-value ≤ 0.05 in the presence of NFATc1 overexpression (in *Nfatc1/A-Bio.BirA* mice) and/or stimulation. Out of the selected genes, some were involved in the early stages of T cell development, such as *Ikzf1*, *Tbx21*, some in the movement of thymocytes along different thymic zones, such as the chemokine receptors *Ccr4*, *Ccr7*, *Ccr8*, and *Ccr9*, and some in cell survival and apoptosis, such as the Bcl2 family members *Bcl2a1a*, *1b*, and *1d*, and *Fas*. Surprisingly, while genes associated with T cell functions and activation were downregulated, such as the *Gzmb* and *Ifng* genes, a great number of genes involved in thymocyte development were also downregulated (Figure 6.24 A)¹.

We sorted out some genes that are known to antagonize the $\alpha\beta$ lineage toward the $\gamma\delta$ T cells differentiation and that are involved in the $\gamma\delta$ T cells effector commitment. Some identified are the *Tcrg* constant region gene segment, and the *Egr2*, *Egr3*, *Sox13*, *Nr4a1*, and *Nr4a3* genes. A more closed view, represented in the volcano plot (Figure 6.24 B), showed that NFATc1 overexpression in combination or without additional stimulation downregulated these $\gamma\delta$ T cell genes. We confirmed the downregulation of these genes in *ex vivo* isolated DN thymocytes from *Nfatc1/A-Bio.BirA* and control *BirA* mice by real-time PCR analysis (Figure 6.24 C).

¹ The RNA-seq analysis was carried out in collaboration with Konrad Knöpper, AG Kastenmüller, Institute of System Immunology, University of Würzburg.

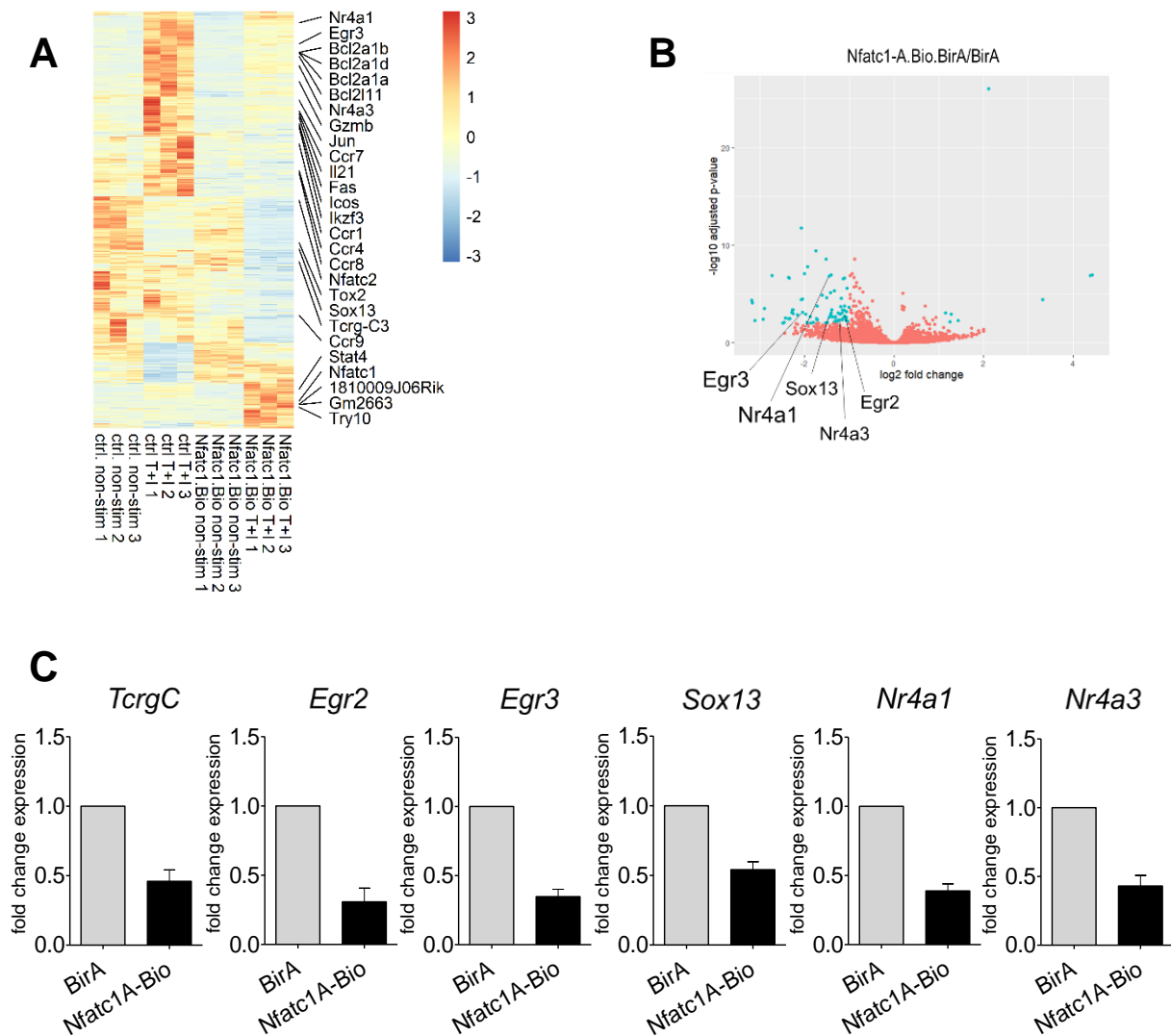


Figure 6.24 Potential NFATc1 target genes in DN thymocytes involved in $\gamma\delta$ T cell development.

(A) Heat-map of selected genes differentially expressed in isolated DN thymocytes from *Nfatc1/A-Bio.BirA* and *BirA* mice. The cells were stimulated for 4h with T+I or left unstimulated. The extracted RNA was subjected to RNA-seq and the results were analysed with DESeq2 package in the R software. The genes were selected for a log₂FC ≥ 1 or ≤ -1 and a p-value < 0.05 . (B) Volcano plot of specific genes involved in $\gamma\delta$ T cell development. The genes resulted from the R analysis and showed a log₂FC ≤ 1 in *Nfatc1/A-Bio.BirA* compared to *BirA* mice. (C) Fold change expression of the $\gamma\delta$ T cell-selected genes in isolated DN thymocytes from *Nfatc1/A-Bio.BirA* and *BirA* mice, analysed by qRT-PCR. Gene expression was normalized to that of *Actb* gene and was expressed as fold induction relative to the gene expression in control *BirA* thymocytes. Data are from at least three independent experiments and are shown as mean \pm SEM.

Furthermore, our ChIP analysis showed NFATc1 binding sites along the loci of these genes. The NFATc1 binding sites were located mostly upstream of the transcription start site (TTS) of each locus, suggesting that NFATc1 binds at the promoter/regulatory elements of the genes (Figure 6.25 A).

A

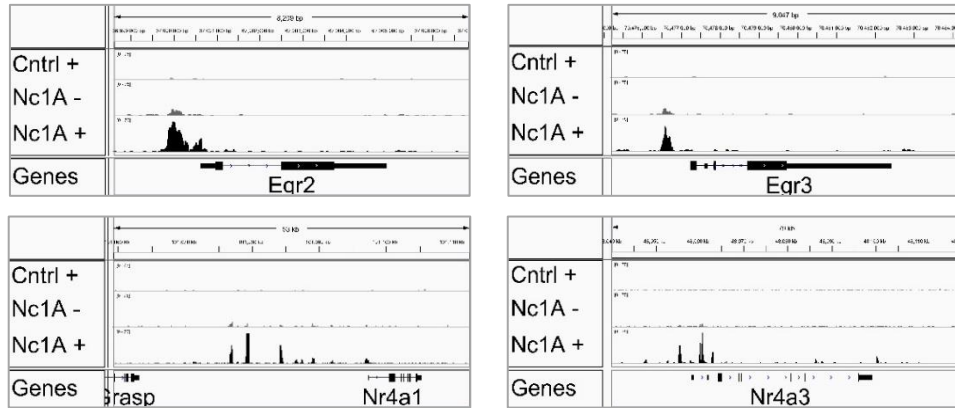


Figure 6.25 Binding of NFATc1/A at the locus of genes involved in $\gamma\delta$ T cell development.

(A) NFATc1 binding sites nearby the loci of *Egr2*, *Egr3*, *Nr4a1* and *Nr4a3* genes. The data are from the ChIP-seq analysis previously described.

We verified the transcriptional regulation of these $\gamma\delta$ genes by real-time PCR in isolated DN thymocytes from *Rag1Cre-Nfatc1^{fl/fl}* and *Rag1Cre-E2^{fl/fl}* mice. The PCRs showed that indeed, in the absence of either the complete NFATc1 or of the NFATc1/ α isoforms, the expression of these genes increased at least by two-fold (Figure 6.26 A and 6.27 A). Taken together these data show that NFATc1 and, in particular, its inducible isoforms regulate directly some of the genes involved in $\gamma\delta$ T cell development.

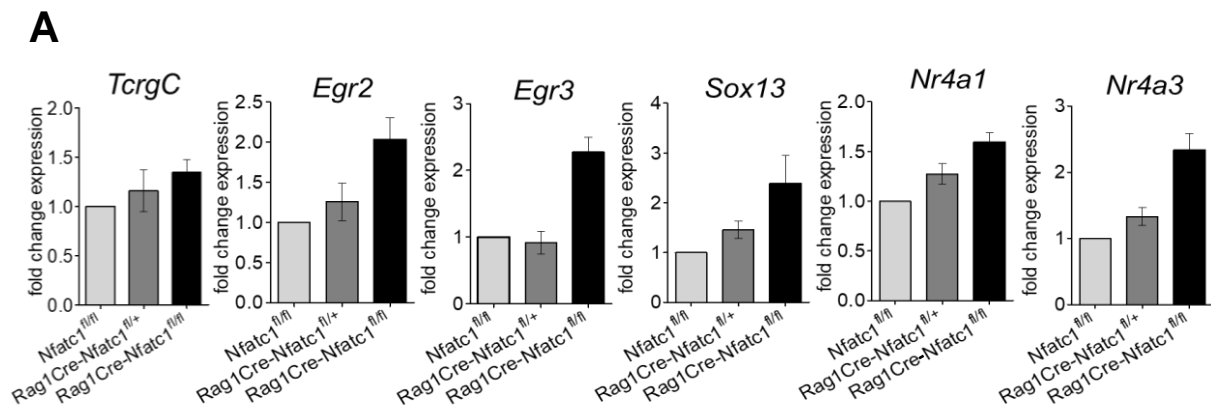


Figure 6.26 Transcriptional regulation of genes involved in $\gamma\delta$ T cell development in DN thymocytes.

(A) Fold change expression of the $\gamma\delta$ T cell-genes in *ex vivo* isolated DN thymocytes from *Rag1Cre-Nfatc1^{fl/fl}* and *Rag1Cre-Nfatc1^{fl/+}* mice compared to *Nfatc1^{fl/fl}* controls, analysed by qRT-PCR. Gene expression was normalized to that of *Actb* gene and expressed as fold induction relative to the gene expression in control *Nfatc1^{fl/fl}* thymocytes. Data are from at least three independent experiments and are shown as mean \pm SEM.

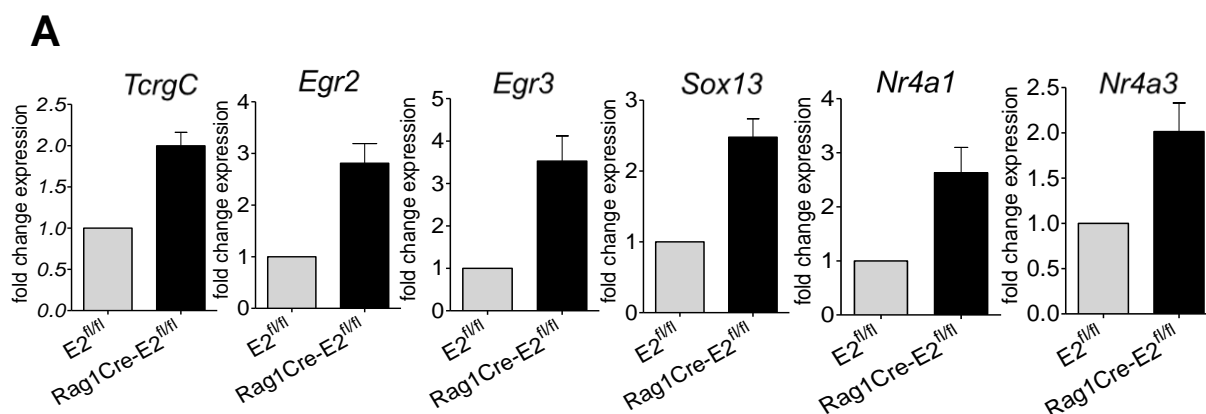


Figure 6.27 Transcriptional regulation of genes involved in $\gamma\delta$ T cell development in DN thymocytes.

(A) Fold change expression of the $\gamma\delta$ - genes in *ex vivo* $Rag1Cre-E2^{fl/fl}$ compared to $Nfatc1^{fl/fl}$ control DN thymocytes, analysed by qRT-PCR. Gene expression was normalized to that of *Actb* gene and expressed as fold induction relative to the gene expression in control $E2^{fl/fl}$ thymocytes. Data are from at least three independent experiments and are shown as mean \pm SEM.

6.13 Differential expression of the Bcl2 family members in NFATc1-deficient $\gamma\delta$ T cells

Another question to be addressed was about the mechanism behind the increased number of $\gamma\delta$ T cells in $Rag1Cre-Nfatc1^{fl/fl}$ mice. We checked the expression levels of some genes related to cell survival, or anti-apoptotic genes, in isolated $\gamma\delta$ from $Rag1Cre-Nfatc1^{fl/fl}$ and control mice. Among the anti-apoptotic Bcl2 family members, we investigated the expression of two members of the Bcl2 family, *Bcl2* and *Bcl2a1a* (encoding A1) genes. Patra *et al.* reported in previous studies that NFATc1 positively regulates the expression of the *Bcl2* gene during the early stages of thymocyte development (DN1-DN3). In addition, in our CHIP assays we demonstrated the binding of NFATc1/A to the *Bcl2* gene, in stimulated thymocytes from $Nfatc1/A-Bio.BirA$ mice (Figure 6.4 C). In our expression analysis in isolated $\gamma\delta$ T cells, the lack of NFATc1 leads to a decrease in *Bcl2* gene expression (Figure 6.28 A), while this was not observed in isolated DN and DP+SP thymocytes from $Rag1Cre-Nfatc1^{fl/fl}$ mice (Figure 6.28 B).

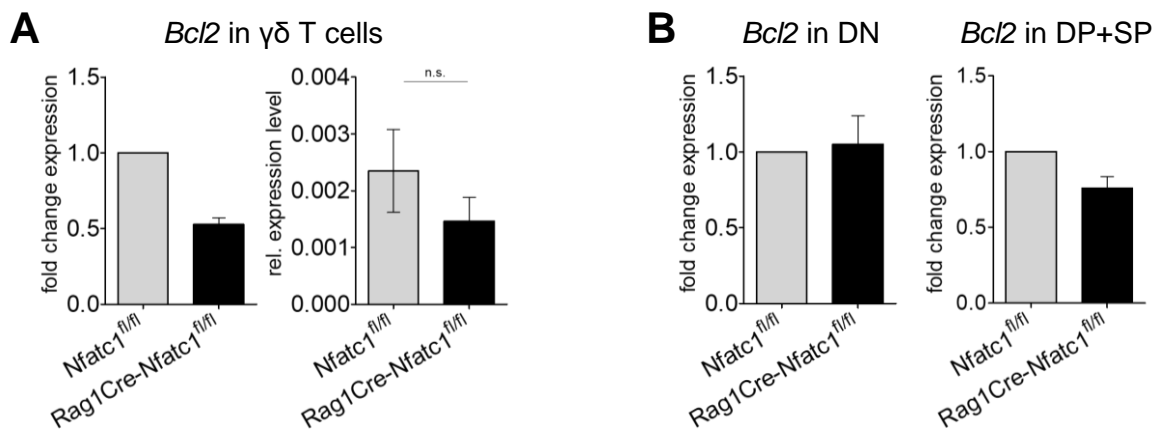


Figure 6.28 Differential *Bcl2* expression in NFATc1-deficient thymocytes.

(A) Fold change and relative expression of the *Bcl2* gene in freshly isolated $\gamma\delta$ T cells from *Nfatc1^{fl/fl}* and *Rag1Cre-Nfatc1^{fl/fl}* mice. The analysis was carried out by qRT-PCR. (B) Fold change expression of the *Bcl2* gene in freshly isolated DN and DP+SP thymocytes from *Nfatc1^{fl/fl}* and *Rag1Cre-Nfatc1^{fl/fl}* mice. The analysis was carried out by qRT-PCR. Gene expression was normalized to that of *Actb* gene and expressed as fold induction relative to *Nfatc1^{fl/fl}* control thymocytes (only for the fold change expression). Data are indicative of at least three independent experiments and are shown as mean \pm SEM.

Interestingly, other members of the *Bcl2* family, the *Bcl2a1a*, *Bcl2a1b*, and *Bcl2a1d* genes were highly upregulated in isolated $\gamma\delta$ thymocytes from *Rag1Cre-Nfatc1^{fl/fl}* mice (Figure 6.29 A and S4). We also confirmed that the *Bcl2a1a* upregulation in NFATc1-deficient thymi occurred in isolated DN thymocytes from *Rag1Cre-Nfatc1^{fl/fl}* mice (Figure 6.29 B). We did not observe the *Bcl2a1a* upregulation in DP+SP thymocyte populations from *Rag1Cre-Nfatc1^{fl/fl}* mice (Figure 6.29 B).

This was a rather unexpected result, as the *Bcl2* gene is positively regulated by NFATc1. These preliminary results could suggest that the increase of the $\gamma\delta$ cell number was due to the higher survival rate of NFATc1-deficient thymocytes.

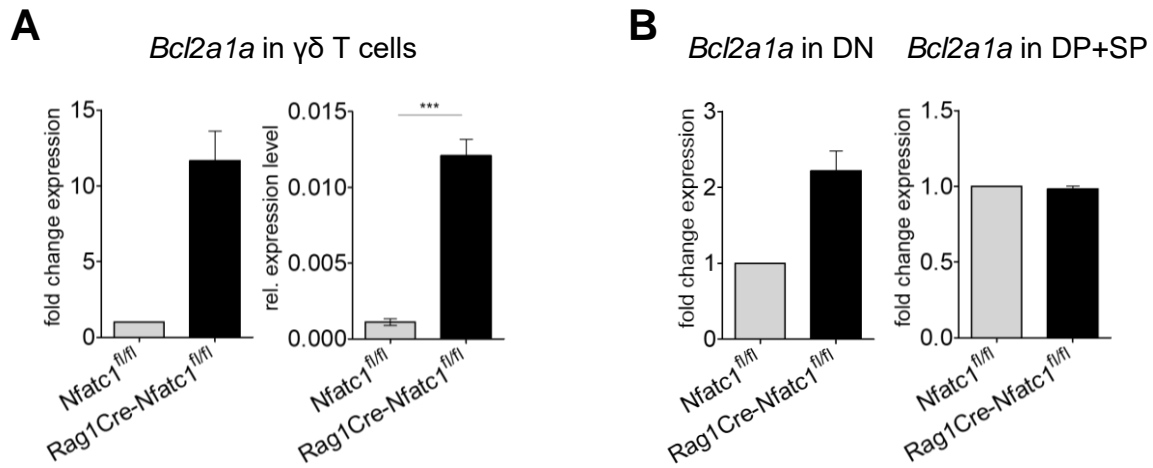


Figure 6.29 Differential expression of the Bcl2 family member *Bcl2a1a* in NFATc1-deficient thymocytes.

(A) Fold change and relative expression of the *Bcl2a1a* gene in freshly isolated $\gamma\delta$ T cells from *Nfatc1^{fl/fl}* and *Rag1Cre-Nfatc1^{fl/fl}* mice. The analysis was carried out by qRT-PCR. (B) Fold change expression of *Bcl2a1a* gene in freshly isolated DN and DP+SP thymocytes from *Nfatc1^{fl/fl}* and *Rag1Cre-Nfatc1^{fl/fl}* mice. The analysis was carried out by qRT-PCR. Gene expression was normalized to that of *Actb* gene and expressed as fold induction relative to *Nfatc1^{fl/fl}* control thymocytes (only for the fold expression).

Data are indicative of at least three independent experiments and are shown as mean \pm SEM.

7 Discussion

7.1 Identification of NFATc1/A target genes that control thymocyte development

In the *VavCre-Nfatc1^{fl/fl}* mouse model, previously studied by Patra *et al.*⁴, the deletion of NFATc1 in hematopoietic lineage cells induces a block at the DN1 stage, resulting in a defect in differentiation and an accumulation of cells at the DN stage of development. The block of thymocyte differentiation is associated with a dramatic reduction in thymic cellularity and the generation of a very small thymus, compared to *Nfatc1^{fl/fl}* control animals⁴. However, in our *Rag1Cre-Nfatc1^{fl/fl}* mouse model, however, we observed a much-moderated decrease in thymic cellularity and no differences in thymic size (Figure 6.10 A). Compared to the *VavCre-Nfatc1^{fl/fl}* mouse model, our *Rag1Cre-Nfatc1^{fl/fl}* model leads to the specific NFATc1 deletion during the DN stages of thymocytes development, when the cells restrict their potential to give rise to myeloid and lymphoid lineages, toward the T cell lineage specification. This suggests that the role of NFATc1 is strictly developmental stage-specific and the difference in the phenotype of the *VavCre-Nfatc1^{fl/fl}* and the *Rag1Cre-Nfatc1^{fl/fl}* mice could be due to the stage where NFATc1 activity is absent in these models.

Besides, in *VavCre-Nfatc1^{fl/fl}* thymocytes, the genes essential for T cell commitment and differentiation, as of *Notch1*, *Bcl11b*, *Tcf7*, and *Gata3* genes are normally expressed⁵. It could be likely that NFATc1 is not involved in the early T cell commitment processes, but later in the control of fate decision between $\alpha\beta$ and $\gamma\delta$ thymocytes.

The results of our study confirm the importance of the role of NFATc1 not only in thymocyte development but also in the lineage fate choice between $\alpha\beta$ and $\gamma\delta$ T cells.

Patra *et al.*⁴ showed an alternative NFATc1 activation system occurring during the pre-TCR-negative DN stages of thymocyte development. This pathway of activation leads the P2 promoter products NFATc1/ β A, NFATc1/ β B, and NFATc1/ β C to be phosphorylated via the IL-7R-JAK3-STAT5 pathway and to translocate from the cytoplasm to the nucleus⁴. The induction of the *Nfatc1* (P1 promoter products-*Nfatc1 α* isoforms) gene occurs upon the pre-TCR and TCR signaling in thymocytes. However, the population of DN3 thymocytes shows the highest level of NFATc1 in the nucleus, compared to pre-TCR bearing DN4 thymocytes^{4, 5, 180}. Nonetheless, the majority of NFATc1 during the DN3 stage is represented by the P2-transcribed β isoforms, compared to the DN4 stage, in which the inducible α forms are mostly present⁵. In the two well-known models of *Rag1^{-/-}* and Δ Cam tg mice, the thymocyte development is arrested at the DN3 stage. In both types of mice, a defect in the pre-TCR signaling is the obvious reason for this block in differentiation⁵.

To clarify the molecular role of NFATc1 in thymocyte development, we wondered which genes are the target of NFATc1 during this process. For this purpose, we performed ChIP-seq and RNA-seq assays. In the past years, our laboratory focused specifically on the identification of genes regulated by the short isoform, NFATc1/A, which differs in numerous properties from all other NFATc proteins. In particular, NFATc1/A supports the survival of T lymphocytes²⁰³ and seems to enhance the anti-tumor activity of cytotoxic T cells (unpublished data). Due to the lack of a specific ChIP-grade antibody against this isoform, a mouse model has been generated, that was designated as *Nfatc1/A-Bio.BirA* tg mice. The characteristics of this line have been previously described (see section 6.1). Thereby, in previous studies, the use of the *Nfatc1/A-Bio.BirA* mouse model allowed the identification of target genes that are controlled by NFATc1/A in cytotoxic CD8⁺ cells¹⁹⁵. This mouse model ensures the high specificity for NFATc1/A bound to chromatin fragments, as it is based on purification by the strong affinity of Biotin/Streptavidin. While in those mice, the bacterial BAC vector contains the complete *Nfatc1* gene locus, only the NFATc1/A isoform is expressed together with the biotin-tag. The integration of the bacterial BAC vector into the mouse genome results in the presence of a third *Nfatc1* allele, leading to NFATc1 overexpression (Figure 6.1 C, D, and E). We made use of this overexpression to identify fold changes in gene expression in *Nfatc1/A-Bio.BirA* thymocytes compared to *BirA* controls in RNA-seq analysis. NFATc1 overexpression in *Nfatc1/A-Bio.BirA* mice seemed to be more close to physiological conditions, compared to the situation in Δ Cam mice, a mouse model expressing a constitutively active Calcineurin A deleted form, leading to overactivated NFATc1 factors^{5, 186}.

It is well known that TPA and ionomycin stimulation, which mimics the pre-TCR and TCR stimulation, induces NFATc1 activation and the translocation of the NFAT factors into the nucleus. In peripheral T and B cells, an increase of the *Nfatc1* gene expression, and in particular of the inducible short isoform *Nfatc1 α A*, is reached after 24h of primary receptor stimulation, and in few hours after a secondary stimulation^{203,197}. Surprisingly, in thymocytes, NFATc1/A-Bio is induced already after 4h of TPA and ionomycin stimulation (Figure S1).

In the first set of experiments, performing ChIP-seq analysis of total thymocytes, we intended to get a broad view about NFATc1/A-regulated genes involved in thymocyte differentiation. The stimulation of thymocytes with TPA and ionomycin increased the activity of NFATc1 and, therefore, enhancing the chances of NFATc1 binding to its target genes. Using the *Nfatc1/A-Bio.BirA* mice and applying multiple assays (ChIP-seq, RNA-seq, qRT-PCR assay, etc.), we have identified several genes that play a critical role in thymocyte differentiation in general and in the $\gamma\delta$ T cell development in particular.

The combination of the RNA-seq together with ChIP-seq analyses allowed us to discriminate between genes that are regulated specifically by NFATc1/A, and those that are controlled by TPA and ionomycin treatment only, or by both in combination.

The regulation of numerous genes, such as *Tcf7*, *Ikzf1*, *Zap70*, *Ccr9*, and *Rorc* genes by NFATc1, that are known to be involved in thymocyte development, confirmed previous observations on the essential role of NFATc1 during thymocyte differentiation. Some of these genes are known to be NFATc1 target genes in peripheral T cells^{204, 205}. An important finding from our analysis is that NFATc1 regulates these genes also during thymocyte development in the thymus.

Ccr4, *Ccr8*, *Ccr7*, and *Ccr9* are four members of the chemokine receptor family that are expressed on thymocytes and involved in the movement of the thymocytes along the various thymic niches^{206, 207, 208}. The expression of *Ccr9* directs the immigration of T cell progenitors into the thymus. After entering the thymus, thymocytes downregulate *Ccr9* expression until they experience the signaling through the pre-TCR^{209,243}. As pre-TCR-positive thymocytes have high NFATc1 activity, an NFATc1-mediated regulation of *Ccr9* expression can be expected. In peripheral CD4⁺T cells, NFATc1 was shown to impair the activity of NFATc2 in regulating the expression of the *Ccr9* gene^{205, 210}.

It has been shown that in stimulated peripheral human CD4⁺ T cells, NFATc1 and NFATc2 bind at the promoter of the *RORC* gene, recruiting p300/CBP histone acetyltransferases, but only NFATc2 contributes to the transcriptional upregulation of the *RORC* gene²⁰⁴.

It has been already shown that *Bcl2* is upregulated during the early stages of thymocyte development (DN1 stage) by NFATc1⁴. However, the results of our ChIP-seq assays demonstrate convincingly that NFATc1/A binds in thymocytes directly to the *Bcl2* gene locus and thereby, confirm and extend the data published previously⁵.

In Th cells, Ets-1 is required for nuclear entry of NFATc1 and, its physical association induces the recruitment of NFATc1 to the *Il2* promoter upon TCR stimulation²¹¹.

The enrichment analysis of binding motifs for TFs in purified chromatin fragments from *Nfatc1/A-Bio.BirA* thymocytes show significant enrichment of motifs for several factors involved in T cell development. The same analysis performed on CTLs showed the enrichment of binding motifs of different factors involved in T cell activation and cytokine signaling pathways (Figure 6.3 A and B).

This is a remarkable result, which suggests that NFATc1/A in association with specific partner transcription factors regulates critical aspects of thymocyte differentiation and in the context of CTLs, it requires a different set of factors to influence the function of mature T cells. We hypothesize that a physical association between NFATc1 and these various other TFs could be possible in a context-dependent manner to regulate thymocyte development and CTLs functions.

7.2 $\gamma\delta$ T cells increase in the absence of NFATc1

Thymocyte development is a well-coordinated process during which the cells go through several steps of differentiation, proliferation, and *Tcr* loci recombination to give rise to mature T cells. The $\alpha\beta$ versus $\gamma\delta$ T cell bifurcation step occurs between the DN2b and DN3a developmental steps when thymocytes start to recombine their *Tcrb*, *Tcrq*, and *Tcrd* loci. In the past, several theories have been proposed to explain the lineage fate of thymocytes. Up to now, the most popular is the strength-model theory: strong signaling coming from the T cell receptor favors the $\gamma\delta$ phenotype, while weaker signaling leads to $\alpha\beta$ lineage fate^{110, 111, 125}. The expression of NFATc1 in the thymus was shown to peak in the nuclei during the DN2-DN3 stage that corresponds well with the lineage fate decision point^{4, 126}. Upon pre-TCR signaling the inducible NFATc1 isoforms NFATc1/ α A, NFATc1/ α B, and NFATc1/ α C start to be upregulated. In DN1, DN2, and DN3 isolated thymocytes, the α isoforms are undetectable, while all the constitutive β isoforms of *Nfatc1*, NFATc1/ β A, NFATc1/ β B, and NFATc1/ β C are expressed at these stages, directed by the P2 promoter⁵. Therefore, since NFATc1 is a key transcription factor for thymocyte development, either in the pre-TCR-negative cells and in cells that have experienced pre-TCR signaling, we wondered if NFATc1/ α induction can be related to determining the lineage fate of developing thymocytes.

While the loss of NFATc1 induced a very moderate decrease in number and the percentage of $\alpha\beta$ T cells, the partial or complete loss of NFATc1 led to a dose-dependent increase of $\gamma\delta$ T cells. These findings lead us to hypothesize that NFATc1 controls the lineage fate decision between the two major T cell phenotypes. The observed weak decrease of $\alpha\beta$ thymocytes was certainly due to the relatively low percentage of $\gamma\delta$ compared to $\alpha\beta$ cells among all the thymocyte population. While, due to the level of NFATc1 expression, subtle changes in the population of $\gamma\delta$ thymocytes could readily be detected, those small changes in the large population of $\alpha\beta$ thymocytes remained undetected (Figure 6.13 B and C). We obtained the same results in the *Rag1Cre-E2^{fl/fl}* mouse model, in which the depletion of the E2 enhancer abolishes the expression of the inducible NFATc1/ α isoforms. In this mouse model, we did not observe a very strong but statistically significant decrease in thymic cellularity (Figure 6.12 A). In addition, in NFATc1/ α isoforms-deficient thymi, we observed a higher increase of $\gamma\delta$ T cells, compared to the increase of $\gamma\delta$ T cells in NFATc1-deficient thymi and a very moderate decrease in $\alpha\beta$ thymocyte population, as well.

The differences observed in our *Rag1Cre-Nfatc1^{fl/fl}* model compared to the *VavCre-Nfatc1^{fl/fl}* concerning the detrimental effects on thymocytes development are likely due to the importance of NFATc1 expression at specific stages during thymocytes development. At the DN stage during which *Rag1* expression occurs, NFATc1 is not crucial for thymocyte survival

as it is during the very early progenitor stages of T cell development⁴, but instead, it is required, as the marked effect on $\gamma\delta$ T cell formation shows, for thymocyte identity specification.

One unanticipated finding was that the $\gamma\delta$ T cells express higher levels of NFATc1 compared to $\alpha\beta$ T cells (Figure 6.15 A). The observed NFATc1 expression level in $\gamma\delta$ T cells could be attributed to the role of NFATc1 in these cells. We favour the hypothesis that NFATc1 keeps $\gamma\delta$ T cells “under control” in terms of proliferation. Indeed, when NFATc1 or NFATc1/ α are missing, as in *Rag1Cre-Nfatc1^{fl/fl}* and *Rag1Cre-E2^{fl/fl}* mice, we observed an expansion of $\gamma\delta$ T cells in the thymus. To support the idea that NFATc1 is involved in the decisional lineage fate between $\alpha\beta$ and $\gamma\delta$ thymocytes our RNA- and CHIP-seq analyses in the *Nfatc1/A-Bio.BirA* mouse model revealed the NFATc1/A binding and downregulation of numerous genes associated with the $\gamma\delta$ T cell development in the thymus (Figure 6.24 and 6.25). We then confirmed the regulatory role of NFATc1 and NFATc1/ α isoforms in the two NFATc1-deficient models, *Rag1Cre-Nfatc1^{fl/fl}* and *Rag1Cre-E2^{fl/fl}*. According to our predictions, the expression of selected genes was upregulated when NFATc1 was depleted (Figure 6.26 A and 6.27 A). The results of those assays indicate a suppressive role of NFATc1 in the regulation of genes important for $\gamma\delta$ T cell commitment. Thereby the absence of NFATc1 is correlated with an increase in the number of $\gamma\delta$ T cells.

Members of the Egr transcription family exert their functions already during the early stages of thymocyte development. It has been shown previously that NFATc1 and EGR1 act in concert to promote thymocyte differentiation beyond the β -selection²¹².

EGR2 and EGR3 are the most important factors for the commitment of early thymocytes toward the $\gamma\delta$ lineage, and important for T cell development at later stages^{110, 212}. In RNA-seq and qRT-PCR experiments with total *Nfatc1/A-Bio.BirA* thymocytes, the overexpression of *Nfatc1* induced an increase in both of these genes (data are not shown), in line with the importance of these genes in T cell development. In contrast, RNA-seq experiments from isolated DN cells showed a decreased expression level of *Egr2* and *Egr3* genes (Figure 6.24). We speculate that NFATc1 can play opposite roles and in the expression of both *Egr* genes in DN and later stages of thymocyte development. During the DN stage, the regulation of *Egr2* and *Egr3* genes, by an optimal level of NFATc1, appears to be essential for the $\alpha\beta$ and $\gamma\delta$ bifurcation step, while at later stages, the NFATc1-mediated regulation of Egr members is essential for the survival (and further differentiation) of thymocytes, and it is independent of the phenotype of thymocytes. In line with this regulation process, we observed an increment of expression levels of these genes in NFATc1 or NFATc1/ α -deficient DN thymocytes from *Rag1Cre-Nfatc1^{fl/fl}* and *Rag1Cre-E2^{fl/fl}* mice (Figure 6.26 A and 6.27 A).

Another important gene involved in $\gamma\delta$ development is the *Sox13* gene¹²⁹. We observed a transcriptional regulation induced by NFATc1 in RNA-seq and confirmed in real-time PCR assays using cells from the *Nfatc1/A-Bio.BirA*, in *Rag1Cre-Nfatc1^{fl/fl}* and *Rag1Cre-E2^{fl/fl}* mouse

models. In ChIP experiments, we did not detect any NFATc1/A binding to a regulatory region of this gene. Therefore, NFATc1 appears to control indirectly the transcription of the *Sox13* gene. *Nr4a1* and *Nr4a3* are known to be NFATc1 target genes²¹³ and upregulated in $\gamma\delta$ T cell development, but up to now, their role in these cells upon NFATc1 regulation has not been shown.

Another interesting finding is the upregulation of genes belonging to the Bcl2-family, the *Bcl2* and *Bcl2a1a* genes^{95, 214, 215} (Figure 6.28 and 6.29). The *Bcl2a1a* gene was strongly upregulated in isolated NFATc1-deficient $\gamma\delta$ T cells and, with a less fold increase in DN thymocytes. We also confirmed the upregulation of other members of the Bcl2a family, the *Bcl2a1b* and *Bcl2a1d* genes in isolated $\gamma\delta$ T cells from *Rag1Cre-Nfatc1^{fl/fl}* mice (Figure S4). Among all the Bcl2-A1 is the most specific pro-survival factor that results upregulated upon the pre-TCR signaling in thymocytes⁹⁵. Interestingly, Patra *et al.* showed no differences in *Bcl2a1a* expression in *VavCre-Nfatc1^{fl/fl}* mouse model. In our *Rag1Cre-Nfatc1^{fl/fl}* mouse model, instead, the absence of NFATc1 in later stages, compared to a hematopoietic depletion, led to a strong upregulation of *Bcl2a1a*. These results lead us to the speculation that NFATc1 at this stage of development downregulates the expression of this anti-apoptotic gene during the β -selection. Our ChIP-seq analysis did not show any NFATc1/A binding along the *Bcl2a1a, 1b*, and *1d* genetic loci, suggesting that NFATc1 regulation on these genes is indirect. In *VavCre-Nfatc1^{fl/fl}* model, it has been shown that the *Bcl2* gene is regulated by NFATc1 during the DN1 stages. In our mouse model, we observed a decrease in the expression of the *Bcl2* gene in isolated $\gamma\delta$ T cells from *Rag1Cre-Nfatc1^{fl/fl}*, which was not confirmed in isolated DN and DP+SP thymocyte populations (Figure 6.28 B). Taken together, these results suggest that *Bcl2*, *Bcl2a1a, 1b*, and *1d* act at different stages of development, and that NFATc1 regulates them at specific steps, *Bcl2* at the early stages, and *Bcl2a* members at the later ones.

The more than ten-fold increase of expression of the Bcl2a members in $\gamma\delta$ T cells suggests a close link to the survival rate of these thymocytes. Although these preliminary results suggest that these $\gamma\delta$ T cells may survive better compared to their control counterpart, AnnexinV, and Ki67 stainings did not reveal any differences between *Rag1Cre-Nfatc1^{fl/fl}* and *Nfatc1^{fl/fl}* control thymocytes (data not shown). On the other hand, we speculate that the overexpression of Bcl2a members may give an advantage to $\gamma\delta$ T cells to survive. As the survival or the death of cells in the thymus is the result of the balance between the Bcl-2 family members (pro- and anti-apoptotic), these results do not rule out the influence of other factors in the $\gamma\delta$ survival.

We characterized the phenotype of the increased $\gamma\delta$ T cell population in *Rag1Cre-Nfatc1^{fl/fl}* and *Rag1Cre-E2^{fl/fl}* mice by stainings $\gamma\delta$ thymocytes with Abs against the CD24 surface marker. The results showed that in *Rag1Cre-Nfatc1^{fl/fl}* and *Rag1Cre-E2^{fl/fl}* mice a greater percentage of $\gamma\delta$ thymocytes missed CD24 expression on the cell surface, compared to their control littermates (Figure 6.21 A and 6.22 A). Among $\gamma\delta$ T cells, CD24⁺ marks more immature

stages of development of the cells, while missing CD24 expression indicates a phenotypical commitment toward one of the two pathways of differentiation, to IFN- γ or IL17-A producing $\gamma\delta$ T cells^{122, 127, 216}. From our experiments, we could not conclude that the deficiency of the CD24 marker on the $\gamma\delta$ cell surface is linked to a more mature phenotype. Further experiments with stimulated $\gamma\delta$ T cells and cytokine production will be carried out to extend our preliminary observations on CD24 expression. However, our ChIP-seq analysis showed the binding of NFATc1/A to the *Cd24a* locus. In addition, the analysis on the transcription level of *Cd24a* in NFATc1- and NFATc1/ α forms-deficient $\gamma\delta$ T cells showed that in the absence of NFATc1 or NFATc1/ α isoforms, *Cd24a* is downregulated compared to control *Nfatc1^{fl/fl}* and *E2^{fl/fl}* $\gamma\delta$ T cells (Figure 6.23 B). These findings suggest that NFATc1 plays an important role in the regulation of the *Cd24a* gene in thymocytes.

The observation that in thymocytes from mouse lines bearing alleles for either complete NFATc1 and NFATc1/ α ablation we observed similar effects on the thymic cellularity, an increase of $\gamma\delta$ T cells and abnormal expression of surface markers, such as CD24 and regulation of $\gamma\delta$ T cell-genes, leads to hypothesize that an essential and more specific role is played by the inducible *Nfatc1 α* isoforms compared to constitutively expressed *Nfatc1* isoforms. Further experiments need to be performed to validate this hypothesis. In this regard, all the previously described effects should not occur in the absence of the longest NFATc1 isoforms, NFATc1/B and NFATc1/C.

We also speculated that the importance of NFATc1 for thymocyte development resides in its total amount. For normal thymocyte development, the complete NFATc1 expression is necessary. The absence of the complete gene expression in *Rag1Cre-Nfatc1^{fl/fl}*, or only of the inducible isoforms, such as in *Rag1Cre-E2^{fl/fl}* mice, leads to the observed effects in thymocytes.

Unpublished data from my colleague Cristina Chiarolla² indicated a cumulative effect on the increase of $\gamma\delta$ T cell number when additional NFAT members are missing. Such as NFATc1 in combination with NFATc2, and/or NFATc3, or all the three members, using a CD4-Cre-triple ko mouse model. In this model, the expression of the single NFAT members or all three is abolished when the *Cd4* gene is expressed.

Taken together these results suggest that for optimal thymocyte development the full expression and function of all the three NFAT family members is necessary.

² Working in the AG of PD Dr. Friederike Berberich-Siebelt, Institute of Pathology, University of Würzburg

7.3 NFATc1 controls the thymocyte lineage fate of $\alpha\beta$ and $\gamma\delta$ T cells

Previous studies showed the essential role of NFATc1 either in pre-TCR negative and in pre-TCR positive thymocytes and the identification of potential NFATc1/A target genes that are involved in thymocyte development^{5,6}. These data confirm that NFATc1 is indeed an important factor for T cell progression in the thymus.

In mice bearing NFATc1-deficient lymphocytes, we observed an increase of $\gamma\delta$ T cells, that was associated with a slight decrease in $\alpha\beta$ T cells (Figure 6.13). As stated previously, in the thymus the $\alpha\beta$ T cells represent 90% of the total cells, therefore, any change in this thymocyte population number and percentage was hard to detect.

In our ChIP-seq assays, we observed the binding of NFATc1/A at the *Tcrb* locus on chromosome 6 (Figure 6.8 A). The strong NFATc1/A binding resides at the 3' region of the *Tcrb* locus, in which the D-J gene segments, the enhancer E β , and the PD β 1 motifs are located^{197, 198}. The PD β 1 region is important for long-range *Tcrb* looping and serves as a chromatin barrier, between the active chromatin at its 3' side, which includes the D-J segments, and the inactive chromatin at its 5' side, encompassing the trypsinogen genes. If the function of PD β 1 is impaired, the active chromatin spreads upstream, toward the 5' side of the *Tcrb* locus, and leads to the transcription of the trypsinogen genes.

We hypothesize that the strong binding of NFATc1/A at the PD β 1 region induces the recruitment of chromatin remodeling complexes, leading to the spreading of active chromatin toward the 5' side of the *Tcrb* locus. Under these conditions, the trypsinogen genes become transcribed. It is known that the TAD-A domain of NFATc1 binds and recruits p300/CBP, a histone deacetylase^{156, 217}. However, under physiological conditions, during the thymocyte development, it is unclear why and how NFATc1 induces this effect on the *Tcrb* locus. Another possible explanation for this finding could be the use of the particular animal model for our ChIP experiments, the *Nfatc1/A-Bio.BirA* mouse model. In those mice, the third allele of *Nfatc1* is expressed from a transgene. As the importance of a distinct threshold level of NFATc1 activity for normal thymocyte development has been reported⁵, the *Nfatc1* overexpression, increased by TPA and ionomycin treatment, could result in the dysregulation of trypsinogen genes, although we never observed any disturbance in the overall expression of *Tcrb* locus in our experimental model.

To shed more light on this process, it will be interesting to check if the epigenetic modifications of the *Tcrb* locus induce alteration in the TCR repertoire. One can speculate that the shift in open chromatin around the trypsinogen genes could be counterbalanced by the closure of the chromatin where some V gene segments are located, and therefore, making them non-available for recombination.

In our phenotypic characterization of $\gamma\delta$ T cells in *Rag1Cre-Nfatc1^{fl/fl}* and *Rag1Cre-E2^{fl/fl}* mice, we stained the cells with antibodies against CD4 and CD8. In both mouse models, $\gamma\delta$ T cells showed an abnormal strong expression of CD4 marker on the cell surface (Figure 6.19 and 6.20). We excluded that this increased $\gamma\delta$ population was represented by the $V\gamma 1^+V\delta 6.3^+$ NKT $\gamma\delta$ T cells²⁸. In mice, this population shows several characteristics like NKT type 1 cells, the expression of Thy1 (CD90), NK1.1⁺ and CD4⁺ surface markers, some transcription factors, and cytokine production²⁸. No changes in expression of the NK1.1 and of the $V\delta 6.3^+$ markers were observed in our FACS analysis (data not shown). In conclusion, our phenotypical analysis of $\gamma\delta$ T cells in *Rag1Cre-Nfatc1^{fl/fl}* and *Rag1Cre-E2^{fl/fl}* shows a strong increase in the percentage of $\gamma\delta$ T cells expressing the CD4 co-receptor on the cell surface, and these cells do not correspond to NKT $\gamma\delta$ T cells. These data may suggest that the NFATc1 or NFATc1/ α isoforms-deficient thymocytes are acquiring characteristics of $\alpha\beta$ thymocytes, but their developmental process is blocked at some point.

The *Tcra* and *Tcrd* genes are organized in a single genetic locus on mouse chromosome 14. As for the other *Tcrb* and *Tcrg* loci, they are equipped with enhancers that mediate the initial germ-line transcription, the accessibility of the recombinase machinery, and the V(D)J recombination. In the *Tcra* locus, the enhancer α ($E\alpha$) is located downstream of $C\alpha$, while in the *Tcrd* locus, the enhancer δ ($E\delta$) is located in the murine $J\delta 2$ - $C\delta$ intron²¹⁸.

As the recombination of the *Tcra* locus induces the deletion of the *Tcrd* locus, the activity of their respective enhancers controls the *Tcra* and *Tcrd* recombination in a developmentally regulated manner. $E\alpha$, as well as the $E\delta$, control the initial germinal transcription and the V(D)J recombination of the overlapping *Tcra/Tcrd* locus²¹⁹. During the early stages of thymocyte development (DN2b-DN3a) the $E\alpha$ is inactive but primed by TFs such as CREB, LEF1/TCF1, RUNX1, and ETS1, GATA3, E2A, HEB, FLI1, SP1, and IKAROS. $E\alpha$ is activated at the DN3 developmental stage, upon the β -selection and enrichment of TFs as NFAT, EGR1, and AP1²²⁰. These preliminary data lead us to conclude that NFATc1 binds and regulates the *Tcra* locus during thymocyte development.

All these data together lead us to propose that NFATc1 is essential for the $\alpha\beta$ thymocyte development and differentiation. During the normal $\alpha\beta$ development path, between the end of DN4 and the initial DP phase, upon the pre-TCR signaling, thymocytes start to recombine and express the *Tcra* locus. During this latest stage of development, CD4 and CD8 are expressed on the cell membrane, giving rise to DP thymocytes. Previous studies hypothesized that the lineage commitment between $\alpha\beta$ and $\gamma\delta$ is dictated during the *Tcra* locus recombination. They have shown that in thymic $\gamma\delta$ T cells, the in-frame recombination of the *Tcrb* locus, but not of the *Tcra* locus, occurs frequently²²¹.

Under normal conditions, thymocytes develop toward the $\alpha\beta$ T cell lineage until the *Tcra* locus recombination point. At this point of development, NFATc1 plays an essential role. In the absence of NFATc1, the missing NFATc1 binding to the *Tcra* locus leads to a defect in proceeding toward the $\alpha\beta$ T cell pathway, and, therefore, thymocytes divert to the $\gamma\delta$ phenotype. According to our model, these $\gamma\delta$ T cells express a high level of the CD4 marker. This idea is also supported by the previously mentioned *CD4Cre-Nfatc1^{fl/fl}-Nfatc2ko-Nfatc3^{fl/fl}* mouse model. The increase of $\gamma\delta$ T cells occurs in parallel with the cumulative depletion of the NFAT factors since the depletion of the NFAT members, under the control of the *Cd4* gene expression, occurs at the time of *Tcra* recombination.

8 Annex

8.1 Supplementary information

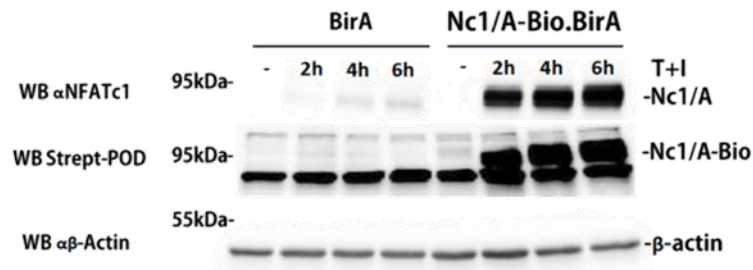


Figure S1 The induction of NFATc1/A-Bio in thymocytes occurs already after 2h of TPA and ionomycin stimulation.

Western Blot analysis of the whole protein extract from *BirA* control and *Nfatc1/A-Bio.BirA* total thymocytes, stimulated for 2h, 4h and 6h with TPA (100µg/ml) and ionomycin (100µg/ml), or left unstimulated. The whole protein extract was blotted with anti-NFATc1 Ab, Strept-POD and β-Actin. The molecular weight of the proteins is indicated. NFATc1/A-Bio protein possess a relative mol wt of ~95kDa.

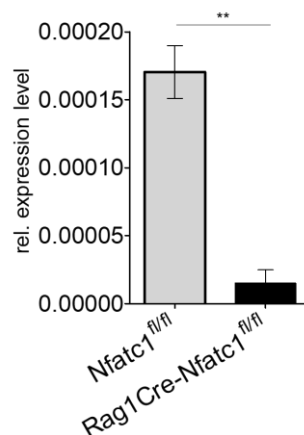


Figure S2 The constitutive *Nfatc1* β isoforms are depleted in *Rag1Cre-Nfatc1^{fl/fl}* thymocytes.

Real-time PCR analysis of the expression of the constitutive *Nfatc1*β isoforms in *Rag1Cre-Nfatc1^{fl/fl}* compared to *Nfatc1^{fl/fl}* total thymocytes. The specific primers bind on the exon 2 and exon 3 of the *Nfatc1* locus.

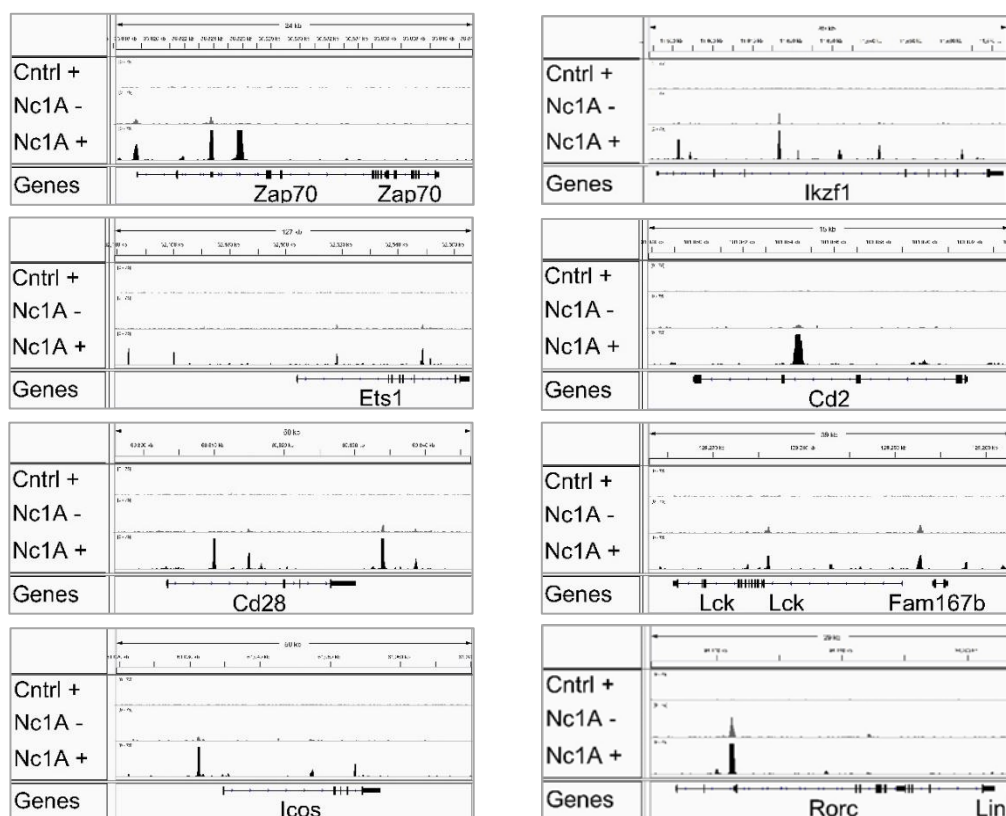


Figure S3 NFATc1/A binds near numerous genes that control thymocyte development

NFATc1/A binding sites at indicated genes in *BirA* stimulated, *Nfatc1/A-Bio.BirA* freshly isolated and stimulated *Nfatc1/A-Bio.BirA* total thymocytes. The binding sites visualized with IGV software.

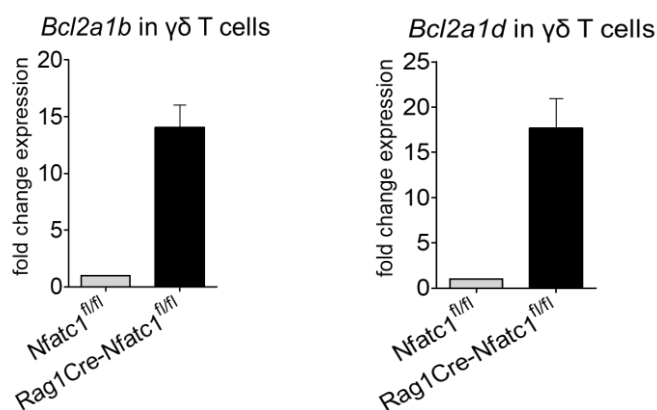


Figure S4 *Bcl2a1b* and *Bcl2a1d* are upregulated in NFATc1-deficient $\gamma\delta$ T cells.

Fold change expression and relative expression of *Bcl2a1b* (on the left) and of *Bcl2a1d* (on the right) genes in freshly isolated $\gamma\delta$ T cells from *Nfatc1^{fl/fl}* and *Rag1Cre-Nfatc1^{fl/fl}* mice. The analysis was carried out by qRT-PCR. Gene expression was normalized to that of *Actb* gene and expressed as fold induction relative to *Nfatc1^{fl/fl}* control thymocytes. Data are indicative of at least three independent experiments and are shown as mean \pm SEM.

8.2 List of abbreviations

A	Ampere
Abs	Antibodies
Abs	absorbance
AICD	activation-induced cell death
Akt	protein kinase B
AP-1	activator protein 1
APC	Antigen-presenting cell
bHLH	Basic helix-loop-helix
BM	Bone marrow
bp	Base pair
BRC	B cell receptor
BSA	Bovine serum albumine
C	constant
°C	Celsius
CBM	(CARMA1-BCL10-MALT1) signalosome complex
CD	Cluster of differentiation
ChIP	Chromatin immunoprecipitation
CKI	Casein kinase I
CLP	Common lymphoid progenitor
CMJ	cortico-medullary junction
CN	calcineurin
CRAC	Calcium release-activated calcium channel
cTEC	cortical thymic epithelial cell
CTL	Cytotoxic T cell
D	diversity
DAG	diacylglycerol
DC	Dendritic cell
DETC	Dendritic epidermal T cell
DN	Double negative
DP	Double positive
E	embryonic day
E2	Enhancer 2
E β	Enhancer β
Ebox	Enhancer box
ER	Endoplasmic reticulum

ERG	Early growth response gene
ERK	Extracellular signal-related kinase
ES	Embryonic stem (cell)
ETP	Early T cell progenitor
FACS	Fluorescence activated cell sorting
FBS	Fetal bovine serum
Fig	Figure
GEF	Guanine-nucleotide exchange factor
GFP	Green fluorescent protein
GO	Gene ontology
GREAT	Genomic Regions Enrichment of Annotations Tool
GSK3	Glycogen synthase kinase
h	hour
HSA	Heat-stable antigen
HSC	Hematopoietic stem cell
I	ionomycin
ICAM	Intercellular adhesion molecule-1
iELP	Intraepithelial lymphocyte
IFN	Interferon
IL	Interleukin
ILC	Innate lymphoid cell
iNKT	Invariant natural killer T cell
IP ₃	Inositol 1,4,5-triphosphate
ITAM	Tyrosine-based activation motif
Itk	Interleukin-2-inducible T cell kinase
J	Joining
JNK3	c-Jun N-terminal kinase 3
Ko	Knockout
LAT	Adaptor protein linker for activated T cells
LDTF	Lineage determining transcription factor
MFI	Mean fluorescence intensity
MHC	Major histocompatibility complex
min	Minute
mTEC	Medullary thymic epithelial cell
NES	Nuclear export signal
NFAT	Nuclear factor of activated T cells
NFκB	Nuclear factor κB
NHR	NFAT homology region

NICD	Notch intracellular domain
NK	Natural killer
NKT	Natural killer T cell
NLS	Nuclear localization signal
nm	Nanometer
nTreg	Natural T regulatory cell
o/n	Over night
P1	Promoter 1
P2	Promoter 2
PBS	Phosphate buffered saline
PDK-1	Phosphoinositide-dependent kinase 1
PH	Pleckstrinin homology
PI ₃	Phosphatidylinositol kinase 3
PIP ₃	Phosphatidylinositol (3,4,5)-triphosphate
PK	Protein kinase
PLC γ	Phosphatase C- γ
PLC	Phospholipase C
PMSF	Phenylmethylsulfonyl fluoride
Pre-TCR	Pre-T cell receptor
PRRS	Pattern recognition receptors
PSGL1	Platelet (P)-selectin glycoprotein ligand 1
RAG	Recombination-activating gene
RNA-seq	RNA sequencing
Rpm	Round per minute
RSD	Rel similarity domain
RSS	Recombination signal sequence
RT	Room temperature
S1P1	Sphingosine-1-phosphate receptor 1
scRNAseq	Single cell RNA sequencing
sec	Second
SLP-76	Leukocyte-specific phosphoprotein of 76kDa
SP	Single positive
SRD	Serine- rich domain
STIM 1 & 2	Stromal interaction molecule
T $\alpha\beta$	$\alpha\beta$ T cell
TBS	Tris-buffered saline
Tcr α	T cell receptor α locus
Tcr β	T cell receptor β locus

T $\gamma\delta$	$\gamma\delta$ T cell
TAD	Transactivation domain
TAD-C	C-terminal transactivation domain
TAD-N	N-terminal transactivation domain
TCR	T cell receptor
TF	Transcription factor
Tfh	T Follicular helper cell
Th	T helper cell
Thy	Thymocyte
TPA	12-O-Tetradecanoylphorbol-13-acetate
TRA	Tissue restricted antigens
Treg	T regulatory cell
TTS	Transcription start site
V	variable
VCAM-1	Vascular cell adhesion molecule-1
vs	Versus
wt	Wild type

9 Bibliography

1. Suda, T. & Zlotnik, A. Origin, differentiation, and repertoire selection of CD3+CD4-CD8- thymocytes bearing either alpha beta or gamma delta T cell receptors. *J Immunol* **150**, 447-455 (1993).
2. Godfrey, D.I., Kennedy, J., Mombaerts, P., Tonegawa, S. & Zlotnik, A. Onset of TCR-beta gene rearrangement and role of TCR-beta expression during CD3-CD4-CD8- thymocyte differentiation. *J Immunol* **152**, 4783-4792 (1994).
3. Godfrey, D.I., Kennedy, J., Suda, T. & Zlotnik, A. A developmental pathway involving four phenotypically and functionally distinct subsets of CD3-CD4-CD8- triple-negative adult mouse thymocytes defined by CD44 and CD25 expression. *J Immunol* **150**, 4244-4252 (1993).
4. Patra, A.K. *et al.* An alternative NFAT-activation pathway mediated by IL-7 is critical for early thymocyte development. *Nature immunology* **14**, 127–135 (2013).
5. Klein-Hessling, S. *et al.* A threshold level of NFATc1 activity facilitates thymocyte differentiation and opposes notch-driven leukaemia development. *Nature communications* **7**, 11841 (2016).
6. Weaver, K.M.C. *Janeway's Immunobiology*, 2017.
7. Ciofani, M. & Zúñiga-Pflücker, J.C. The thymus as an inductive site for T lymphopoiesis. *Annual review of cell and developmental biology* **23**, 463–493 (2007).
8. Yamane, T., Hosen, N., Yamazaki, H. & Weissman, I.L. Expression of AA4.1 marks lymphohematopoietic progenitors in early mouse development. *Proc Natl Acad Sci U S A* **106**, 8953-8958 (2009).
9. Yokota, T. *et al.* Tracing the first waves of lymphopoiesis in mice. *Development* **133**, 2041-2051 (2006).
10. Yamane, T. Mouse Yolk Sac Hematopoiesis. *Front Cell Dev Biol* **6**, 80 (2018).
11. Seo, W. & Taniuchi, I. Transcriptional regulation of early T-cell development in the thymus. *European journal of immunology* **46**, 531–538 (2016).
12. Kawamoto, H., Ohmura, K. & Katsura, Y. Presence of progenitors restricted to T, B, or myeloid lineage, but absence of multipotent stem cells, in the murine fetal thymus. *J Immunol* **161**, 3799-3802 (1998).
13. Harman, B.C. *et al.* T/B lineage choice occurs prior to intrathymic Notch signaling. *Blood* **106**, 886-892 (2005).
14. Zaharie, D., Moleriu, R.D. & Mic, F.A. Modeling the development of the post-natal mouse thymus in the absence of bone marrow progenitors. *Sci Rep* **6**, 36159 (2016).
15. Yong Park S., Saijo K., Takahashi T., Osawa M., Areas H., Hirayama N., Miyake K., Nakauchi, H., Shirasawa T., Saito T. Developmental defects of lymphoid cells in Jak3 kinase-deficient mice. *Immunity* **3**, 667-824 (1995).
16. Xiao, S.Y., Li, Y. & Chen, W.F. Kinetics of thymocyte developmental process in fetal and neonatal mice. *Cell Res* **13**, 265-273 (2003).
17. Takahama, Y. Journey through the thymus: stromal guides for T-cell development and selection. *Nat Rev Immunol* **6**, 127-135 (2006).

18. Porritt, H.E. *et al.* Heterogeneity among DN1 prothymocytes reveals multiple progenitors with different capacities to generate T cell and non-T cell lineages. *Immunity* **20**, 735-745 (2004).
19. Lind, E.F., Prockop, S.E., Porritt, H.E. & Petrie, H.T. Mapping precursor movement through the postnatal thymus reveals specific microenvironments supporting defined stages of early lymphoid development. *J Exp Med* **194**, 127-134 (2001).
20. Hosokawa, H. & Rothenberg, E.V. How transcription factors drive choice of the T cell fate. *Nat Rev Immunol* (2020).
21. Shah, D.K. & Zuniga-Pflucker, J.C. An overview of the intrathymic intricacies of T cell development. *J Immunol* **192**, 4017-4023 (2014).
22. Taghon, T., Yui, M.A., Pant, R., Diamond, R.A. & Rothenberg, E.V. Developmental and molecular characterization of emerging beta- and gammadelta-selected pre-T cells in the adult mouse thymus. *Immunity* **24**, 53-64 (2006).
23. Scollay, R.G., Butcher, E.C. & Weissman, I.L. Thymus cell migration. Quantitative aspects of cellular traffic from the thymus to the periphery in mice. *Eur J Immunol* **10**, 210-218 (1980).
24. Zuklys, S. *et al.* Normal thymic architecture and negative selection are associated with Aire expression, the gene defective in the autoimmune-polyendocrinopathy-candidiasis-ectodermal dystrophy (APECED). *J Immunol* **165**, 1976-1983 (2000).
25. Abramson, J. & Anderson, G. Thymic Epithelial Cells. *Annual review of immunology* **35**, 85–118 (2017).
26. Starr, T.K., Jameson, S.C. & Hogquist, K.A. Positive and negative selection of T cells. *Annu Rev Immunol* **21**, 139-176 (2003).
27. Egerton, M., Scollay, R. & Shortman, K. Kinetics of mature T-cell development in the thymus. *Proc Natl Acad Sci U S A* **87**, 2579-2582 (1990).
28. Pellicci, D.G., Koay, H.F. & Berzins, S.P. Thymic development of unconventional T cells: how NKT cells, MAIT cells and gammadelta T cells emerge. *Nat Rev Immunol* **20**, 756-770 (2020).
29. Hosokawa, H. & Rothenberg, E.V. Cytokines, Transcription Factors, and the Initiation of T-Cell Development. *Cold Spring Harb Perspect Biol* **10** (2018).
30. Radtke, F., MacDonald, H.R. & Tacchini-Cottier, F. Regulation of innate and adaptive immunity by Notch. *Nat Rev Immunol* **13**, 427-437 (2013).
31. Thompson, P.K. & Zuniga-Pflucker, J.C. On becoming a T cell, a convergence of factors kick it up a Notch along the way. *Semin Immunol* **23**, 350-359 (2011).
32. Robey, E.A. & Bluestone, J.A. Notch signaling in lymphocyte development and function. *Curr Opin Immunol* **16**, 360-366 (2004).
33. Radtke, F. *et al.* Deficient T cell fate specification in mice with an induced inactivation of Notch1. *Immunity* **10**, 547-558 (1999).
34. Hozumi, K. *et al.* Delta-like 4 is indispensable in thymic environment specific for T cell development. *J Exp Med* **205**, 2507-2513 (2008).
35. Schmitt, T.M. & Zuniga-Pflucker, J.C. Induction of T cell development from hematopoietic progenitor cells by delta-like-1 in vitro. *Immunity* **17**, 749-756 (2002).
36. Bray, S.J. Notch signalling: a simple pathway becomes complex. *Nat Rev Mol Cell Biol* **7**, 678-689 (2006).

37. Yashiro-Ohtani, Y., Ohtani, T. & Pear, W.S. Notch regulation of early thymocyte development. *Semin Immunol* **22**, 261-269 (2010).
38. Ciofani, M. & Zuniga-Pflucker, J.C. A survival guide to early T cell development. *Immunol Res* **34**, 117-132 (2006).
39. Yui, M.A. & Rothenberg, E.V. Developmental gene networks: a triathlon on the course to T cell identity. *Nat Rev Immunol* **14**, 529-545 (2014).
40. Rothenberg, E.V., Ungerback, J. & Champhekar, A. Forging T-Lymphocyte Identity: Intersecting Networks of Transcriptional Control. *Adv Immunol* **129**, 109-174 (2016).
41. Zhou, W. *et al.* Single-Cell Analysis Reveals Regulatory Gene Expression Dynamics Leading to Lineage Commitment in Early T Cell Development. *Cell Syst* **9**, 321-337 e329 (2019).
42. Lu, M. *et al.* The earliest thymic progenitors in adults are restricted to T, NK, and dendritic cell lineage and have a potential to form more diverse TCRbeta chains than fetal progenitors. *J Immunol* **175**, 5848-5856 (2005).
43. Champhekar, A. *et al.* Regulation of early T-lineage gene expression and developmental progression by the progenitor cell transcription factor PU.1. *Genes Dev* **29**, 832-848 (2015).
44. Kawamoto, H. *et al.* Extensive proliferation of T cell lineage-restricted progenitors in the thymus: an essential process for clonal expansion of diverse T cell receptor beta chains. *Eur J Immunol* **33**, 606-615 (2003).
45. Scott, E.W., Simon, M.C., Anastasi, J. & Singh, H. Requirement of transcription factor PU.1 in the development of multiple hematopoietic lineages. *Science* **265**, 1573-1577 (1994).
46. Reizis, B. & Leder, P. Direct induction of T lymphocyte-specific gene expression by the mammalian Notch signaling pathway. *Genes Dev* **16**, 295-300 (2002).
47. Del Real, M.M. & Rothenberg, E.V. Architecture of a lymphomyeloid developmental switch controlled by PU.1, Notch and Gata3. *Development* **140**, 1207-1219 (2013).
48. Kueh, H.Y., Champhekar, A., Nutt, S.L., Elowitz, M.B. & Rothenberg, E.V. Positive feedback between PU.1 and the cell cycle controls myeloid differentiation. *Science* **341**, 670-673 (2013).
49. Zhang, J.A., Mortazavi, A., Williams, B.A., Wold, B.J. & Rothenberg, E.V. Dynamic transformations of genome-wide epigenetic marking and transcriptional control establish T cell identity. *Cell* **149**, 467-482 (2012).
50. Mingueneau, M. *et al.* The transcriptional landscape of alphabeta T cell differentiation. *Nat Immunol* **14**, 619-632 (2013).
51. De Obaldia, M.E. *et al.* T cell development requires constraint of the myeloid regulator C/EBP-alpha by the Notch target and transcriptional repressor Hes1. *Nat Immunol* **14**, 1277-1284 (2013).
52. Kondo, M., Akashi, K., Domen, J., Sugamura, K. & Weissman, I.L. Bcl-2 rescues T lymphopoiesis, but not B or NK cell development, in common gamma chain-deficient mice. *Immunity* **7**, 155-162 (1997).
53. Zohren, F. *et al.* The transcription factor Lyl-1 regulates lymphoid specification and the maintenance of early T lineage progenitors. *Nat Immunol* **13**, 761-769 (2012).
54. Goodings, C. *et al.* Hhex is Required at Multiple Stages of Adult Hematopoietic Stem and Progenitor Cell Differentiation. *Stem Cells* **33**, 2628-2641 (2015).

55. Germar, K. *et al.* T-cell factor 1 is a gatekeeper for T-cell specification in response to Notch signaling. *Proc Natl Acad Sci U S A* **108**, 20060-20065 (2011).
56. Weber, B.N. *et al.* A critical role for TCF-1 in T-lineage specification and differentiation. *Nature* **476**, 63-68 (2011).
57. Zaret, K.S. & Carroll, J.S. Pioneer transcription factors: establishing competence for gene expression. *Genes Dev* **25**, 2227-2241 (2011).
58. Hozumi, K. *et al.* Notch signaling is necessary for GATA3 function in the initiation of T cell development. *Eur J Immunol* **38**, 977-985 (2008).
59. Garcia-Ojeda, M.E. *et al.* GATA-3 promotes T-cell specification by repressing B-cell potential in pro-T cells in mice. *Blood* **121**, 1749-1759 (2013).
60. Scripture-Adams, D.D. *et al.* GATA-3 dose-dependent checkpoints in early T cell commitment. *J Immunol* **193**, 3470-3491 (2014).
61. Ebihara, T., Seo, W. & Taniuchi, I. Roles of RUNX Complexes in Immune Cell Development. *Adv Exp Med Biol* **962**, 395-413 (2017).
62. Kueh, H.Y. *et al.* Asynchronous combinatorial action of four regulatory factors activates Bcl11b for T cell commitment. *Nat Immunol* **17**, 956-965 (2016).
63. Liu, P., Li, P. & Burke, S. Critical roles of Bcl11b in T-cell development and maintenance of T-cell identity. *Immunol Rev* **238**, 138-149 (2010).
64. Kominami, R. Role of the transcription factor Bcl11b in development and lymphomagenesis. *Proc Jpn Acad Ser B Phys Biol Sci* **88**, 72-87 (2012).
65. Avram, D. & Califano, D. The multifaceted roles of Bcl11b in thymic and peripheral T cells: impact on immune diseases. *J Immunol* **193**, 2059-2065 (2014).
66. Li, L., Leid, M. & Rothenberg, E.V. An early T cell lineage commitment checkpoint dependent on the transcription factor Bcl11b. *Science* **329**, 89-93 (2010).
67. Longabaugh, W.J.R. *et al.* Bcl11b and combinatorial resolution of cell fate in the T-cell gene regulatory network. *Proc Natl Acad Sci U S A* **114**, 5800-5807 (2017).
68. Li, P. *et al.* Reprogramming of T cells to natural killer-like cells upon Bcl11b deletion. *Science* **329**, 85-89 (2010).
69. Ciofani, M. *et al.* Obligatory role for cooperative signaling by pre-TCR and Notch during thymocyte differentiation. *J Immunol* **172**, 5230-5239 (2004).
70. Semerad, C.L., Mercer, E.M., Inlay, M.A., Weissman, I.L. & Murre, C. E2A proteins maintain the hematopoietic stem cell pool and promote the maturation of myelolymphoid and myeloerythroid progenitors. *Proc Natl Acad Sci U S A* **106**, 1930-1935 (2009).
71. Yang, Q. *et al.* E47 controls the developmental integrity and cell cycle quiescence of multipotential hematopoietic progenitors. *J Immunol* **181**, 5885-5894 (2008).
72. Dias, S., Mansson, R., Gurbuxani, S., Sigvardsson, M. & Kee, B.L. E2A proteins promote development of lymphoid-primed multipotent progenitors. *Immunity* **29**, 217-227 (2008).
73. Braunstein, M. & Anderson, M.K. HEB in the spotlight: Transcriptional regulation of T-cell specification, commitment, and developmental plasticity. *Clin Dev Immunol* **2012**, 678705 (2012).

74. Bain, G. *et al.* E2A deficiency leads to abnormalities in alphabeta T-cell development and to rapid development of T-cell lymphomas. *Mol Cell Biol* **17**, 4782-4791 (1997).
75. Ikawa, T., Kawamoto, H., Goldrath, A.W. & Murre, C. E proteins and Notch signaling cooperate to promote T cell lineage specification and commitment. *J Exp Med* **203**, 1329-1342 (2006).
76. Jones, M.E. & Zhuang, Y. Regulation of V(D)J recombination by E-protein transcription factors. *Adv Exp Med Biol* **650**, 148-156 (2009).
77. Miyazaki, M. *et al.* The E-Id Protein Axis Specifies Adaptive Lymphoid Cell Identity and Suppresses Thymic Innate Lymphoid Cell Development. *Immunity* **46**, 818-834.e814 (2017).
78. Wojciechowski, J., Lai, A., Kondo, M. & Zhuang, Y. E2A and HEB are required to block thymocyte proliferation prior to pre-TCR expression. *J Immunol* **178**, 5717-5726 (2007).
79. Jones, M.E. & Zhuang, Y. Acquisition of a functional T cell receptor during T lymphocyte development is enforced by HEB and E2A transcription factors. *Immunity* **27**, 860-870 (2007).
80. Miyazaki, M. *et al.* The opposing roles of the transcription factor E2A and its antagonist Id3 that orchestrate and enforce the naive fate of T cells. *Nature immunology* **12**, 992-1001 (2011).
81. D'Cruz, L.M., Knell, J., Fujimoto, J.K. & Goldrath, A.W. An essential role for the transcription factor HEB in thymocyte survival, Tcra rearrangement and the development of natural killer T cells. *Nat Immunol* **11**, 240-249 (2010).
82. Yuan, J., Crittenden, R.B. & Bender, T.P. c-Myb promotes the survival of CD4+CD8+ double-positive thymocytes through upregulation of Bcl-xL. *J Immunol* **184**, 2793-2804 (2010).
83. Wang, R. *et al.* Transcription factor network regulating CD(+)CD8(+) thymocyte survival. *Crit Rev Immunol* **31**, 447-458 (2011).
84. Van De Wiele, C.J. *et al.* Thymocytes between the beta-selection and positive selection checkpoints are nonresponsive to IL-7 as assessed by STAT-5 phosphorylation. *J Immunol* **172**, 4235-4244 (2004).
85. Zacarias-Cabeza, J. *et al.* Transcription-dependent generation of a specialized chromatin structure at the TCRbeta locus. *J Immunol* **194**, 3432-3443 (2015).
86. Krimpenfort, P. *et al.* Transcription of T cell receptor beta-chain genes is controlled by a downstream regulatory element. *EMBO J* **7**, 745-750 (1988).
87. McDougall, S., Peterson, C.L. & Calame, K. A transcriptional enhancer 3' of C beta 2 in the T cell receptor beta locus. *Science* **241**, 205-208 (1988).
88. Bories, J.C., Demengeot, J., Davidson, L. & Alt, F.W. Gene-targeted deletion and replacement mutations of the T-cell receptor beta-chain enhancer: the role of enhancer elements in controlling V(D)J recombination accessibility. *Proc Natl Acad Sci U S A* **93**, 7871-7876 (1996).
89. Bouvier, G. *et al.* Deletion of the mouse T-cell receptor beta gene enhancer blocks alphabeta T-cell development. *Proc Natl Acad Sci U S A* **93**, 7877-7881 (1996).
90. Saint-Ruf, C. *et al.* Different initiation of pre-TCR and gammadeltaTCR signalling. *Nature* **406**, 524-527 (2000).
91. Fehling, H.J., Krotkova, A., Saint-Ruf, C. & von Boehmer, H. Crucial role of the pre-T-cell receptor alpha gene in development of alpha beta but not gamma delta T cells. *Nature* **375**, 795-798 (1995).
92. von Boehmer, H. Unique features of the pre-T-cell receptor alpha-chain: not just a surrogate. *Nat Rev Immunol* **5**, 571-577 (2005).

93. Aifantis, I., Gounari, F., Scorrano, L., Borowski, C. & von Boehmer, H. Constitutive pre-TCR signaling promotes differentiation through Ca²⁺ mobilization and activation of NF-kappaB and NFAT. *Nat Immunol* **2**, 403-409 (2001).
94. Engel, I., Johns, C., Bain, G., Rivera, R.R. & Murre, C. Early thymocyte development is regulated by modulation of E2A protein activity. *J Exp Med* **194**, 733-745 (2001).
95. Mandal, M. *et al.* The BCL2A1 gene as a pre-T cell receptor-induced regulator of thymocyte survival. *The Journal of experimental medicine* **201**, 603–614 (2005).
96. Zweemer, A.J., Toraskar, J., Heitman, L.H. & AP, I.J. Bias in chemokine receptor signalling. *Trends Immunol* **35**, 243-252 (2014).
97. Norment, A.M. & Bevan, M.J. Role of chemokines in thymocyte development. *Semin Immunol* **12**, 445-455 (2000).
98. Lind E.F., Prockop S.E., Porritt H.E., and Petrie H.T. Mapping Precursor Movement through the Postnatal Thymus Reveals Specific Microenvironments Supporting Defined Stages of Early Lymphoid Development. *J. Exp. Med* **194**, 127–134 (2001).
99. Liu, C. *et al.* Coordination between CCR7- and CCR9-mediated chemokine signals in prevascular fetal thymus colonization. *Blood* **108**, 2531-2539 (2006).
100. Liu, C. *et al.* The role of CCL21 in recruitment of T-precursor cells to fetal thymus. *Blood* **105**, 31-39 (2005).
101. Wurbel, M.A. *et al.* Mice lacking the CCR9 CC-chemokine receptor show a mild impairment of early T- and B-cell development and a reduction in T-cell receptor gamma delta(+) gut intraepithelial lymphocytes. *Blood* **98**, 2626-2632 (2001).
102. Plotkin, J., Prockop, S.E., Lepique, A. & Petrie, H.T. Critical role for CXCR4 signaling in progenitor localization and T cell differentiation in the postnatal thymus. *J Immunol* **171**, 4521-4527 (2003).
103. Misslitz, A. *et al.* Thymic T cell development and progenitor localization depend on CCR7. *J Exp Med* **200**, 481-491 (2004).
104. Lancaster, J.N., Li, Y. & Ehrlich, L.I.R. Chemokine-Mediated Choreography of Thymocyte Development and Selection. *Trends Immunol* **39**, 86-98 (2018).
105. Matloubian, M. *et al.* Lymphocyte egress from thymus and peripheral lymphoid organs is dependent on S1P receptor 1. *Nature* **427**, 355-360 (2004).
106. Allende, M.L., Dreier, J.L., Mandala, S. & Proia, R.L. Expression of the sphingosine 1-phosphate receptor, S1P1, on T-cells controls thymic emigration. *J Biol Chem* **279**, 15396-15401 (2004).
107. Prinz, I. *et al.* Visualization of the earliest steps of gamma delta T cell development in the adult thymus. *Nat Immunol* **7**, 995-1003 (2006).
108. Hayes, S.M., Shores, E.W. & Love, P.E. An architectural perspective on signaling by the pre-, alphabeta and gamma delta T cell receptors. *Immunol Rev* **191**, 28-37 (2003).
109. Zarin, P., Chen, E.L., In, T.S., Anderson, M.K. & Zuniga-Pflucker, J.C. Gamma delta T-cell differentiation and effector function programming, TCR signal strength, when and how much? *Cell Immunol* **296**, 70-75 (2015).
110. Haks, M.C. *et al.* Attenuation of gamma delta TCR signaling efficiently diverts thymocytes to the alphabeta lineage. *Immunity* **22**, 595-606 (2005).

111. Hayes, S.M., Li, L. & Love, P.E. TCR signal strength influences alphabeta/gammadelta lineage fate. *Immunity* **22**, 583-593 (2005).
112. Lee, S.Y., Stadanlick, J., Kappes, D.J. & Wiest, D.L. Towards a molecular understanding of the differential signals regulating alphabeta/gammadelta T lineage choice. *Semin Immunol* **22**, 237-246 (2010).
113. Pardoll, D.M. *et al.* Differential expression of two distinct T-cell receptors during thymocyte development. *Nature* **326**, 79-81 (1987).
114. Ciofani, M. & Zuniga-Pflucker, J.C. Determining gammadelta versus alpha T cell development. *Nat Rev Immunol* **10**, 657-663 (2010).
115. Wong, G.W. & Zuniga-Pflucker, J.C. gammadelta and alphabeta T cell lineage choice: resolution by a stronger sense of being. *Semin Immunol* **22**, 228-236 (2010).
116. Terrence, K., Pavlovich, C.P., Matechak, E.O. & Fowlkes, B.J. Premature expression of T cell receptor (TCR)alphabeta suppresses TCRgammadelta gene rearrangement but permits development of gammadelta lineage T cells. *J Exp Med* **192**, 537-548 (2000).
117. Jensen, K.D. *et al.* Thymic selection determines gammadelta T cell effector fate: antigen-naive cells make interleukin-17 and antigen-experienced cells make interferon gamma. *Immunity* **29**, 90-100 (2008).
118. Lewis, J.M. *et al.* Selection of the cutaneous intraepithelial gammadelta+ T cell repertoire by a thymic stromal determinant. *Nat Immunol* **7**, 843-850 (2006).
119. Boyden, L.M. *et al.* Skint1, the prototype of a newly identified immunoglobulin superfamily gene cluster, positively selects epidermal gammadelta T cells. *Nat Genet* **40**, 656-662 (2008).
120. Prinz, I., Silva-Santos, B. & Pennington, D.J. Functional development of gammadelta T cells. *Eur J Immunol* **43**, 1988-1994 (2013).
121. Haas, J.D. *et al.* Development of interleukin-17-producing gammadelta T cells is restricted to a functional embryonic wave. *Immunity* **37**, 48-59 (2012).
122. Parker, M.E. & Ciofani, M. Regulation of gammadelta T Cell Effector Diversification in the Thymus. *Front Immunol* **11**, 42 (2020).
123. Vantourout, P. & Hayday, A. Six-of-the-best: unique contributions of gammadelta T cells to immunology. *Nat Rev Immunol* **13**, 88-100 (2013).
124. Chien, Y.-h., Zeng, X. & Prinz, I. The natural and the inducible: interleukin (IL)-17-producing $\gamma\delta$ T cells. *Trends in Immunology* **34**, 151-154 (2013).
125. Munoz-Ruiz, M. *et al.* TCR signal strength controls thymic differentiation of discrete proinflammatory gammadelta T cell subsets. *Nat Immunol* **17**, 721-727 (2016).
126. Sagar *et al.* Deciphering the regulatory landscape of fetal and adult gammadelta T-cell development at single-cell resolution. *EMBO J* **39**, e104159 (2020).
127. Sumaria, N., Grandjean, C.L., Silva-Santos, B. & Pennington, D.J. Strong TCRgammadelta Signaling Prohibits Thymic Development of IL-17A-Secreting gammadelta T Cells. *Cell Rep* **19**, 2469-2476 (2017).
128. Schilham, M.W. *et al.* Critical involvement of Tcf-1 in expansion of thymocytes. *J Immunol* **161**, 3984-3991 (1998).

129. Melichar, H.J. *et al.* Regulation of gammadelta versus alphabeta T lymphocyte differentiation by the transcription factor SOX13. *Science* **315**, 230-233 (2007).
130. Spidale, N.A. *et al.* Interleukin-17-Producing gammadelta T Cells Originate from SOX13(+) Progenitors that Are Independent of gammadeltaTCR Signaling. *Immunity* **49**, 857-872 e855 (2018).
131. Zuberbuehler, M.K. *et al.* The transcription factor c-Maf is essential for the commitment of IL-17-producing gammadelta T cells. *Nat Immunol* **20**, 73-85 (2019).
132. Maki, K., Sunaga, S. & Ikuta, K. The V-J recombination of T cell receptor-gamma genes is blocked in interleukin-7 receptor-deficient mice. *J Exp Med* **184**, 2423-2427 (1996).
133. Malhotra, N. *et al.* A network of high-mobility group box transcription factors programs innate interleukin-17 production. *Immunity* **38**, 681-693 (2013).
134. Lauritsen, J.P. *et al.* Marked induction of the helix-loop-helix protein Id3 promotes the gammadelta T cell fate and renders their functional maturation Notch independent. *Immunity* **31**, 565-575 (2009).
135. Ciofani, M., Knowles, G.C., Wiest, D.L., von Boehmer, H. & Zuniga-Pflucker, J.C. Stage-specific and differential notch dependency at the alphabeta and gammadelta T lineage bifurcation. *Immunity* **25**, 105-116 (2006).
136. Shibata, K. *et al.* Notch-Hes1 pathway is required for the development of IL-17-producing gammadelta T cells. *Blood* **118**, 586-593 (2011).
137. Yamashita, S. *et al.* Analysis of mechanism for human gammadelta T cell recognition of nonpeptide antigens. *Biochem Biophys Res Commun* **334**, 349-360 (2005).
138. Zhang, L. *et al.* Gamma delta T cell receptors confer autonomous responsiveness to the insulin-peptide B:9-23. *J Autoimmun* **34**, 478-484 (2010).
139. Born, W.K. *et al.* Hybridomas expressing gammadelta T-cell receptors respond to cardiolipin and beta2-glycoprotein 1 (apolipoprotein H). *Scand J Immunol* **58**, 374-381 (2003).
140. Bonneville, M. *et al.* Recognition of a self major histocompatibility complex TL region product by gamma delta T-cell receptors. *Proc Natl Acad Sci U S A* **86**, 5928-5932 (1989).
141. Ito, K. *et al.* Recognition of the product of a novel MHC TL region gene (27b) by a mouse gamma delta T cell receptor. *Cell* **62**, 549-561 (1990).
142. Adams, E.J., Chien, Y.H. & Garcia, K.C. Structure of a gammadelta T cell receptor in complex with the nonclassical MHC T22. *Science* **308**, 227-231 (2005).
143. Metkar, S.S. *et al.* Human and mouse granzyme A induce a proinflammatory cytokine response. *Immunity* **29**, 720-733 (2008).
144. Bonneville, M., O'Brien, R.L. & Born, W.K. Gammadelta T cell effector functions: a blend of innate programming and acquired plasticity. *Nat Rev Immunol* **10**, 467-478 (2010).
145. Chien, Y.H., Meyer, C. & Bonneville, M. gammadelta T cells: first line of defense and beyond. *Annu Rev Immunol* **32**, 121-155 (2014).
146. Northrop, J.P. *et al.* NF-AT components define a family of transcription factors targeted in T-cell activation. *Nature* **369**, 497-502 (1994).
147. Vaeth, M. & Feske, S. NFAT control of immune function: New Frontiers for an Abiding Trooper. *F1000Research* **7**, 260 (2018).

148. Lopez-Rodriguez, C., Aramburu, J., Rakeman, A.S. & Rao, A. NFAT5, a constitutively nuclear NFAT protein that does not cooperate with Fos and Jun. *Proc Natl Acad Sci U S A* **96**, 7214-7219 (1999).
149. Serfling, E. *et al.* The role of NF-AT transcription factors in T cell activation and differentiation. *Biochim Biophys Acta* **1498**, 1-18 (2000).
150. de la Pompa, J.L. *et al.* Role of the NF-ATc transcription factor in morphogenesis of cardiac valves and septum. *Nature* **392**, 182-186 (1998).
151. Ranger, A.M. *et al.* The transcription factor NF-ATc is essential for cardiac valve formation. *Nature* **392**, 186-190 (1998).
152. Hodge, M.R. *et al.* Hyperproliferation and dysregulation of IL-4 expression in NF-ATp-deficient mice. *Immunity* **4**, 397-405 (1996).
153. Xanthoudakis, S. *et al.* An enhanced immune response in mice lacking the transcription factor NFAT1. *Science* **272**, 892-895 (1996).
154. Ranger, A.M., Oukka, M., Rengarajan, J. & Glimcher, L.H. Inhibitory function of two NFAT family members in lymphoid homeostasis and Th2 development. *Immunity* **9**, 627-635 (1998).
155. Klein-Hessling, S. *et al.* NFATc1 controls the cytotoxicity of CD8+ T cells. *Nature communications* **8**, 511 (2017).
156. Serfling, E., Berberich-Siebelt, F., Chuvpilo, S., Jankevics, E., Klein-Hessling, S., Twardzik, T., Avots, A. The role of NF-AT transcription factors in T cell activation and differentiation. *Biochimica et Biophysica Acta* **1498**, 1-18 (2000).
157. Bhattacharyya, S. *et al.* NFATc1 affects mouse splenic B cell function by controlling the calcineurin--NFAT signaling network. *J Exp Med* **208**, 823-839 (2011).
158. Vaeth, M. *et al.* Follicular regulatory T cells control humoral autoimmunity via NFAT2-regulated CXCR5 expression. *J Exp Med* **211**, 545-561 (2014).
159. Oestreich, K.J., Yoon, H., Ahmed, R. & Boss, J.M. NFATc1 regulates PD-1 expression upon T cell activation. *J Immunol* **181**, 4832-4839 (2008).
160. Tsytsykova, A.V., Tsitsikov, E.N. & Geha, R.S. The CD40L promoter contains nuclear factor of activated T cells-binding motifs which require AP-1 binding for activation of transcription. *J Biol Chem* **271**, 3763-3770 (1996).
161. Kim, H.P., Korn, L.L., Gamero, A.M. & Leonard, W.J. Calcium-dependent activation of interleukin-21 gene expression in T cells. *J Biol Chem* **280**, 25291-25297 (2005).
162. Monticelli, S. & Rao, A. NFAT1 and NFAT2 are positive regulators of IL-4 gene transcription. *Eur J Immunol* **32**, 2971-2978 (2002).
163. Bandukwala, H.S. *et al.* Structure of a domain-swapped FOXP3 dimer on DNA and its function in regulatory T cells. *Immunity* **34**, 479-491 (2011).
164. Tone, Y. *et al.* Smad3 and NFAT cooperate to induce Foxp3 expression through its enhancer. *Nat Immunol* **9**, 194-202 (2008).
165. Oh-hora, M. & Rao, A. The calcium/NFAT pathway: role in development and function of regulatory T cells. *Microbes and infection* **11**, 612-619 (2009).
166. Vaeth, M. *et al.* Dependence on nuclear factor of activated T-cells (NFAT) levels discriminates conventional T cells from Foxp3+ regulatory T cells. *Proc Natl Acad Sci U S A* **109**, 16258-16263 (2012).

167. Wu, Y. *et al.* FOXP3 controls regulatory T cell function through cooperation with NFAT. *Cell* **126**, 375-387 (2006).
168. Soto-Nieves, N. *et al.* Transcriptional complexes formed by NFAT dimers regulate the induction of T cell tolerance. *J Exp Med* **206**, 867-876 (2009).
169. Macian, F., Garcia-Rodriguez, C. & Rao, A. Gene expression elicited by NFAT in the presence or absence of cooperative recruitment of Fos and Jun. *EMBO J* **19**, 4783-4795 (2000).
170. Nurieva, R.I. *et al.* The E3 ubiquitin ligase GRAIL regulates T cell tolerance and regulatory T cell function by mediating T cell receptor-CD3 degradation. *Immunity* **32**, 670-680 (2010).
171. Asai, K. *et al.* T cell hyporesponsiveness induced by oral administration of ovalbumin is associated with impaired NFAT nuclear translocation and p27kip1 degradation. *J Immunol* **169**, 4723-4731 (2002).
172. Abe, B.T., Shin, D.S., Mocholi, E. & Macian, F. NFAT1 supports tumor-induced anergy of CD4(+) T cells. *Cancer Res* **72**, 4642-4651 (2012).
173. Hogan, P.G. Calcium-NFAT transcriptional signalling in T cell activation and T cell exhaustion. *Cell calcium* **63**, 66–69 (2017).
174. Rudolf, R. *et al.* Architecture and expression of the *nfatc1* gene in lymphocytes. *Front Immunol* **5**, 21 (2014).
175. Chuvpilo, S. *et al.* Alternative polyadenylation events contribute to the induction of NF-ATc in effector T cells. *Immunity* **10**, 261-269 (1999).
176. Chuvpilo, S. *et al.* Multiple NF-ATc isoforms with individual transcriptional properties are synthesized in T lymphocytes. *J Immunol* **162**, 7294-7301 (1999).
177. Chuvpilo, S. *et al.* Autoregulation of NFATc1/A Expression Facilitates Effector T Cells to Escape from Rapid Apoptosis. *Immunity* **16**, 881–895 (2002).
178. Ranger, A.M. *et al.* Delayed lymphoid repopulation with defects in IL-4-driven responses produced by inactivation of NF-ATc. *Immunity* **8**, 125-134 (1998).
179. Mognol, G.P., Carneiro, F.R., Robbs, B.K., Faget, D.V. & Viola, J.P. Cell cycle and apoptosis regulation by NFAT transcription factors: new roles for an old player. *Cell Death Dis* **7**, e2199 (2016).
180. Hock, M. *et al.* NFATc1 induction in peripheral T and B lymphocytes. *J Immunol* **190**, 2345-2353 (2013).
181. Serfling, E., Berberich-Siebelt, F. & Avots, A. NFAT in lymphocytes: a factor for all events? *Sci STKE* **2007**, pe42 (2007).
182. Xiao, Y. *et al.* Lack of NFATc1 SUMOylation prevents autoimmunity and alloreactivity. *J Exp Med* **218** (2021).
183. Jiang, Q. *et al.* Cell biology of IL-7, a key lymphotrophin. *Cytokine Growth Factor Rev* **16**, 513-533 (2005).
184. von Freeden-Jeffry, U. *et al.* Lymphopenia in interleukin (IL)-7 gene-deleted mice identifies IL-7 as a nonredundant cytokine. *J Exp Med* **181**, 1519-1526 (1995).
185. Peschon, J.J. *et al.* Early lymphocyte expansion is severely impaired in interleukin 7 receptor-deficient mice. *J Exp Med* **180**, 1955-1960 (1994).

186. Patra, A.K. *et al.* PKB Rescues Calcineurin/NFAT-Induced Arrest of Rag Expression and Pre-T Cell Differentiation. *The Journal of Immunology* **177**, 4567–4576 (2006).
187. Jalili, V. *et al.* The Galaxy platform for accessible, reproducible and collaborative biomedical analyses: 2020 update. *Nucleic Acids Res* **48**, W395-W402 (2020).
188. Feng, J., Liu, T., Qin, B., Zhang, Y. & Liu, X.S. Identifying ChIP-seq enrichment using MACS. *Nat Protoc* **7**, 1728-1740 (2012).
189. Zhang, Y. *et al.* Model-based analysis of ChIP-Seq (MACS). *Genome Biol* **9**, R137 (2008).
190. McLean, C.Y. *et al.* GREAT improves functional interpretation of cis-regulatory regions. *Nat Biotechnol* **28**, 495-501 (2010).
191. Eden, E., Navon, R., Steinfeld, I., Lipson, D. & Yakhini, Z. GOrilla: a tool for discovery and visualization of enriched GO terms in ranked gene lists. *BMC Bioinformatics* **10**, 48 (2009).
192. Eden, E., Lipson, D., Yogev, S. & Yakhini, Z. Discovering motifs in ranked lists of DNA sequences. *PLoS Comput Biol* **3**, e39 (2007).
193. Duttke, S.H., Chang, M.W., Heinz, S. & Benner, C. Identification and dynamic quantification of regulatory elements using total RNA. *Genome Res* **29**, 1836-1846 (2019).
194. Patra, A.K. *et al.* PKB rescues calcineurin/NFAT-induced arrest of Rag expression and pre-T cell differentiation. *J Immunol* **177**, 4567-4576 (2006).
195. Klein-Hessling, S. *et al.* NFATc1 controls the cytotoxicity of CD8(+) T cells. *Nat Commun* **8**, 511 (2017).
196. Heng, T.S., Painter, M.W. & Immunological Genome Project, C. The Immunological Genome Project: networks of gene expression in immune cells. *Nat Immunol* **9**, 1091-1094 (2008).
197. Majumder, K. *et al.* Domain-Specific and Stage-Intrinsic Changes in Tcrb Conformation during Thymocyte Development. *Journal of immunology (Baltimore, Md. : 1950)* **195**, 1262–1272 (2015).
198. Carabana, J., Watanabe, A., Hao, B. & Krangel, M.S. A barrier-type insulator forms a boundary between active and inactive chromatin at the murine TCRbeta locus. *J Immunol* **186**, 3556-3562 (2011).
199. Patra, A.K. *et al.* An alternative NFAT-activation pathway mediated by IL-7 is critical for early thymocyte development. *Nat Immunol* **14**, 127-135 (2013).
200. Fisher, A.G. & Ceredig, R. Gamma delta T cells expressing CD8 or CD4low appear early in murine foetal thymus development. *Int Immunol* **3**, 1323-1328 (1991).
201. Sato, K., Ohtsuka, K., Watanabe, H., Asakura, H. & Abo, T. Detailed characterization of gamma delta T cells within the organs in mice: classification into three groups. *Immunology* **80**, 380-387 (1993).
202. Kadivar, M., Petersson, J., Svensson, L. & Marsal, J. CD8alphabeta+ gammadelta T Cells: A Novel T Cell Subset with a Potential Role in Inflammatory Bowel Disease. *J Immunol* **197**, 4584-4592 (2016).
203. Serfling, E. *et al.* NFATc1/alphaA: The other Face of NFAT Factors in Lymphocytes. *Cell Commun Signal* **10**, 16 (2012).
204. Yahia-Cherbal, H. *et al.* NFAT primes the human RORC locus for RORgammat expression in CD4(+) T cells. *Nat Commun* **10**, 4698 (2019).

205. Ohoka, Y., Yokota, A., Takeuchi, H., Maeda, N. & Iwata, M. Retinoic acid-induced CCR9 expression requires transient TCR stimulation and cooperativity between NFATc2 and the retinoic acid receptor/retinoid X receptor complex. *J Immunol* **186**, 733-744 (2011).
206. Uehara, S., Grinberg, A., Farber, J.M. & Love, P.E. A role for CCR9 in T lymphocyte development and migration. *J Immunol* **168**, 2811-2819 (2002).
207. Schulz, O., Hammerschmidt, S.I., Moschovakis, G.L. & Forster, R. Chemokines and Chemokine Receptors in Lymphoid Tissue Dynamics. *Annu Rev Immunol* **34**, 203-242 (2016).
208. Svensson, M. *et al.* Involvement of CCR9 at multiple stages of adult T lymphopoiesis. *J Leukoc Biol* **83**, 156-164 (2008).
209. Krishnamoorthy, V. *et al.* Repression of Ccr9 transcription in mouse T lymphocyte progenitors by the Notch signaling pathway. *J Immunol* **194**, 3191-3200 (2015).
210. Norment, A.M., Bogatzki, L.Y., Gantner, B.N. & Bevan, M.J. Murine CCR9, a chemokine receptor for thymus-expressed chemokine that is up-regulated following pre-TCR signaling. *J Immunol* **164**, 639-648 (2000).
211. Tsao, H.W. *et al.* Ets-1 facilitates nuclear entry of NFAT proteins and their recruitment to the IL-2 promoter. *Proc Natl Acad Sci U S A* **110**, 15776-15781 (2013).
212. Koltsova, E.K. *et al.* Early growth response 1 and NF-ATc1 act in concert to promote thymocyte development beyond the beta-selection checkpoint. *J Immunol* **179**, 4694-4703 (2007).
213. Jennings, E., Elliot, Thomas, A. E., Thawait, N., Kanabar, S., Yam-Puc, J.C., Ono, M., Toellner, K.M., Wraith, D.C., Anderson, G., Bending, D. Distinct regulation of Nr4a receptors by NFAT and ERK signalling during T cell activation
214. Hernandez, J.B., Newton, R.H. & Walsh, C.M. Life and death in the thymus--cell death signaling during T cell development. *Curr Opin Cell Biol* **22**, 865-871 (2010).
215. Schenk, R.L. *et al.* Characterisation of mice lacking all functional isoforms of the pro-survival BCL-2 family member A1 reveals minor defects in the haematopoietic compartment. *Cell Death Differ* **24**, 534-545 (2017).
216. Narayan, K. *et al.* Intrathymic programming of effector fates in three molecularly distinct gammadelta T cell subtypes. *Nat Immunol* **13**, 511-518 (2012).
217. Garcia-Rodriguez, C. & Rao, A. Nuclear factor of activated T cells (NFAT)-dependent transactivation regulated by the coactivators p300/CREB-binding protein (CBP). *J Exp Med* **187**, 2031-2036 (1998).
218. Rodriguez-Caparros, A. *et al.* Regulation of T-cell Receptor Gene Expression by Three-Dimensional Locus Conformation and Enhancer Function. *Int J Mol Sci* **21** (2020).
219. Hernandez-Munain, C. Recent insights into the transcriptional control of the Tcra/Tcrd locus by distant enhancers during the development of T-lymphocytes. *Transcription* **6**, 65-73 (2015).
220. del Blanco, B., Garcia-Mariscal, A., Wiest, D.L. & Hernandez-Munain, C. Tcra enhancer activation by inducible transcription factors downstream of pre-TCR signaling. *J Immunol* **188**, 3278-3293 (2012).
221. Burtrum, D.B., Kim, S., Dudley, E.C., Hayday, A.C. & Petrie, H.T. TCR gene recombination and alpha beta-gamma delta lineage divergence: productive TCR-beta rearrangement is neither exclusive nor preclusive of gamma delta cell development. *J Immunol* **157**, 4293-4296 (1996).

10 Acknowledgments

I would like to sincerely express my deep regards to my first supervisor and head of my workgroup, Prof. Dr. Edgar Serfling for giving me the possibility of being a member of his amazing group, and for helping me during all the critical situations that occurred during these years. He supported me a lot in scientific growth and guided me with his scientific and academic experience.

My sincere gratitude goes to Prof. Dr. Andreas Rosenwald, the director of the Institute of Pathology, for the financial support during my last years of PhD.

I would also like to thank the ideator and pioneer of my project, Prof. Dr. Amiya Patra. As the main expert on my topic, he gave me suggestions and advice during these years, encouraging my scientific ideas and discussing my experiments and theories.

A sincere thank is due to the members of my thesis committee, PD Dr. Friederike Berberich-Siebelt, and PD Dr. med. Niklas Beyersdorf for the intense scientific discussions within the annual meetings. In particular, a special mention goes to PD Dr. Friederike Berberich-Siebelt for the deep exchange of scientific opinions and for her constant willingness in giving suggestions. I would like to express my gratitude for the personal support she gave me during these years.

My immense thankfulness goes to my mentor, my colleague, my guide, my friend Dr. Stefan Klein-Hessling. It is difficult for me to put on paper all the gratefulness I would like to express. He has been one of the most important people for me during these years. He trained me, guided me, supported me, and made me become a scientist when I was only a little student with a lot of hopes. All I have learned and the scientific confidence I have acquired during these years come from his guidance. His patience counterbalanced my explosive and lunatic attitude. He supported me whenever I needed help, whenever I was happy and enthusiastic, and whenever I didn't know how to proceed. He always showed me always "the other side of the moon" when I was not able to see it carefully. I hope he will keep being my guide wherever my path will lead me.

I would also like to thank my former and current colleagues. More than colleagues, they became friends and a second family for me, Azeem Muhammad, Cristina Chiarolla, Yin Xiao, Snigdha Majumder, Rishav Seal, Nadine Hundhausen, Anika König, Viola Schmitt, Delicia Xavier, Felix Schüssler, Max Straub, Salvador Sampere. We enjoyed our daily lab life altogether and supported each other under every aspect, scientific and personal. My PhD years would not have been the same without all of them. We created an amazing group and I am so glad to have them in my life.

I can not forget to thank Cristina Chiarolla, my friend and flatmate, who spent every day with me, whether they were good or bad times. I am thankful for her support and patience with me. But most of all, I have the key idea and results of this thesis due to our evening-home discussions. She taught me when I needed to learn something new, suggested when I needed to plan new experiments, making things clear for me. We shared information, knowledge, and scientific ideas, and I would be glad to have her as a co-authorship of my paper. Her support has been precious from the scientific and personal point of view.

Konrad Knöpper, my “unexpected” friend, has been an inestimable help to me. He is one of the nicest and most generous people I have ever met. He helped me out with my RNA-seq analysis, which was a completely new world to me. His friendship became inestimable and his support has been essential especially during these last PhD years.

But these years would have not been special without the presence of other important people met during this journey. My friends and PhD colleague Teresa Wiese, with whom I share the great skill of talking endlessly and with whom I shared each room during all the conferences we attended. Thanks to Anne Rech, Emilia Vendelova, with whom I have spent joyful moments outside of the scientific world.

Thanks to my friend Clara, for the time together, for taking care of me, for our experiences while travelling, for the nights and the days, for the capacity of reading each other’s mind, for the laughs, for the going back to being younger and stupid, for ringing at my door with a “six pack”, for the support when I was not strong enough to stand alone.

My gratitude goes to Matteo da Viá, the first person taking care of me during the first weeks I was in Würzburg. His support and wiseness helped me immensely.

Thanks to Giuseppe d’Ortona, one of the people I felt closest to during these last four years, even though being physically distant. His support for my mind has been precious and irreplaceable.

Thanks to Inga for our nights of dancing and “we found the love in hopeless places”. These nights freed my mind.

Thanks so much to Daniele Spinozzi, my friend and colleague since university, for our “around the world” meetings, and for never losing our friendship during all these years.

Last, but not least, I must thank “my person”, Chiara, the best friend I have always had. The person that understands my mind, my soul, and my thoughts, no explanation is necessary. She was and she is always there for me.

All my love goes to my parents and my family for always understanding the importance of letting me go far away to realize my dreams.

Thanks to all the people that made these four years amazing for this little Italian alien.

At the end of this path, what I love to do is jump up and down while recalling the memories of these years and look at all the faces of the people... some faces made me laugh, some made

me cry, some made me challenge myself, some made me think, but each of them has a value, a story and a lesson I have learned. People made the place and I have loved this place because I have loved the people around me.

Resilience: Resilience is a term used in psychology to describe the capacity of people to cope with stress and catastrophe. It is also used to indicate a characteristic of resistance to future negative events. This psychological meaning of resilience is often contrasted with "risk factors". (Wikipedia)

*"Io so' testardo, c'ho la capoccia dura e per natura non abbasso mai lo sguardo,
è n'esigenza [...]"*

*E so' testardo, e nun me ferma niente, vado sempre avanti fino al mio traguardo indifferente,
e non me frega niente se ritardo [...]"*

Daniele Silvestri, Testardo

"No man burdens his mind with small matters unless he has some very good reason for doing so"

Arthur Conan Doyle, A Study in Scarlet

"What you do in this world is a matter of no consequence. The question is what can you make people believe you have done."

Arthur Conan Doyle, A Study in Scarlet

"My mind," he said, "rebels at stagnation. Give me problems, give me work, give me the most abstruse cryptogram or the most intricate analysis, and I am in my own proper atmosphere. I can dispense then with artificial stimulants. But I abhor the dull routine of existence. I crave for mental exaltation. That is why I have chosen my own particular profession, or rather created it, for I am the only one in the world."

Arthur Conan Doyle, The Sign of Four